EMORY UNIVERSITY SCHOOL OF MEDICINE

EMORY WINSHIP CANCER INSTITUTE

NCI–Designated

Introduction to Tomosynthesis

Ioannis Sechopoulos, Ph.D., DABR
Diagnostic Medical Physics Laboratory
Department of Radiology and Imaging Sciences
& Winship Cancer Institute
Emory University
Atlanta, Georgia

Disclosure

- Institutional Research Collaborations:
  - Barco
  - Hologic
- Consultant:
  - Fuji Medical Systems USA

Learning Objectives

- To understand the fundamental principles behind tomosynthesis
- To explain the possible different system designs
- To explain the determinants of image quality
- To list the factors that affect radiation dose
- To understand the common artifacts in tomosynthesis

Outline

Motivation

Introduction

System Design and Design Considerations

Image Reconstruction

Radiation Dose

X-Ray Scatter

Artifacts

Synthetic Mammograms

MOTIVATION

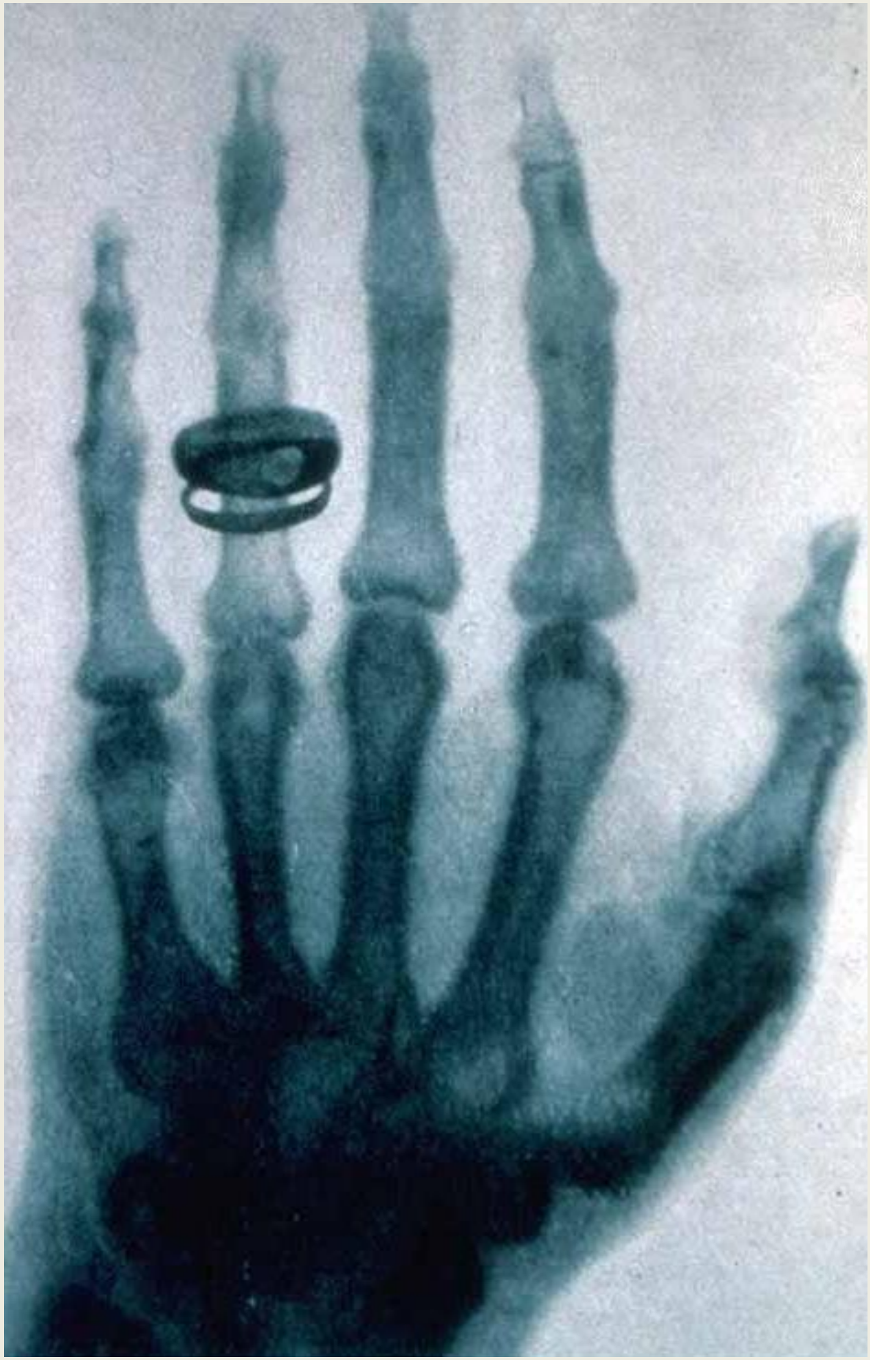

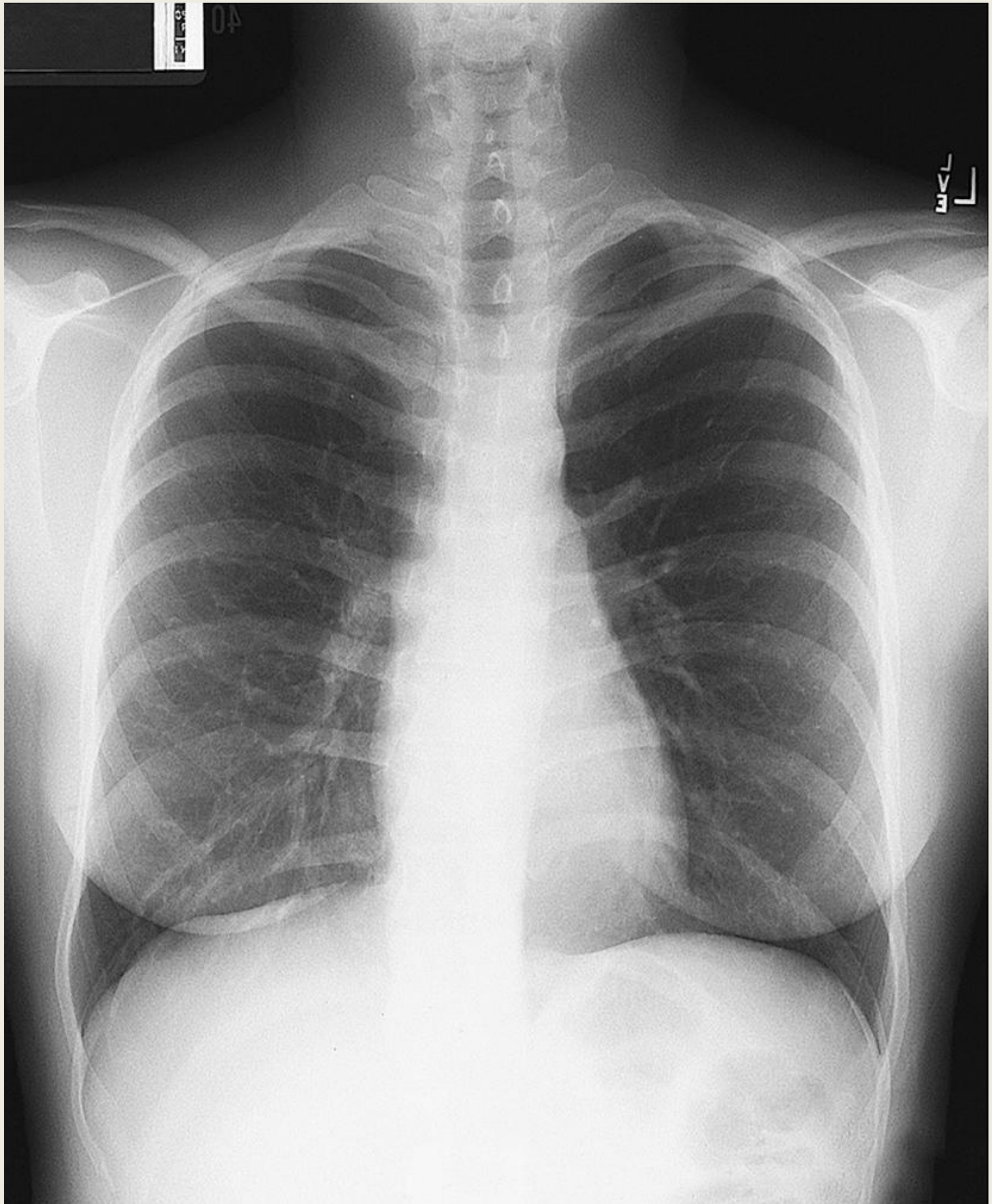

0.16 lesion localization fraction

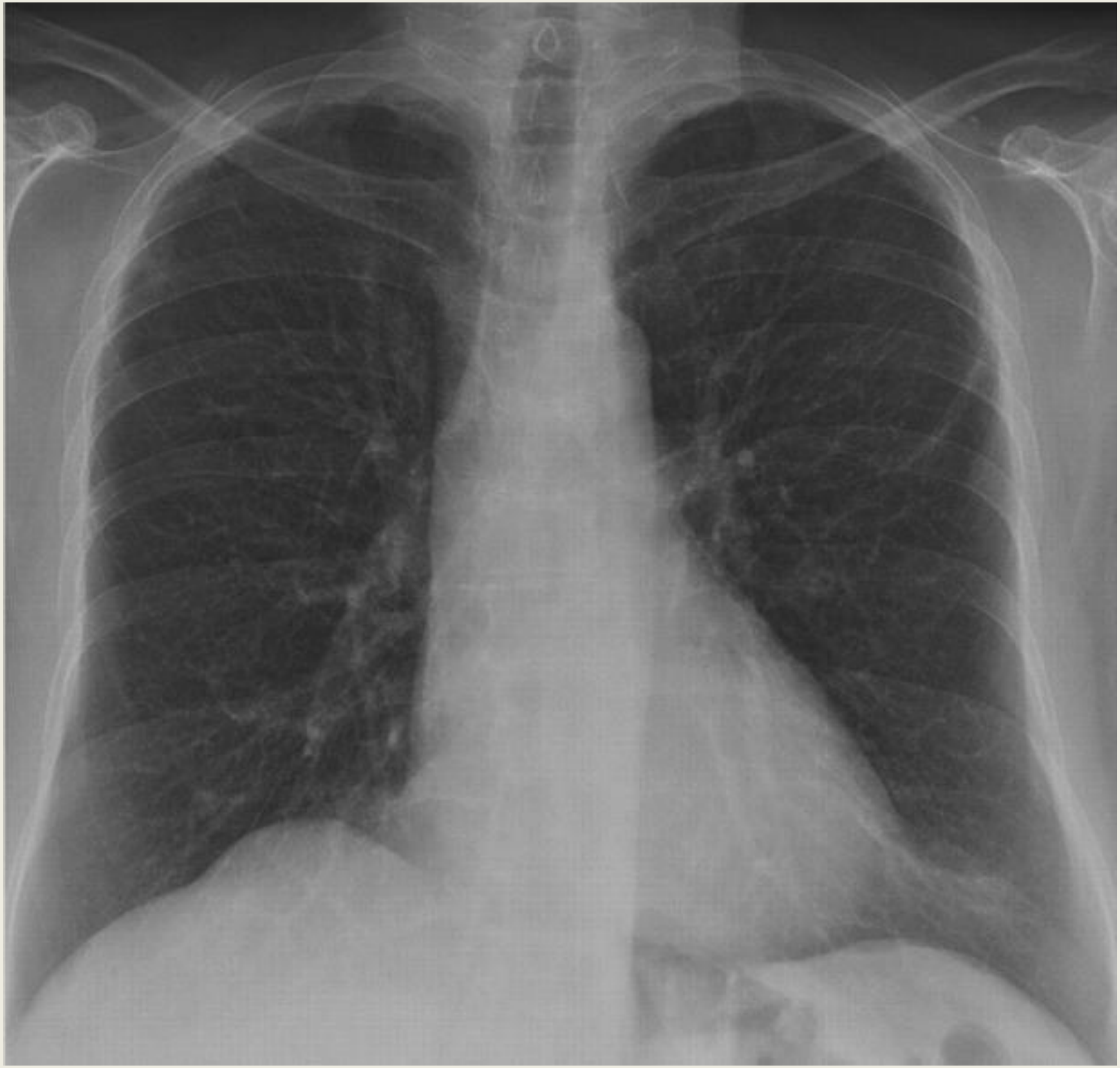

Vikgren et al, Radiology 249(3), 1034-1041 (2008).

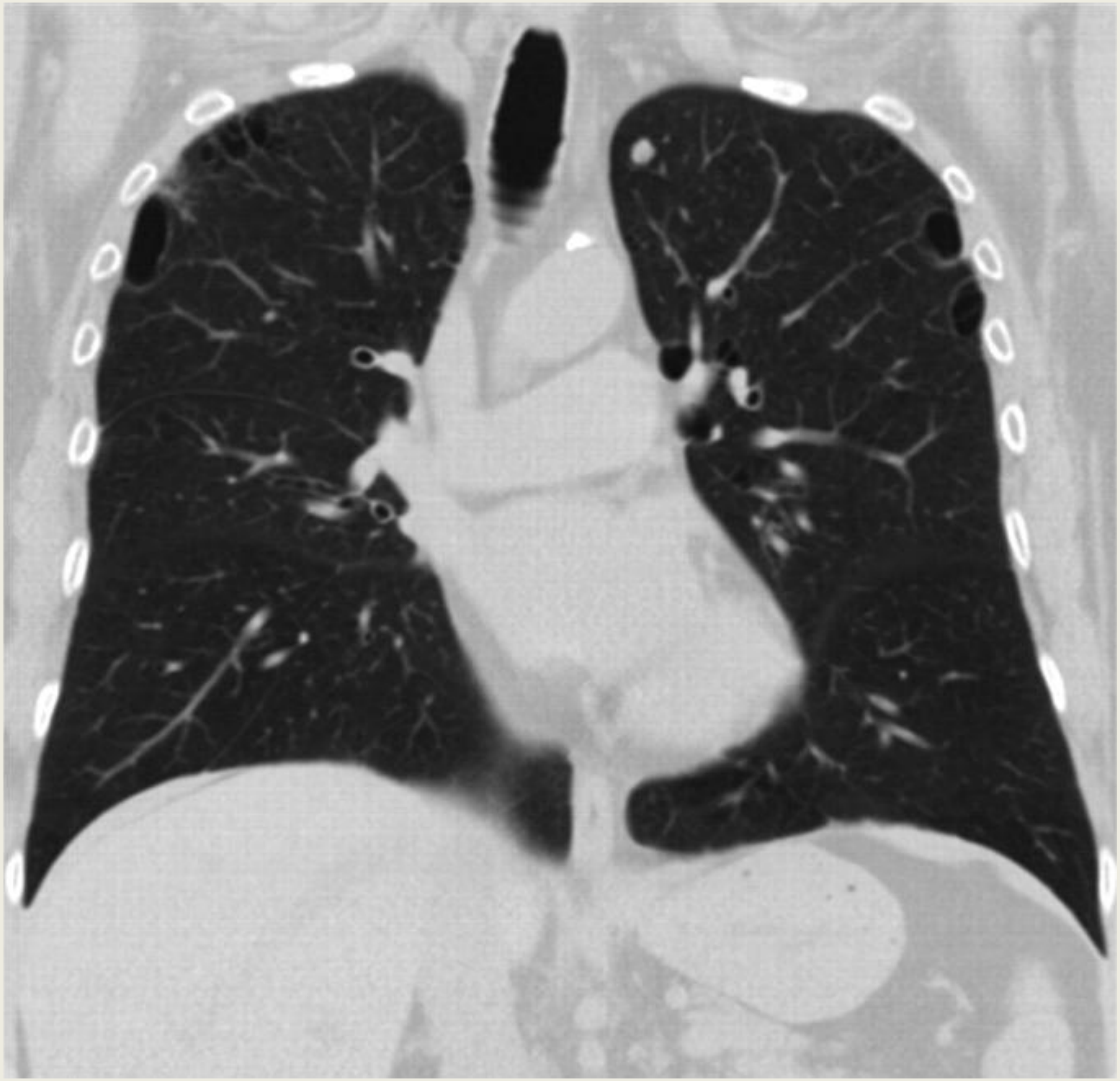

Vikgren et al, Radiology 249(3), 1034-1041 (2008).

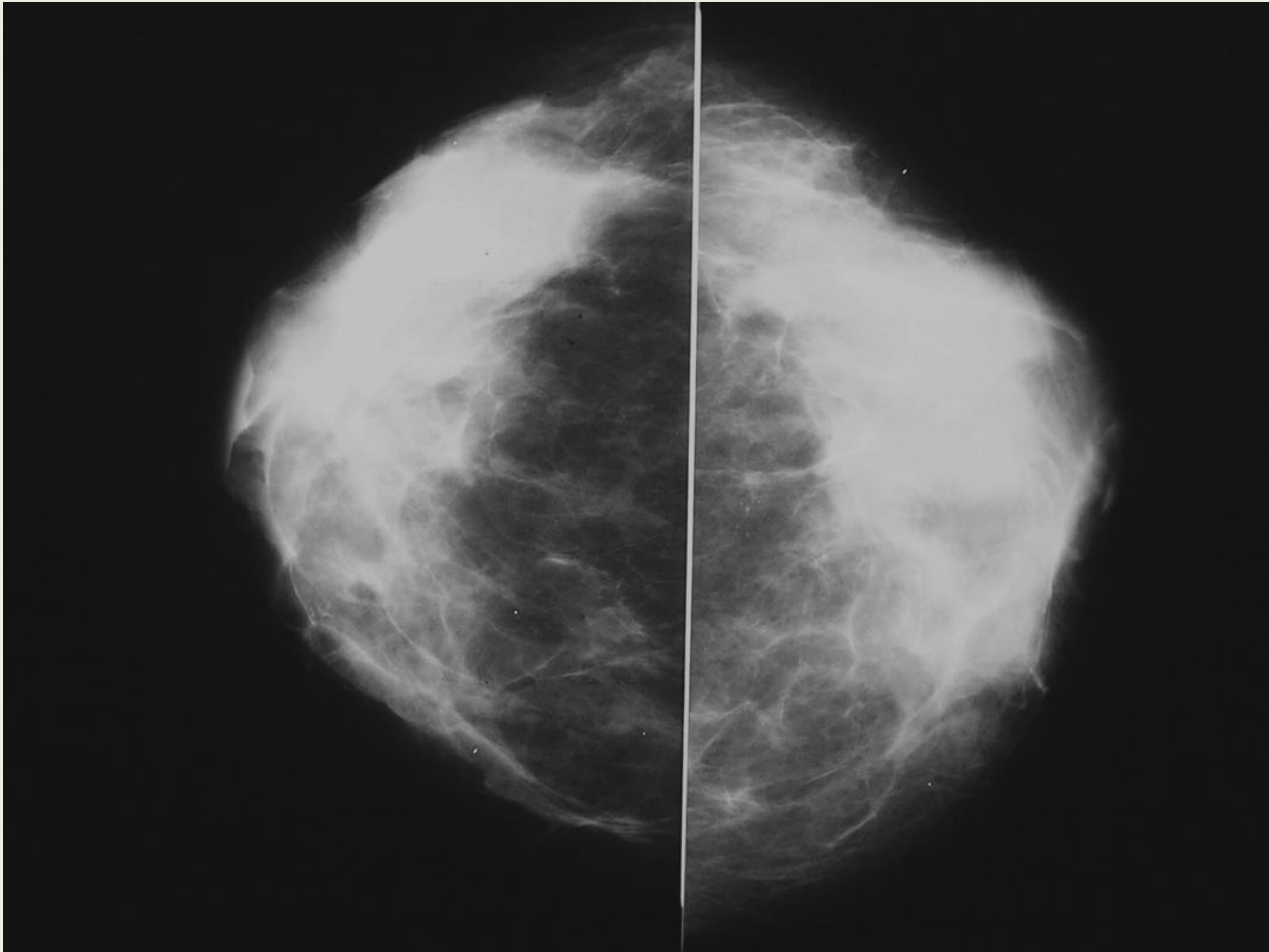

29% of missed cancers were missed due to being “obscured by overlying tissue”

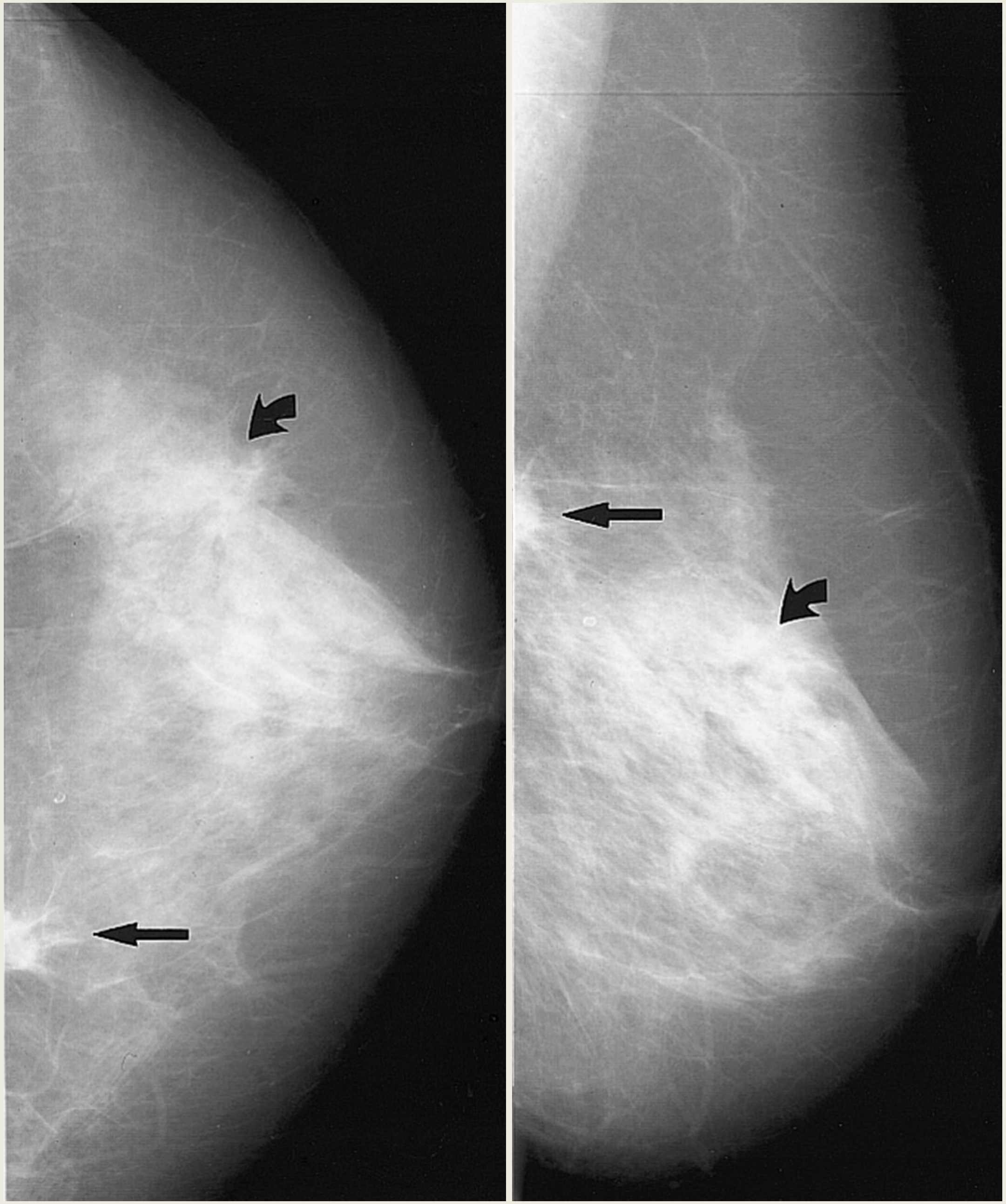

Birdwell et al, Radiology 219, 192-202 (2001).


H
R
L
F
R A


© 2007 Terese Winslow
U.S. Govt. has certain rights


Optima

Courtesy GE Medical Systems

Computed Tomography

More expensive
Higher radiation dose
- 100x chest CT over chest radiograph
- 2-5x breast CT over mammography

Metal problematic
Slower to read (?)

….otherwise, fantastic!

Is there a halfway??

(can we get the best of both worlds?)

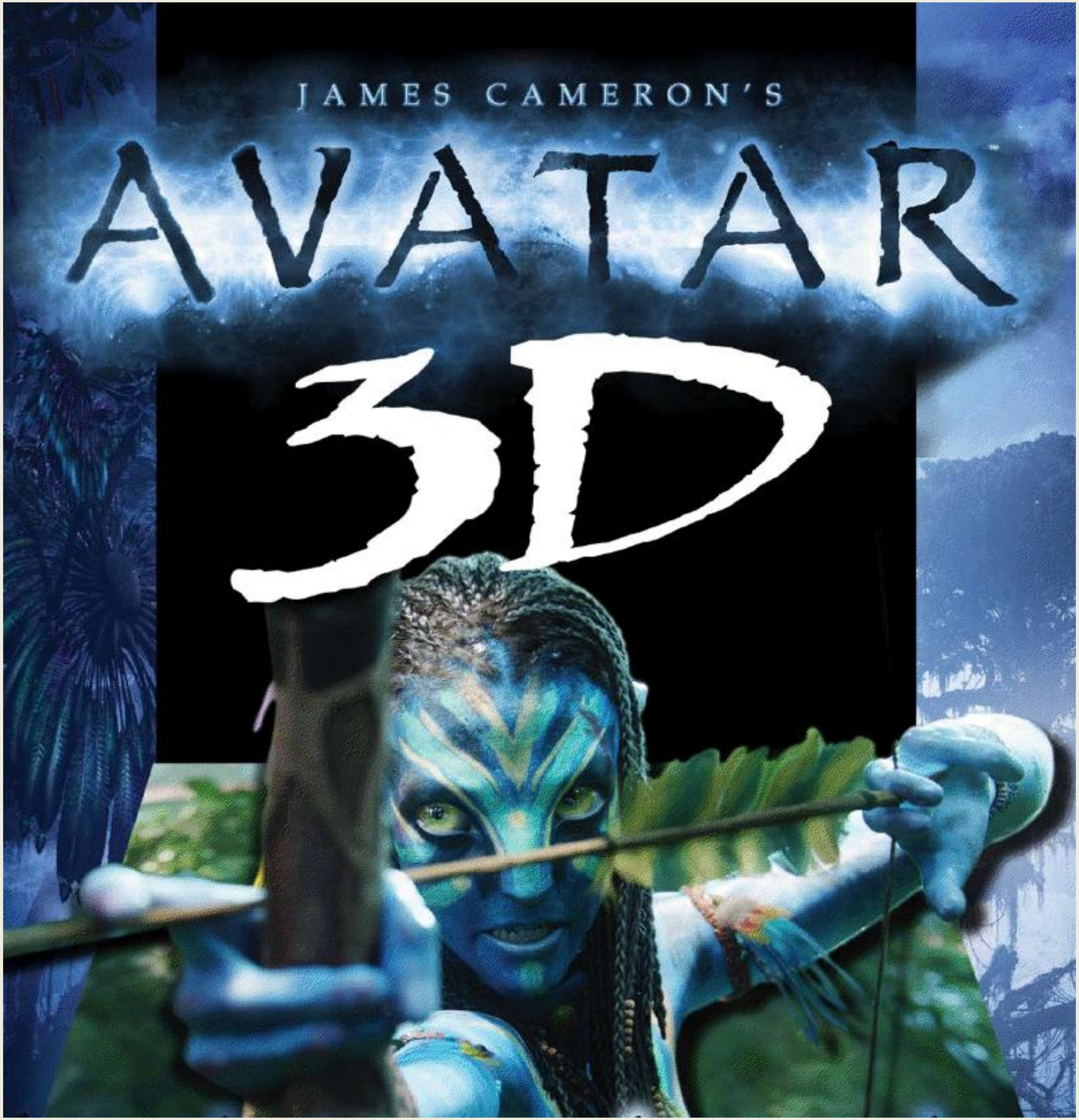
JAMES CAMERON'S
AVATAR
3D

Linear Tomography

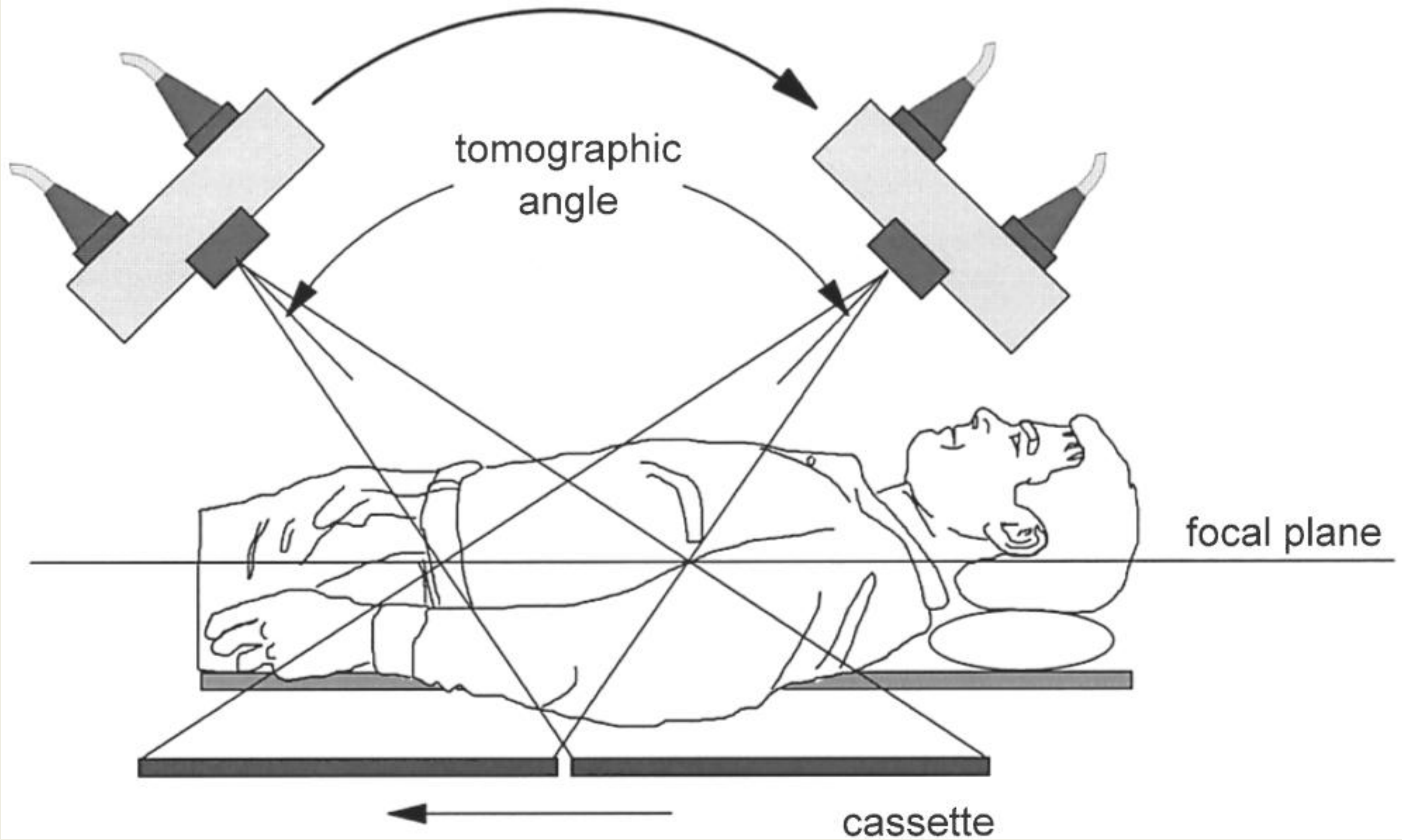

Bushberg et al, The Essential Physics of Medical Imaging, 2nd edition.

Towards Tomographic Imaging

2 D	2+ D	2.1 D	2.2 D	3 D
Standard Transmission Imaging	Stereoscopic Imaging	Linear Tomography	Digital Tomosynthesis	Computed Tomography
	(If your optical system can handle it!)	(If you plan ahead!)		(Is more always better?)

DIGITAL TOMOSYNTHESIS

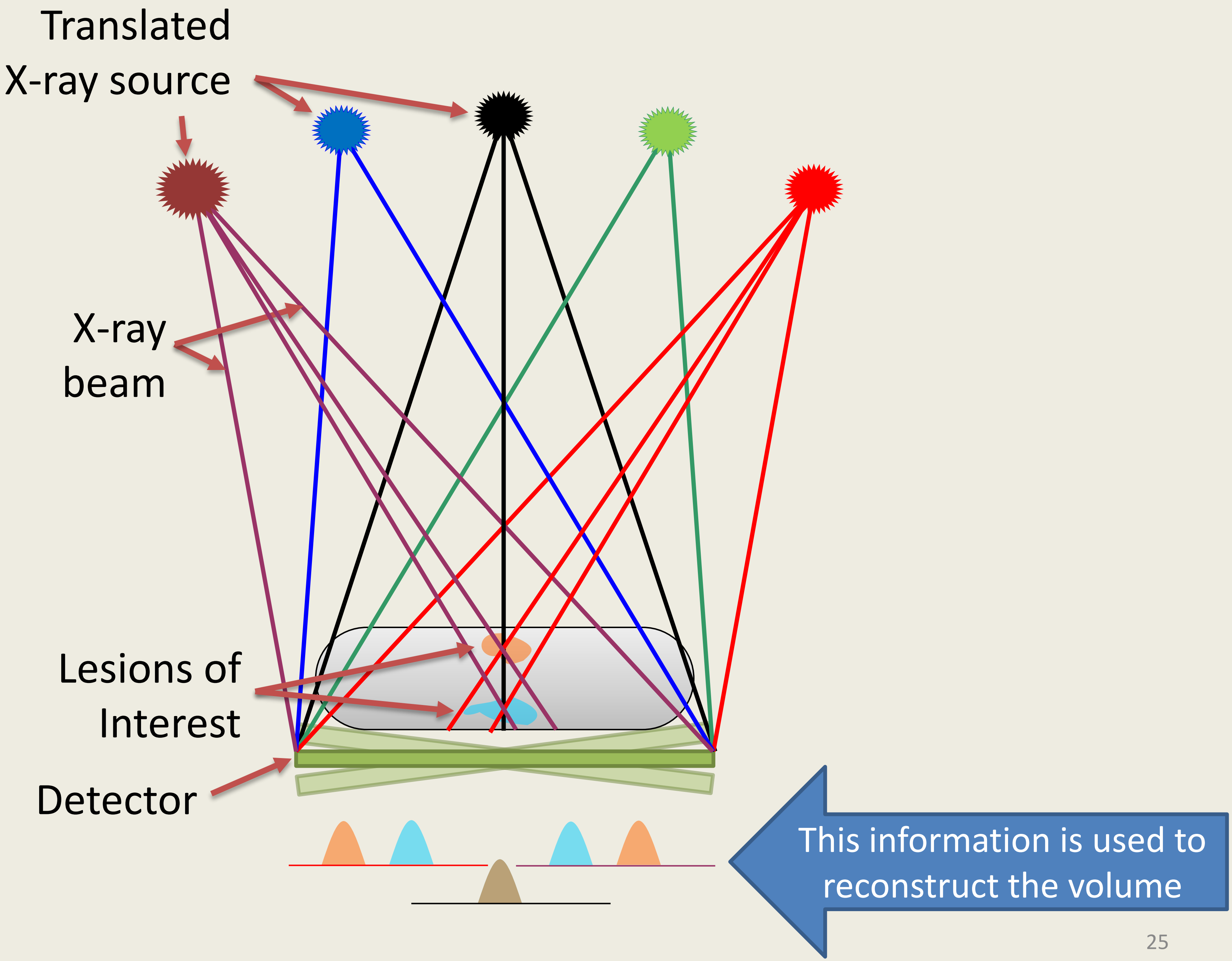
Translated
X-ray source
X-ray
beam
Lesions of
Interest
Detector
This information is used to
reconstruct the volume

Shift correlates with vertical location

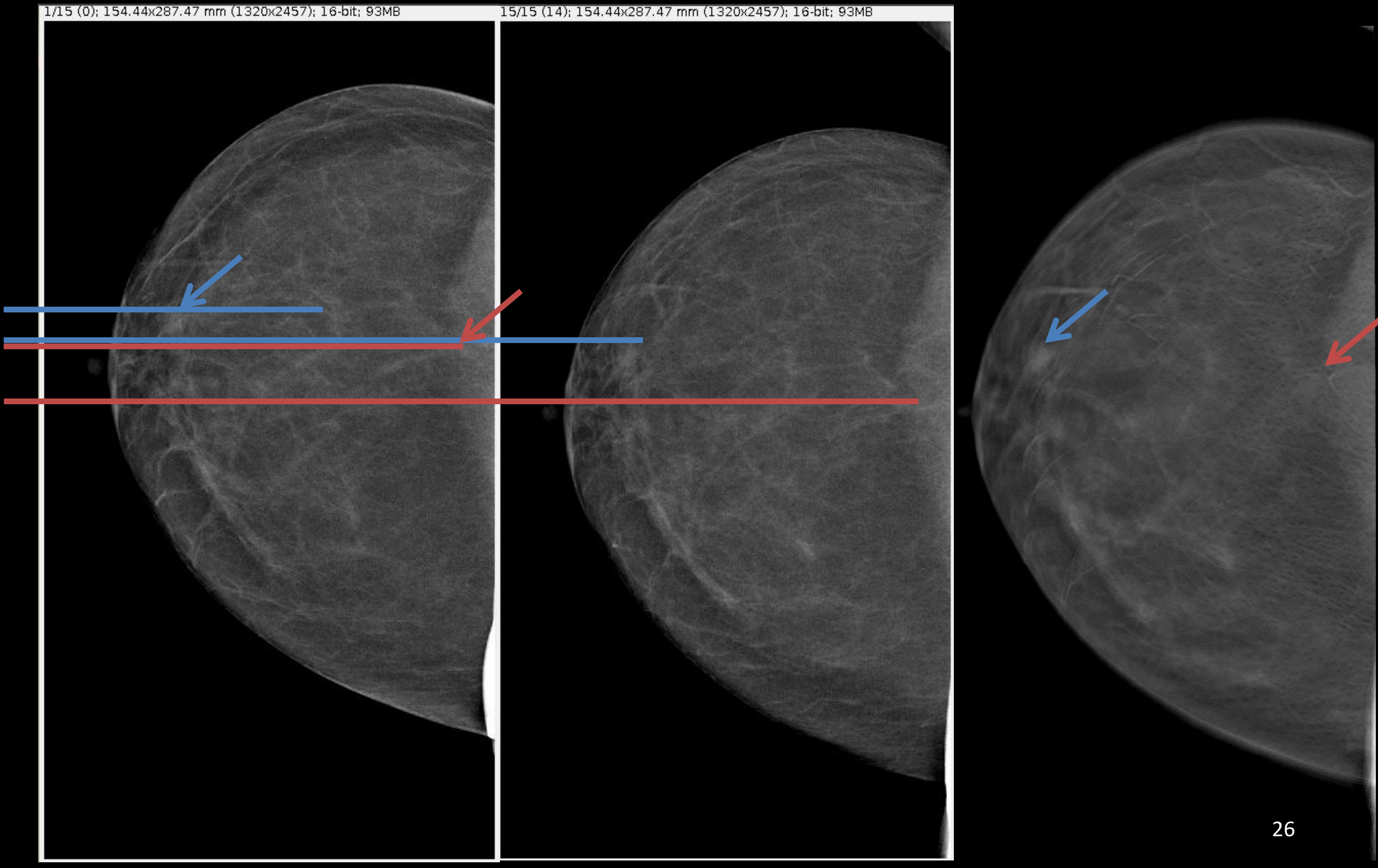

Courtesy of Hologic Inc.

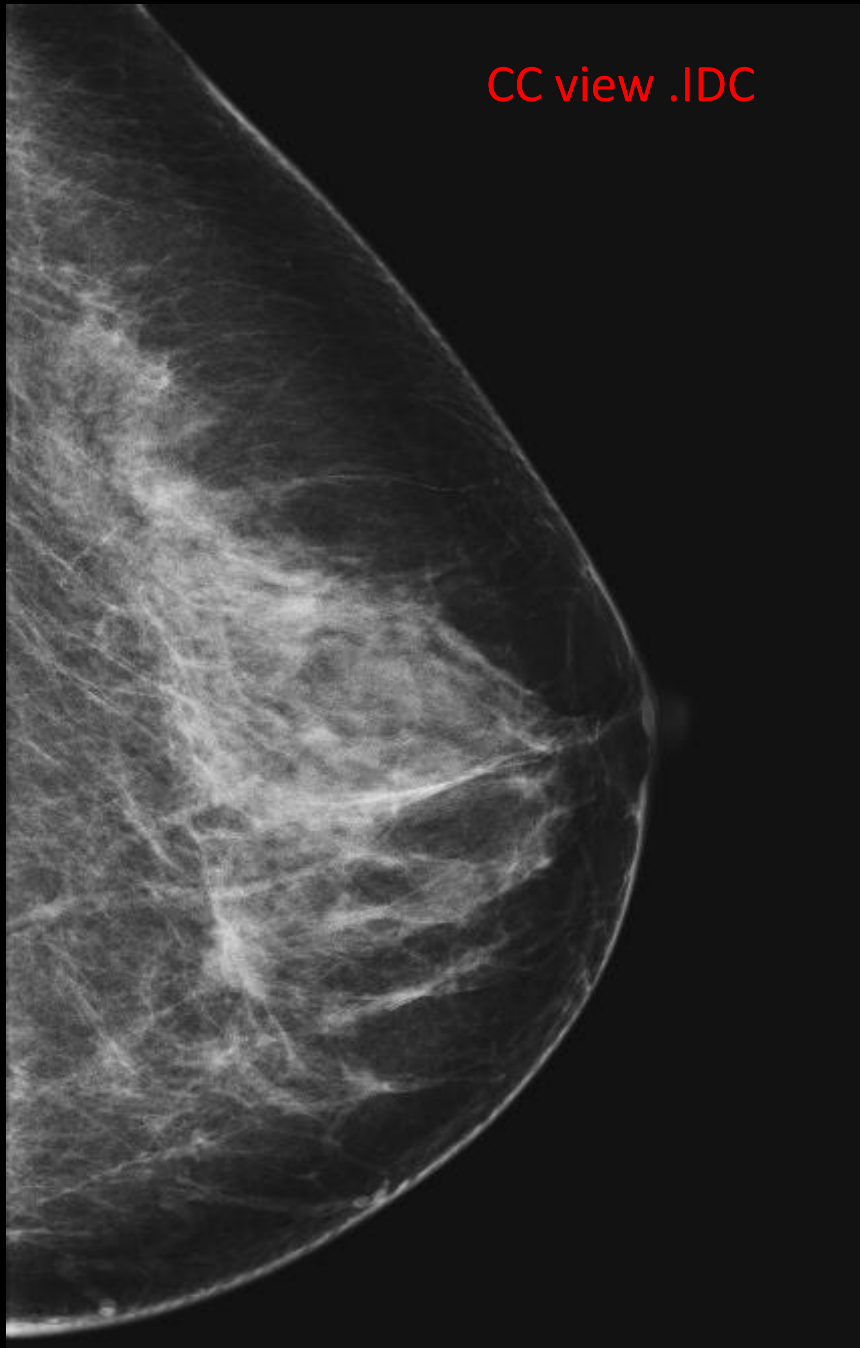

Courtesy of Hologic Inc.

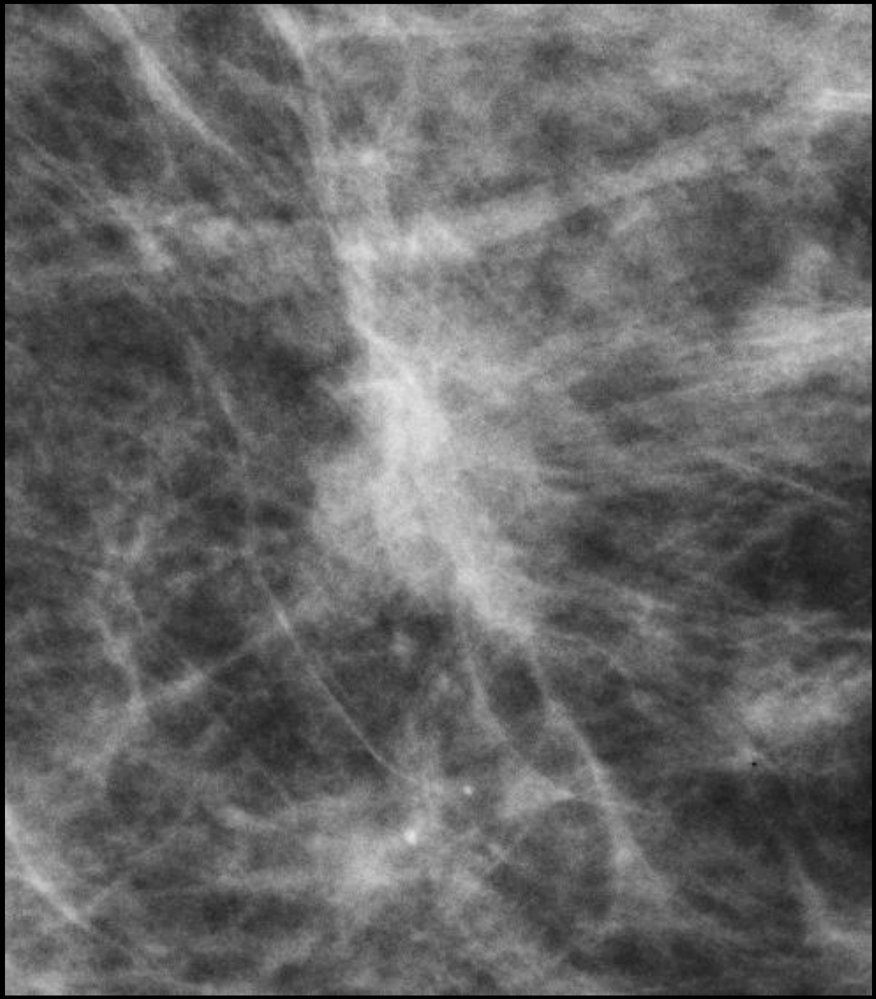

Courtesy of Hologic Inc.

Benefits

Similar to Radiography/Mammography

- System
- Workflow
- Interpretation
- Dose

…but with some discrimination of vertical position!

SYSTEM DESIGN AND DESIGN CONSIDERATIONS

FFDM System

Breast Tomo System

Courtesy Joseph Lo (via youtube)

https://www.youtube.com/watch?v=g9AjqhQJwAs

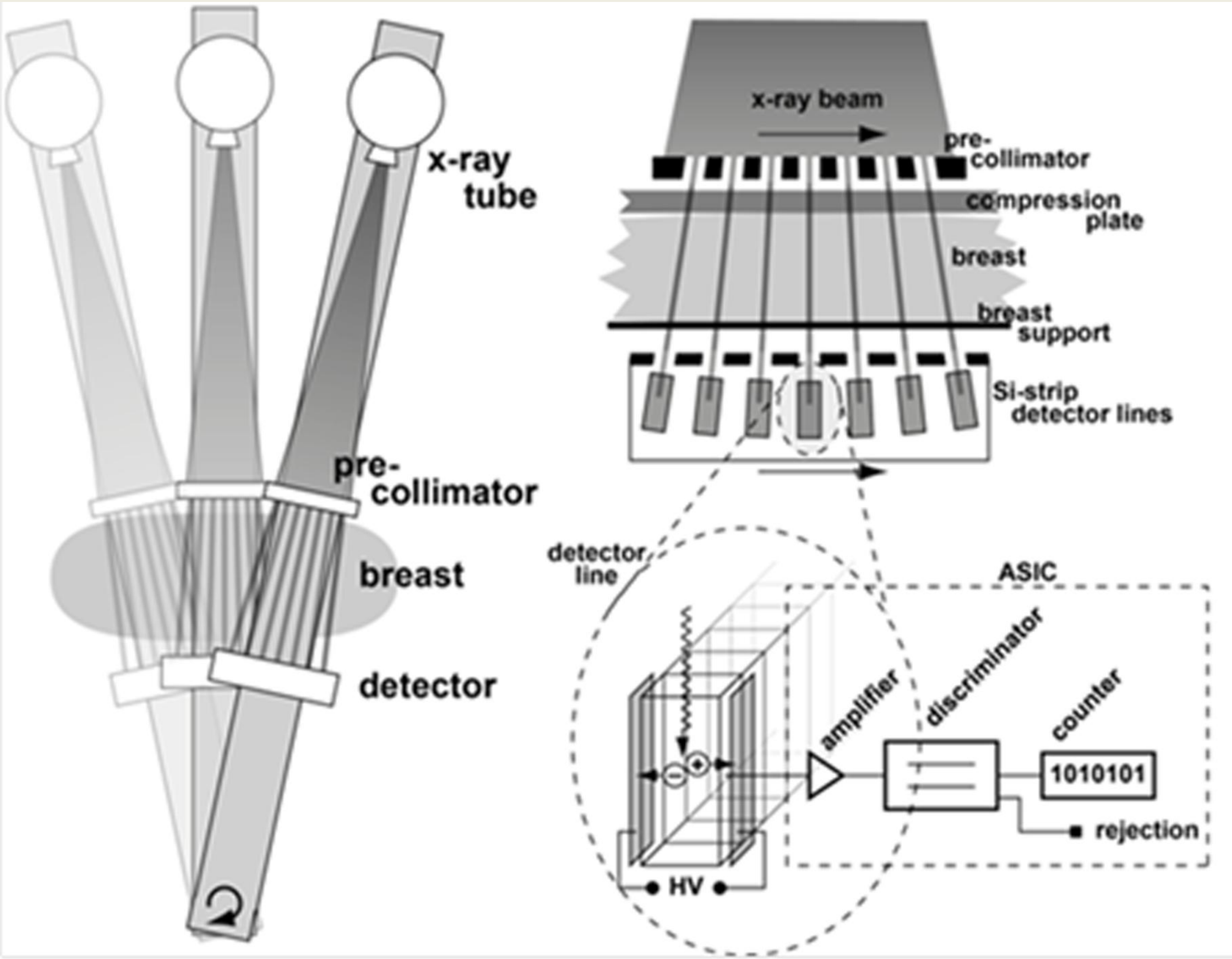

Courtesy of Philips Digital Mammography AB

System	Fuji AMULET Innovality	GE Essential	Hologic Selenia Dimensions	IMS Giotto TOMO	Philips MicroDose	Planmed Nuance Excel DBT	Siemens MAMMOMAT Inspiration
Detector Type	Full field - Direct (a-Se) (Hexagonal pixels)	Full field - Indirect	Full field - Direct (a-Se)	Full field - Direct (a-Se)	Linear Slit Scan – Spectral Photon Counting (Si)	Full field - Direct (a-Se)	Full field - Direct (a-Se)
Detector Motion	Static	Static	Rotating	Static	Continuous Slit Scan	Rotating during exposure	Static
X-Ray Tube Motion	Continuous	Step-and-Shoot	Continuous	Step-and-Shoot	Continuous	Continuous	Continuous
Detector to Center of Rotation Distance (cm)	4	4	0	2	-40	4.37	4.7
Angular Range	15	25	15	40	11	30	50
Number of Projections	15	9	15	13	21	15	25
Scan Time (sec)	4	7	3.7	12	3 – 10	20	25
Reconstruction Method	Modified FBP	Iterative	FBP	Iterative with Total Variation Regularization	Iterative	Iterative	FBP
Development Stage	Commercial System**	Commercial System	Commercial System	Commercial System**	Prototype	Prototype	Commercial System

***Currently not approved for clinical use in the U.S. by the Food and Drug Administration (FDA)*

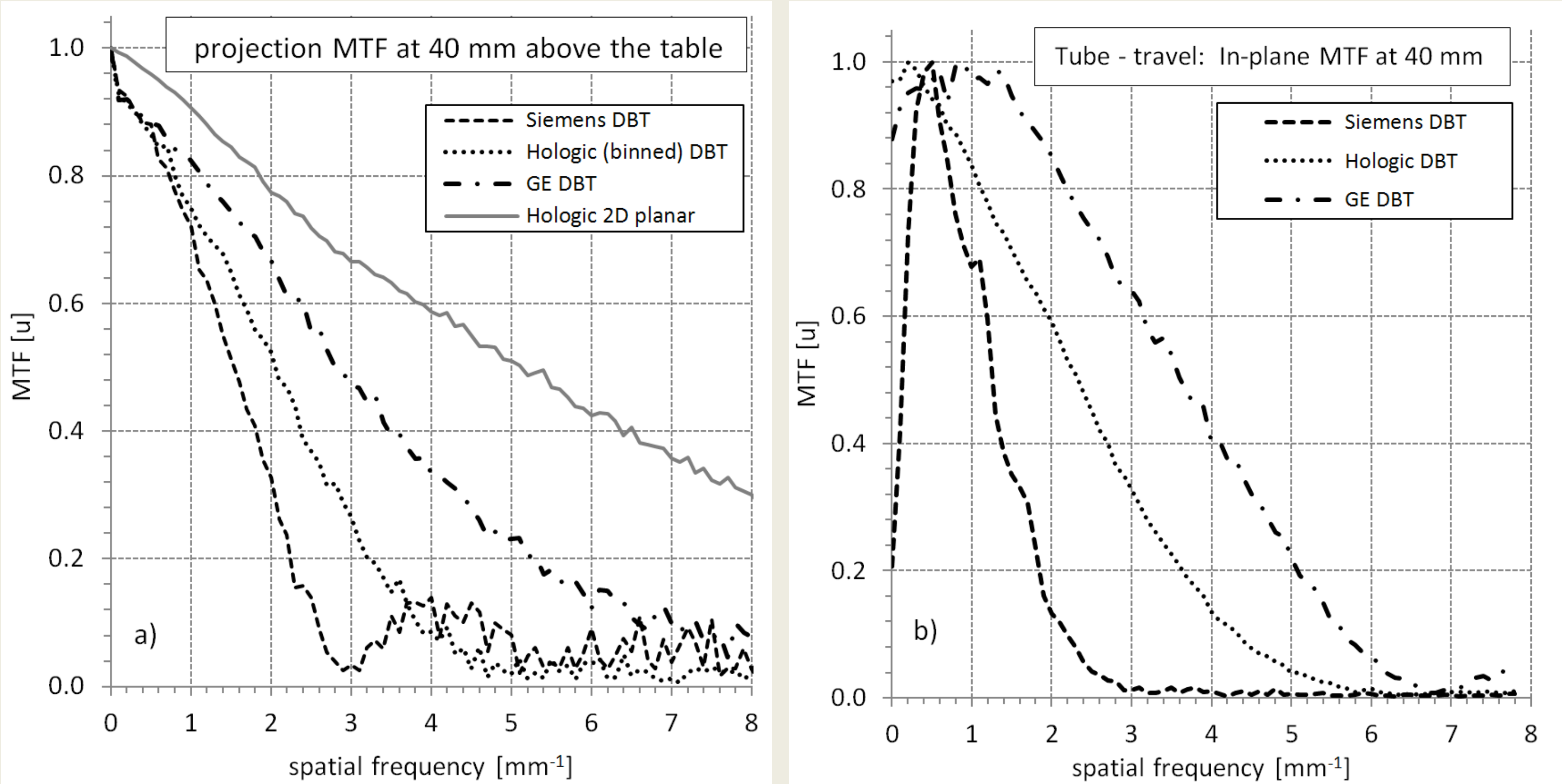

http://2014.bhpa.eu/wp-content/uploads/formidable/Marshall_Nicolas.pdf

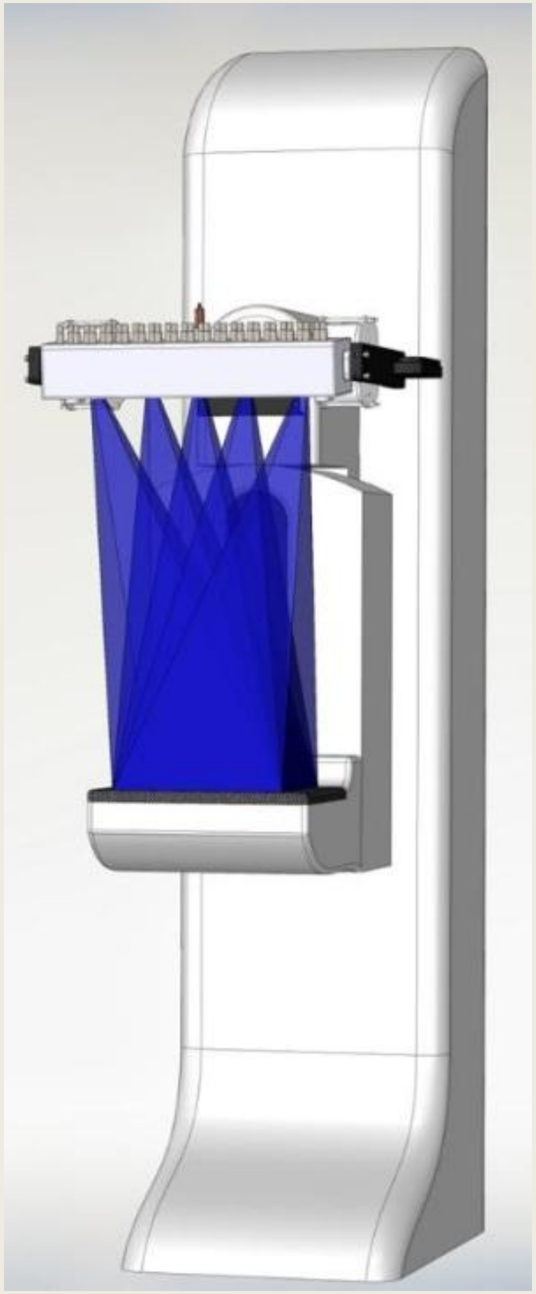

Courtesy of Otto Zhou, Applied Nanotechnology Laboratory, University of North Carolina at Chapel Hill

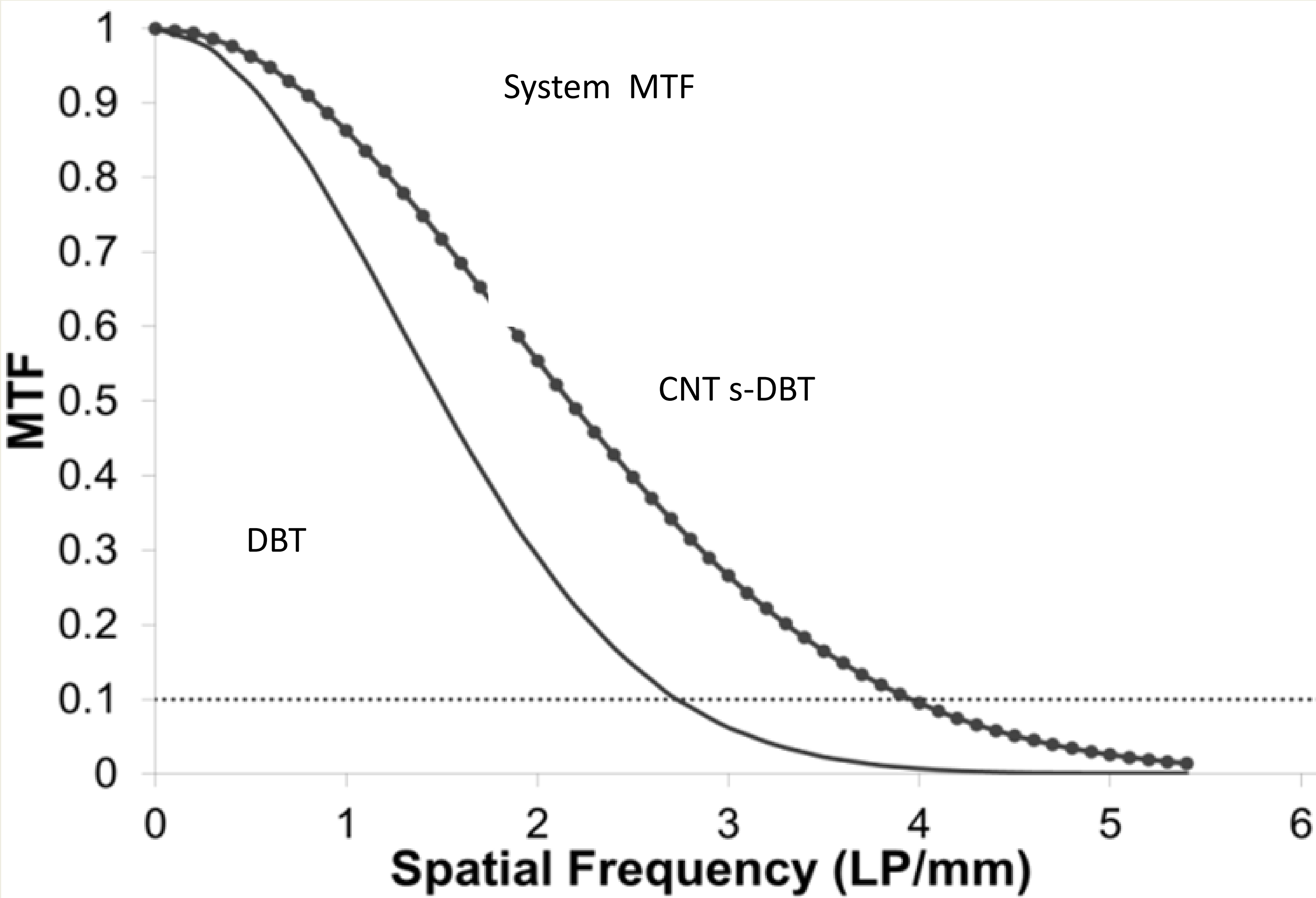

~30% increase in system resolution for standard 15 degree, 15 view scan

A. Tucker, et al, Med Phys 2012

Micro-calcification visibility

S-DBT reconstructions above

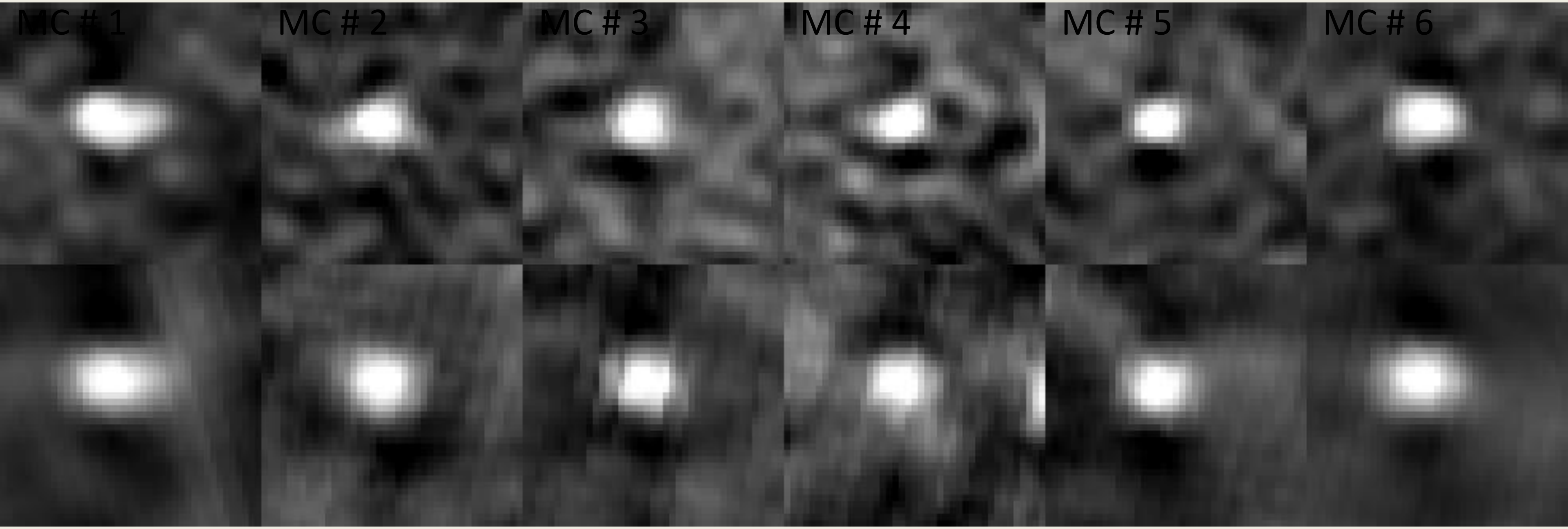

Continuous motion DBT reconstructions

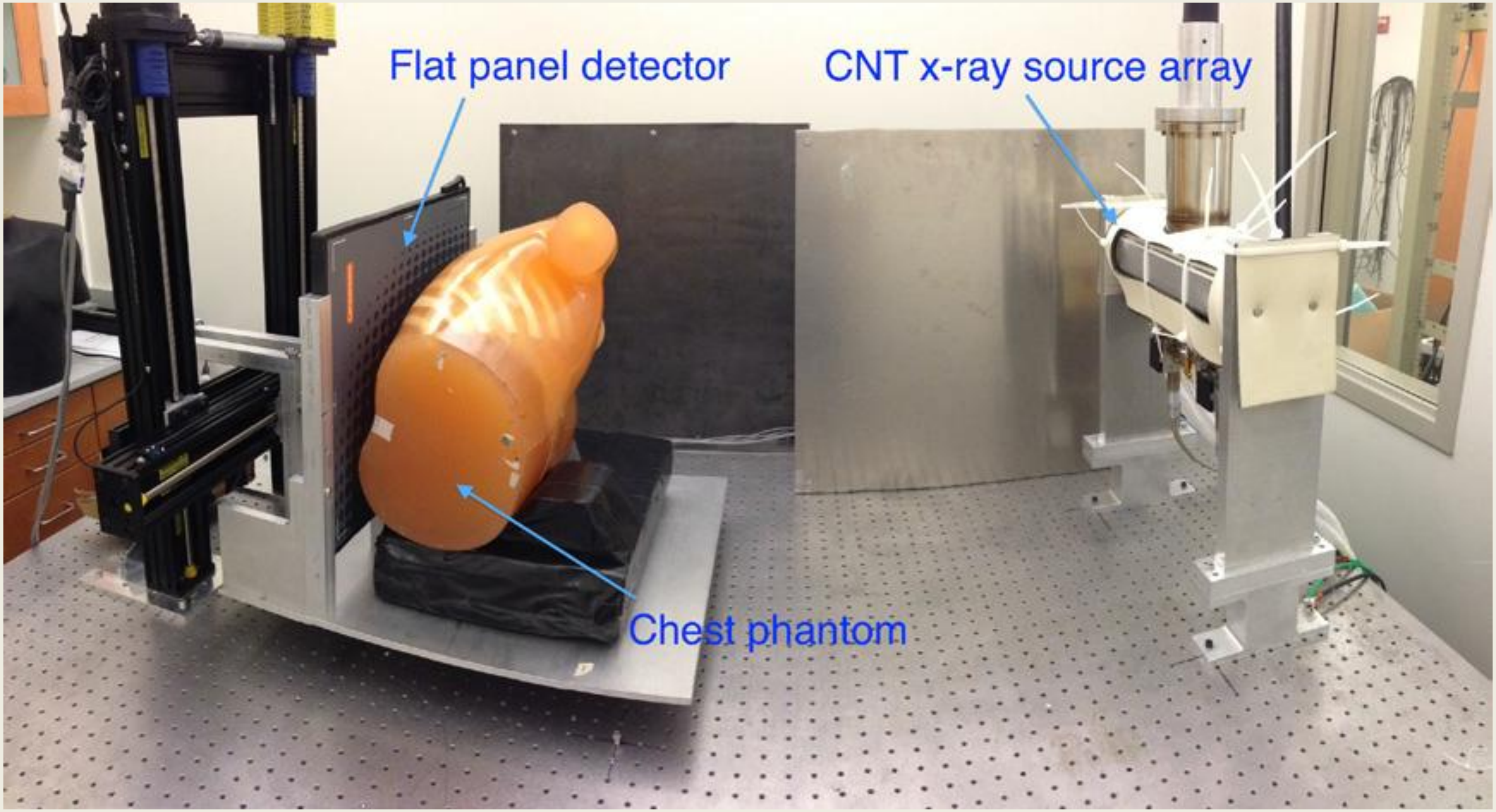

Shan et al, Phys. Med. Biol. 60, 81-101, 2015

System	Fuji AMULET Innovality	GE Essential	Hologic Selenia Dimensions	IMS Giotto TOMO	Philips MicroDose	Planmed Nuance Excel DBT	Siemens MAMMOMAT Inspiration
Detector Type	Full field - Direct (a-Se) (Hexagonal pixels)	Full field - Indirect	Full field - Direct (a-Se)	Full field - Direct (a-Se)	Linear Slit Scan – Spectral Photon Counting (Si)	Full field - Direct (a-Se)	Full field - Direct (a-Se)
Detector Motion	Static	Static	Rotating	Static	Continuous Slit Scan	Rotating during exposure	Static
X-Ray Tube Motion	Continuous	Step-and-Shoot	Continuous	Step-and-Shoot	Continuous	Continuous	Continuous
Detector to Center of Rotation Distance (cm)	4	4	0	2	-40	4.37	4.7
Angular Range	15	25	15	40	11	30	50
Number of Projections	15	9	15	13	21	15	25
Scan Time (sec)	4	7	3.7	12	3 – 10	20	25
Reconstruction Method	Modified FBP	Iterative	FBP	Iterative with Total Variation Regularization	Iterative	Iterative	FBP
Development Stage	Commercial System**	Commercial System	Commercial System	Commercial System**	Prototype	Prototype	Commercial System

***Currently not approved for clinical use in the U.S. by the Food and Drug Administration (FDA)*

Total Angular Range
Oblique Incidence

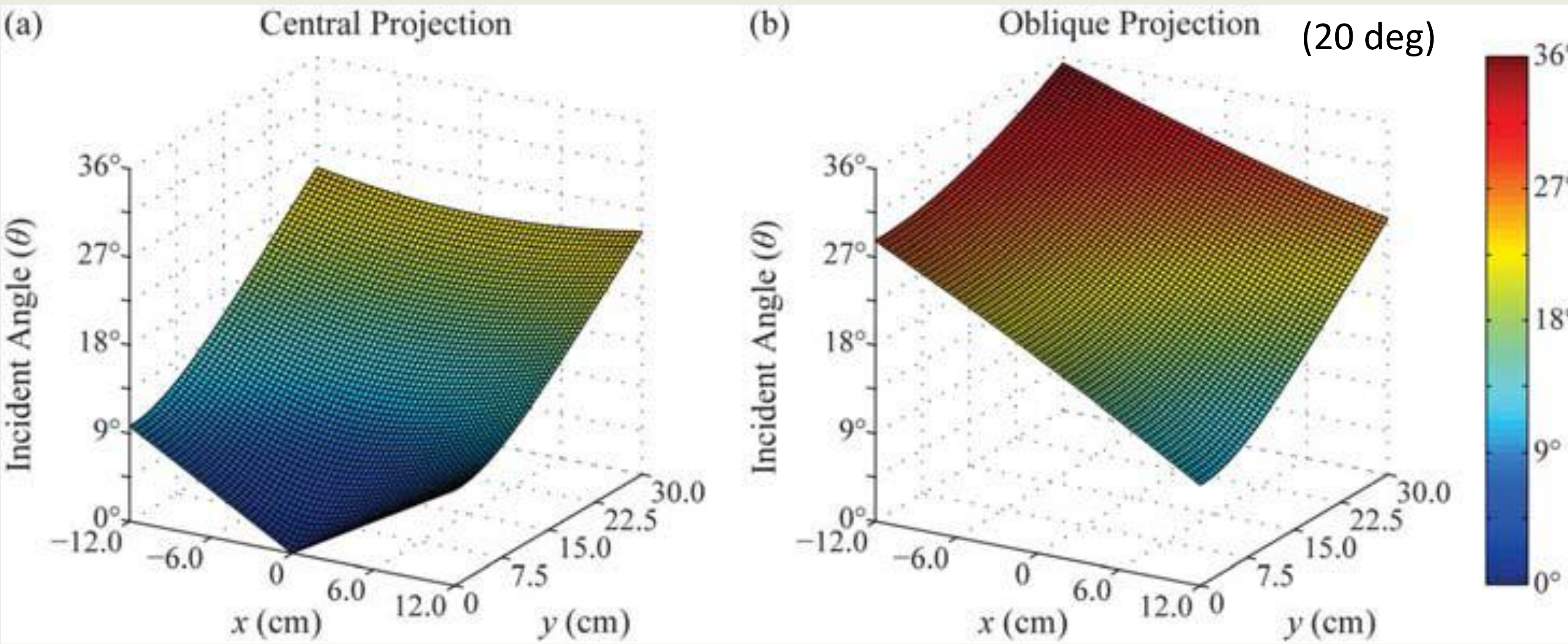

Acciavatti and Maidment, Medical Physics, 38(11), 2011

Oblique Incidence – Direct Detectors

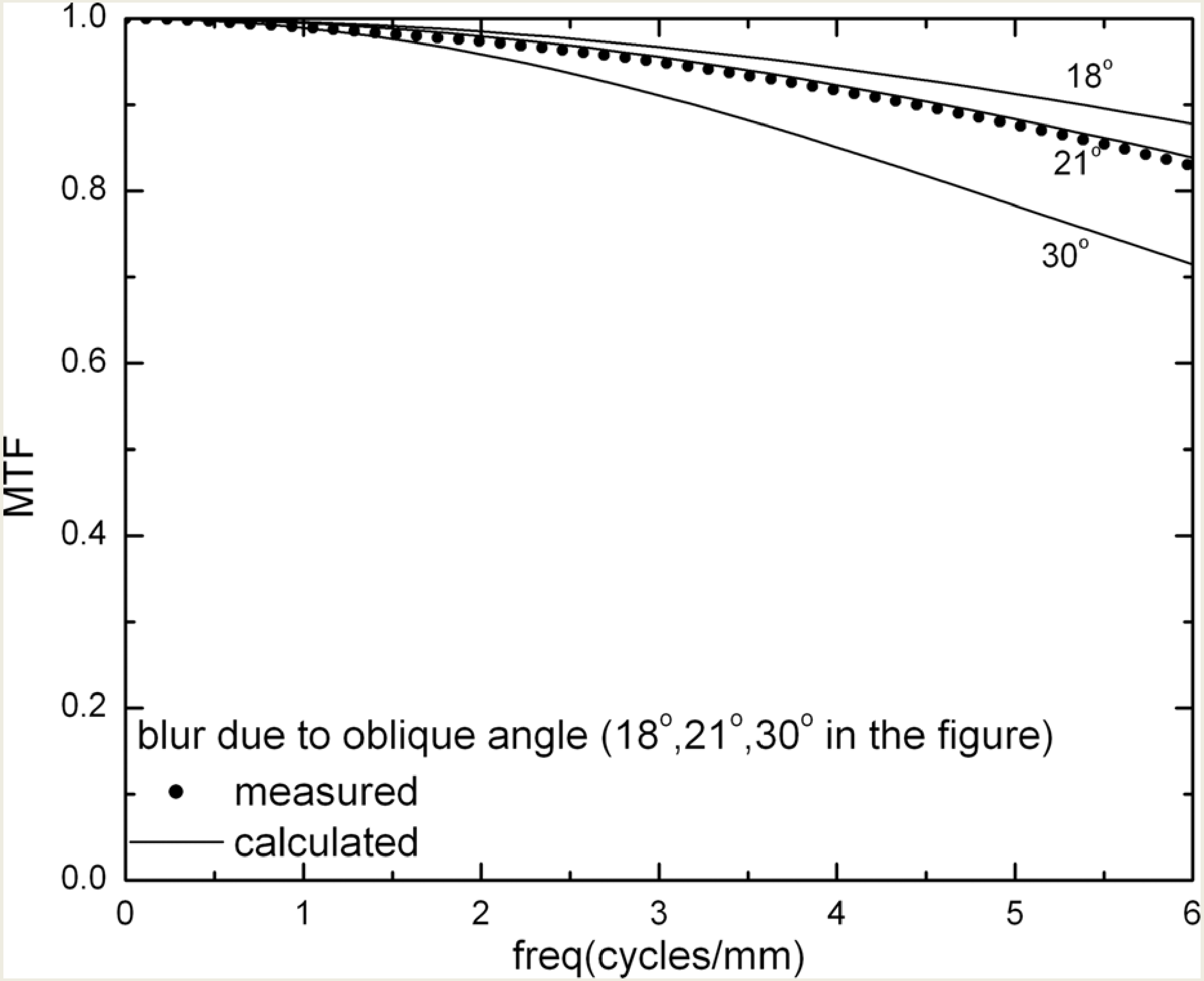

Zhao and Zhao, Medical Physics, 35(5), 2008

Oblique Incidence – Indirect Detectors

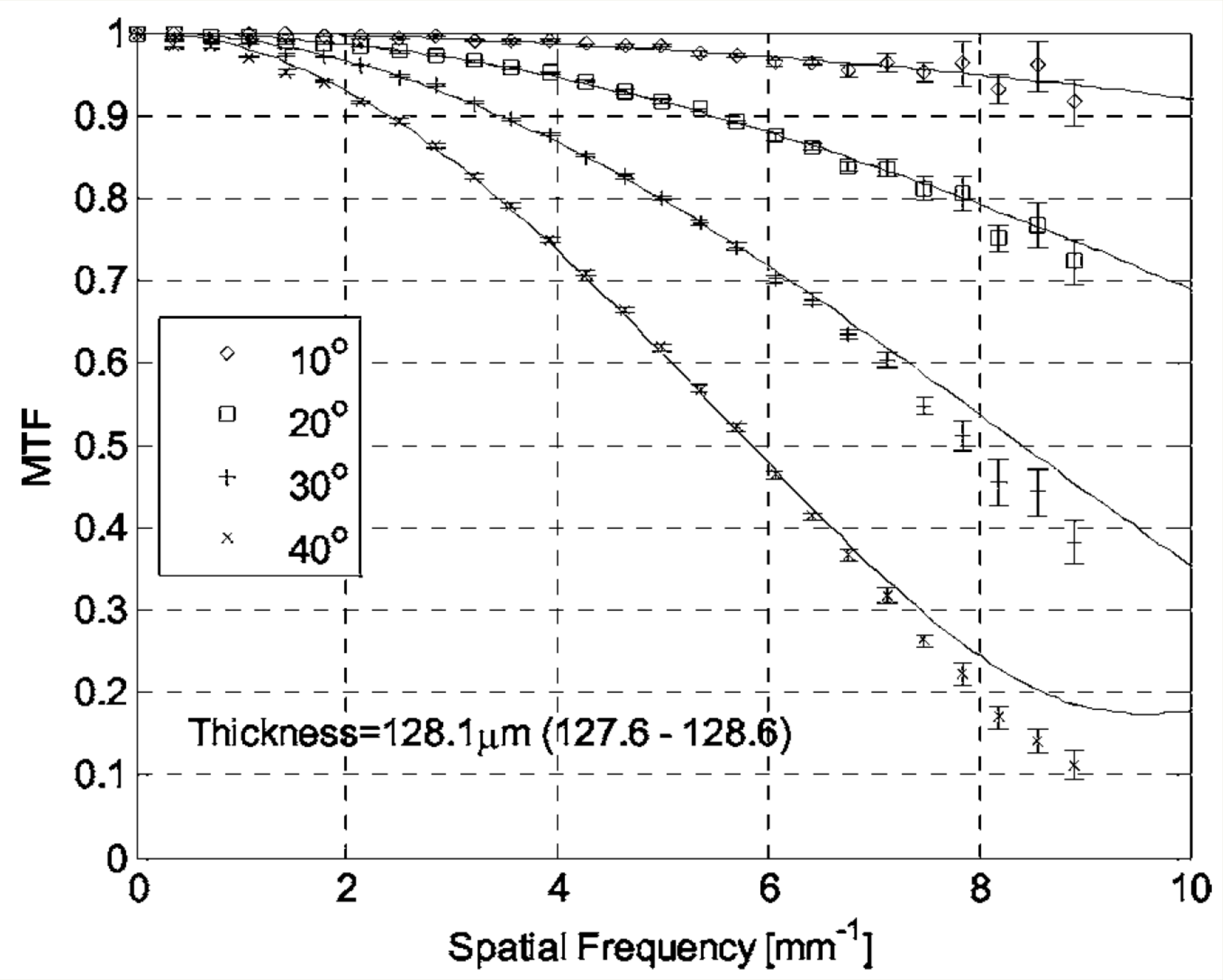

Mainprize et al, Medical Physics, 33(9), 2006

Acquisition Geometry

Radiography:

1 position, 1 shot

CT:

full revolution, 1000 shots

Tomosynthesis:

???

Acquisition Geometry Optimization

Acquisition parameters:

- Angular range
- Number of projection angles

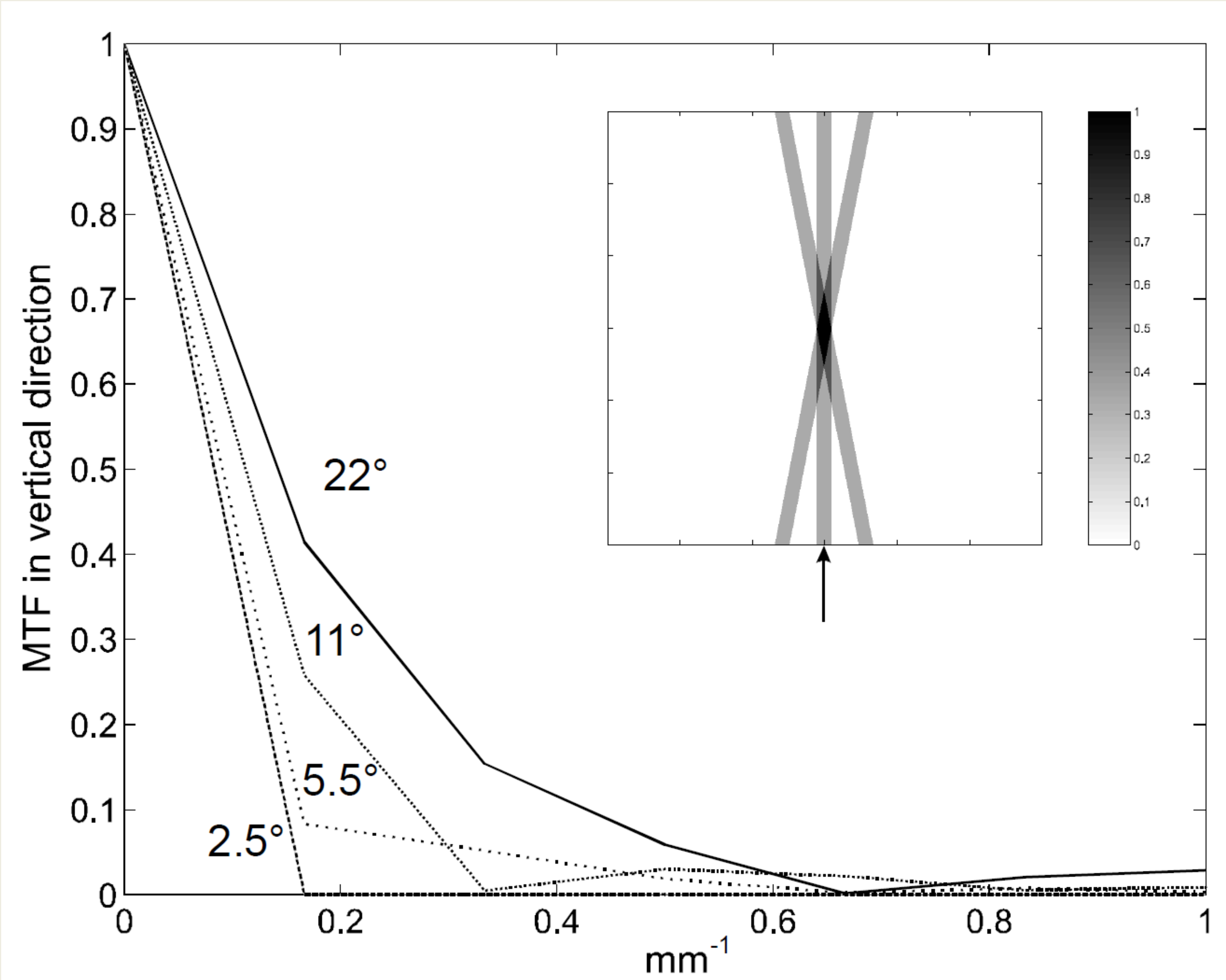

Maidment et al, Proceedings of SPIE, 5745, 2005

Artifact Spread Function

$$ASF(z) = \frac{I_s(z) - I_{BG}(z)}{I_s(z_0) - I_{BG}(z_0)}$$

Wu et al, Medical Physics, 31(9), 2004

Angular Range

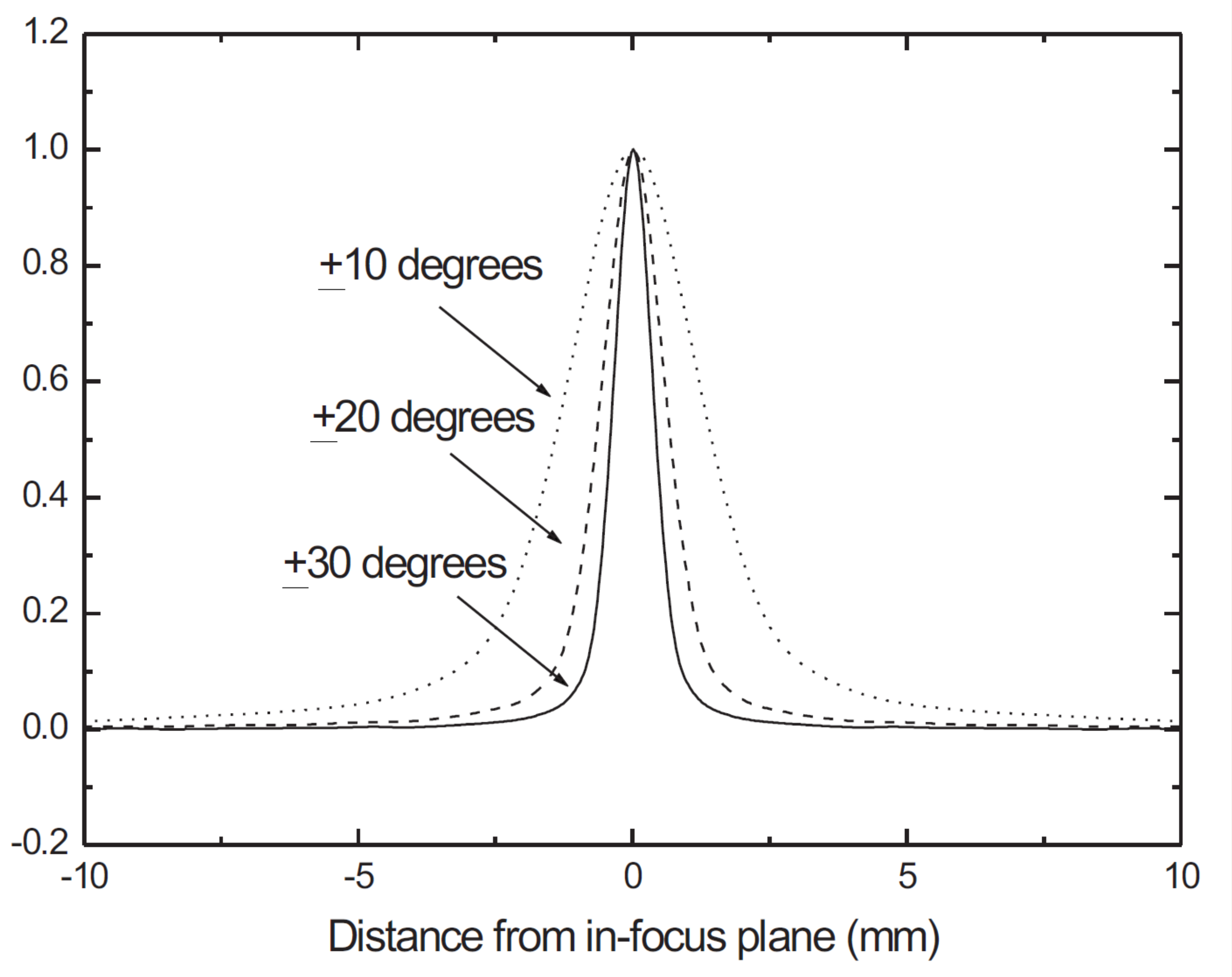

Hu et al, Medical Physics, 35(12), 2008

Image Acquisition Optimization

Computer simulated breast volume and lesions

63 different acquisition geometries

In-plane quality and vertical resolution

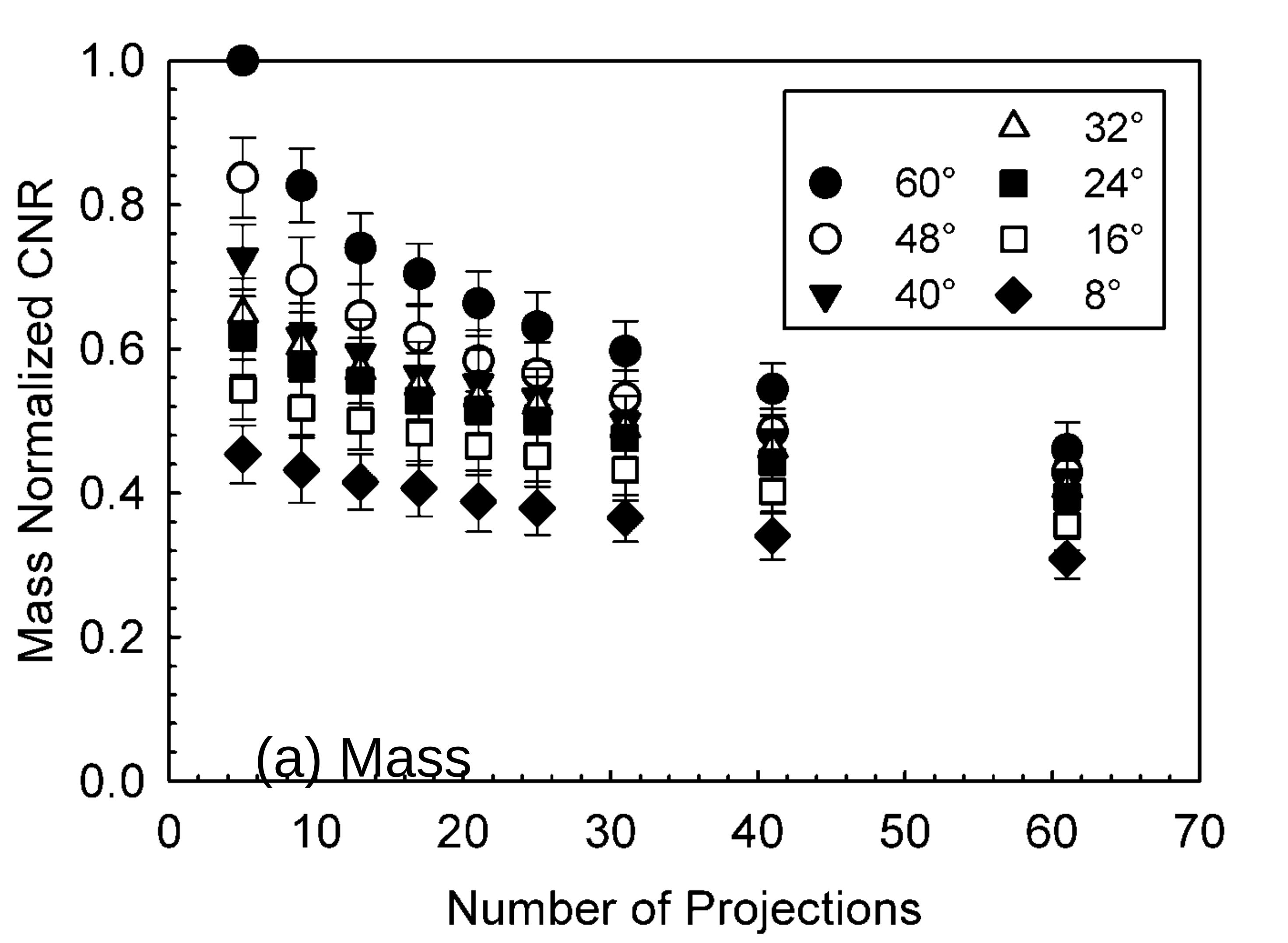

Masses: Increased in-plane quality with increased angular range, fewer projections

Sechopoulos and Ghetti, Medical Physics 2009, 36, 1199-1207.

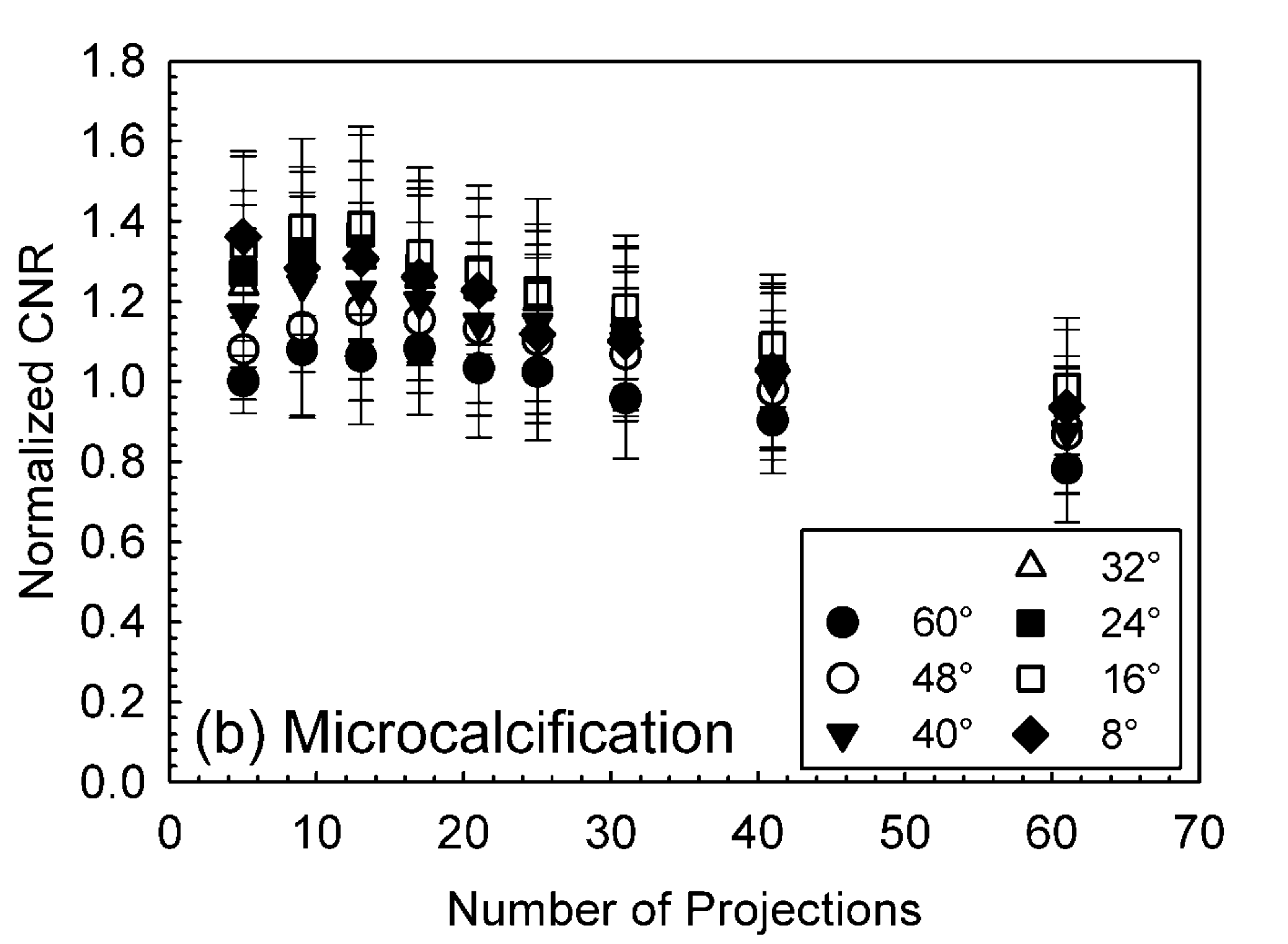

μCa: Increased in-plane quality with decreased angular range (→ mammo), fewer projections (small effect)

Sechopoulos and Ghetti, Medical Physics 2009, 36, 1199-1207.

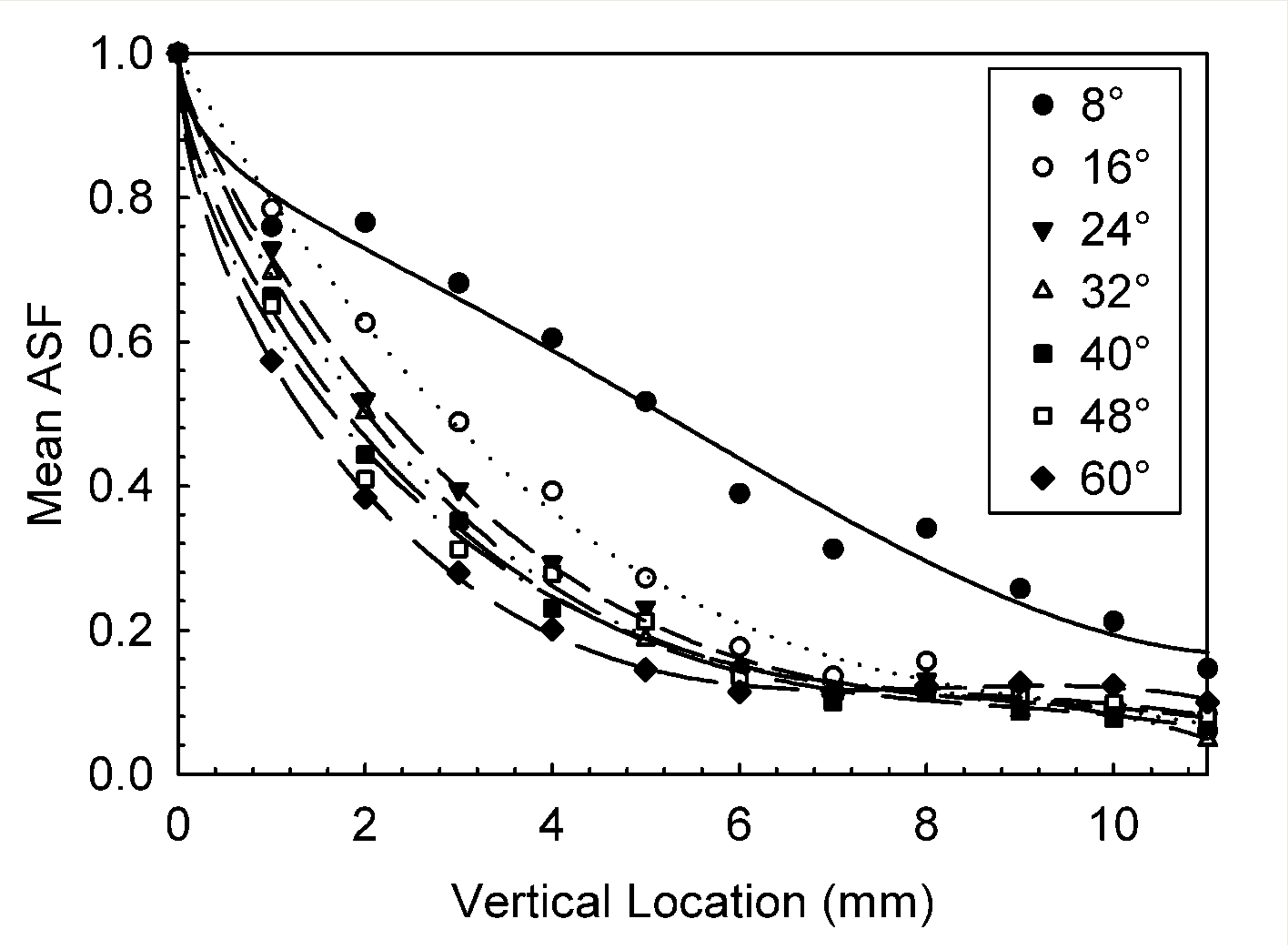

Vertical resolution increases with angular range

Sechopoulos and Ghetti, Medical Physics 2009, 36, 1199-1207.

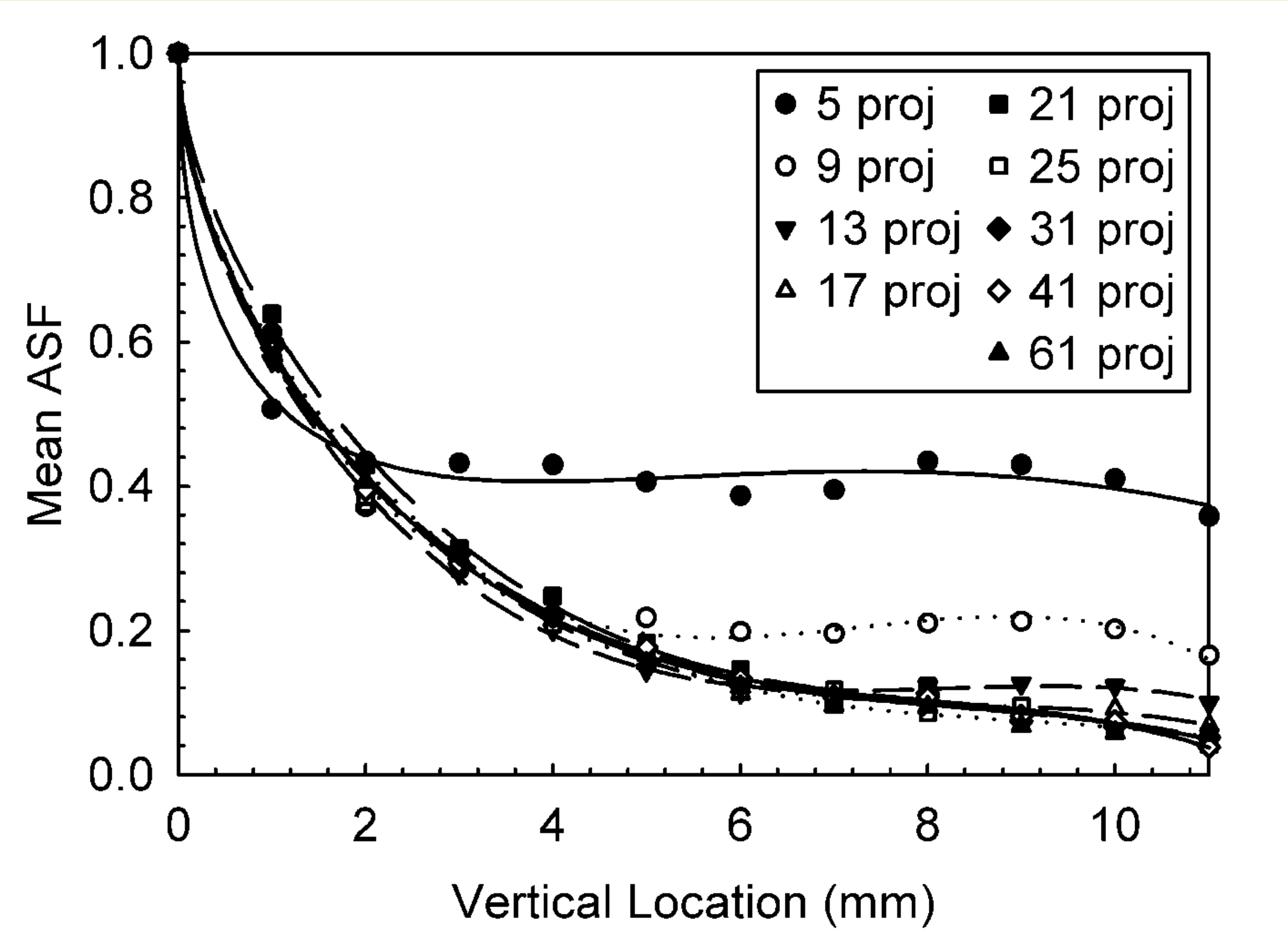

Threshold number of projections to improve vertical resolution

Sechopoulos and Ghetti, Medical Physics 2009, 36, 1199-1207.

Acquisition Geometry and Vertical Resolution

Angular range	Number of projections beyond which ASF improvement is minimal
8[a]	5
16[a]	5
24	9
32	9
40	9
48	13
60	13

[a]Substantial artifacts due to narrow angular range

Sechopoulos and Ghetti, Medical Physics 2009, 36, 1199-1207.

Subsequent studies:

Threshold number of projections for each angular range was confirmed by others

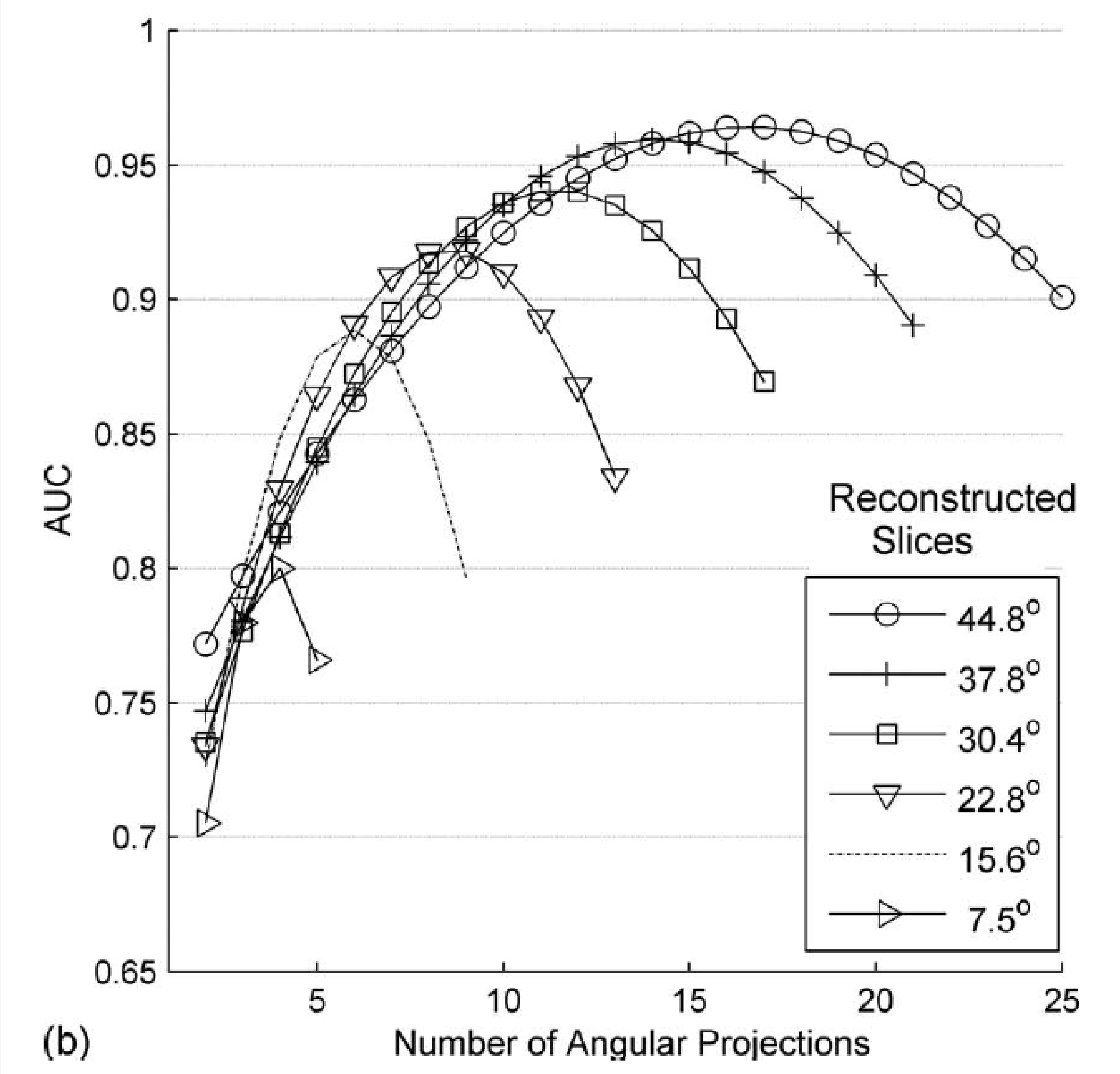

Tucker et al, Proc. SPIE 8313, 831307-831310 (2012)
A. S. Chawla et al, Med. Phys. 36, 4859-4869 (2009)
I. Reiser and R. M. Nishikawa, Med. Phys. 37, 1591-1600 (2010)
Goodsitt et al, Phys. Med. Biol. 59 (2014) 5883

Chest Tomosynthesis

No gain in increase in projections beyond a certain number

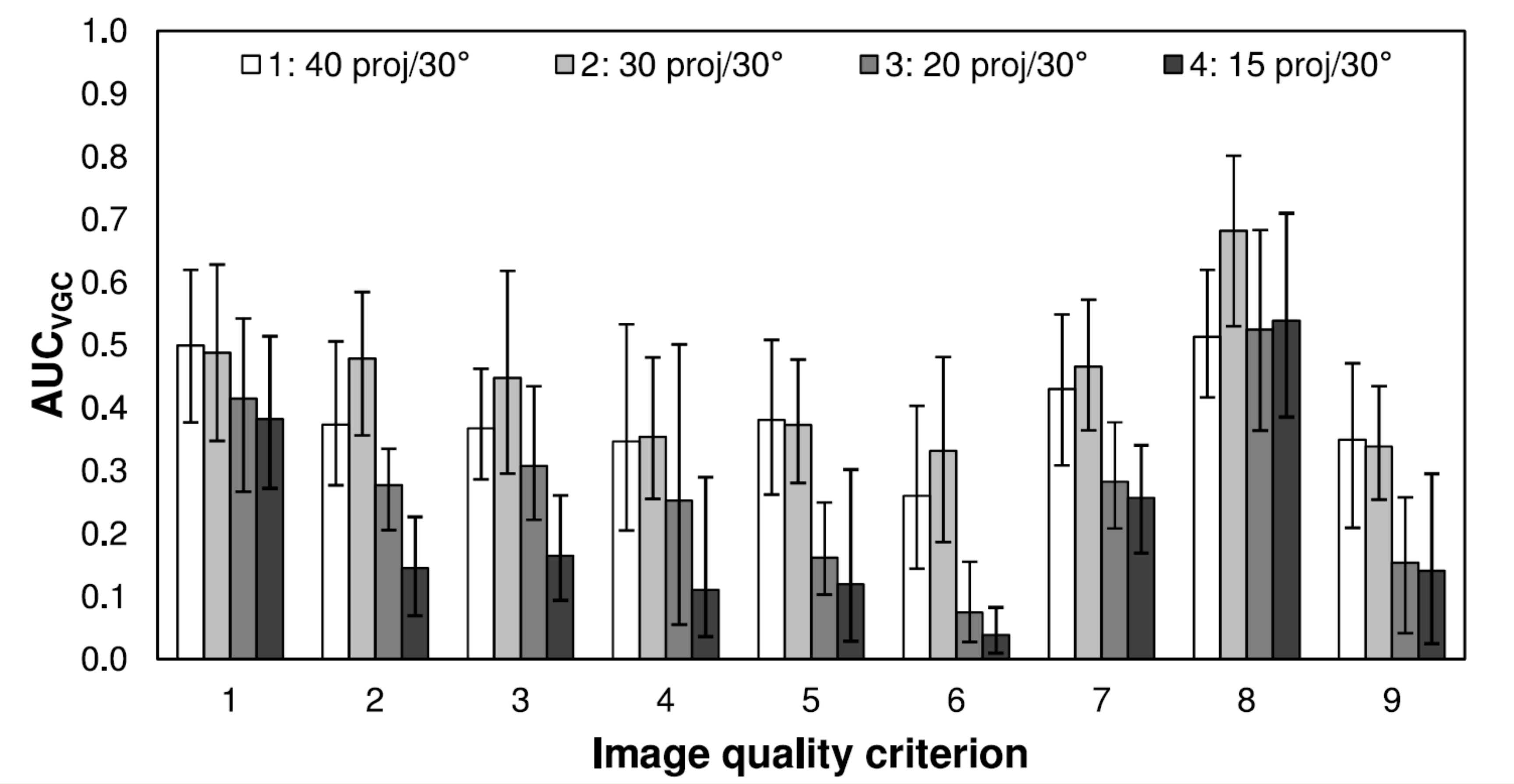

Söderman et al, Medical Physics, Vol. 42, No. 3, 2015

Acquisition Geometry

↑ angular range → ↑ vertical resolution

↑ # of projections → ↑ vertical resolution up to a point

Have to consider:

scan time

anatomy

detector size

ACQUISITION TECHNIQUE

Tube Voltage Selection

Multiple studies reported higher kV than mammo optimal for tomo

Ren et al, Proceedings of SPIE 5745, 550–561 (2005).
Zhao et al, Proceedings of SPIE 5745, 1272–1281 (2005).
Wu et al, Proceedings of SPIE 6142, 61425E (2006)

One study reported lower energies beneficial

Glick and Gong, Proceedings of SPIE 6142, 61421L–61429L (2006).

Technique and Dosimetric Characterization of a Clinical System

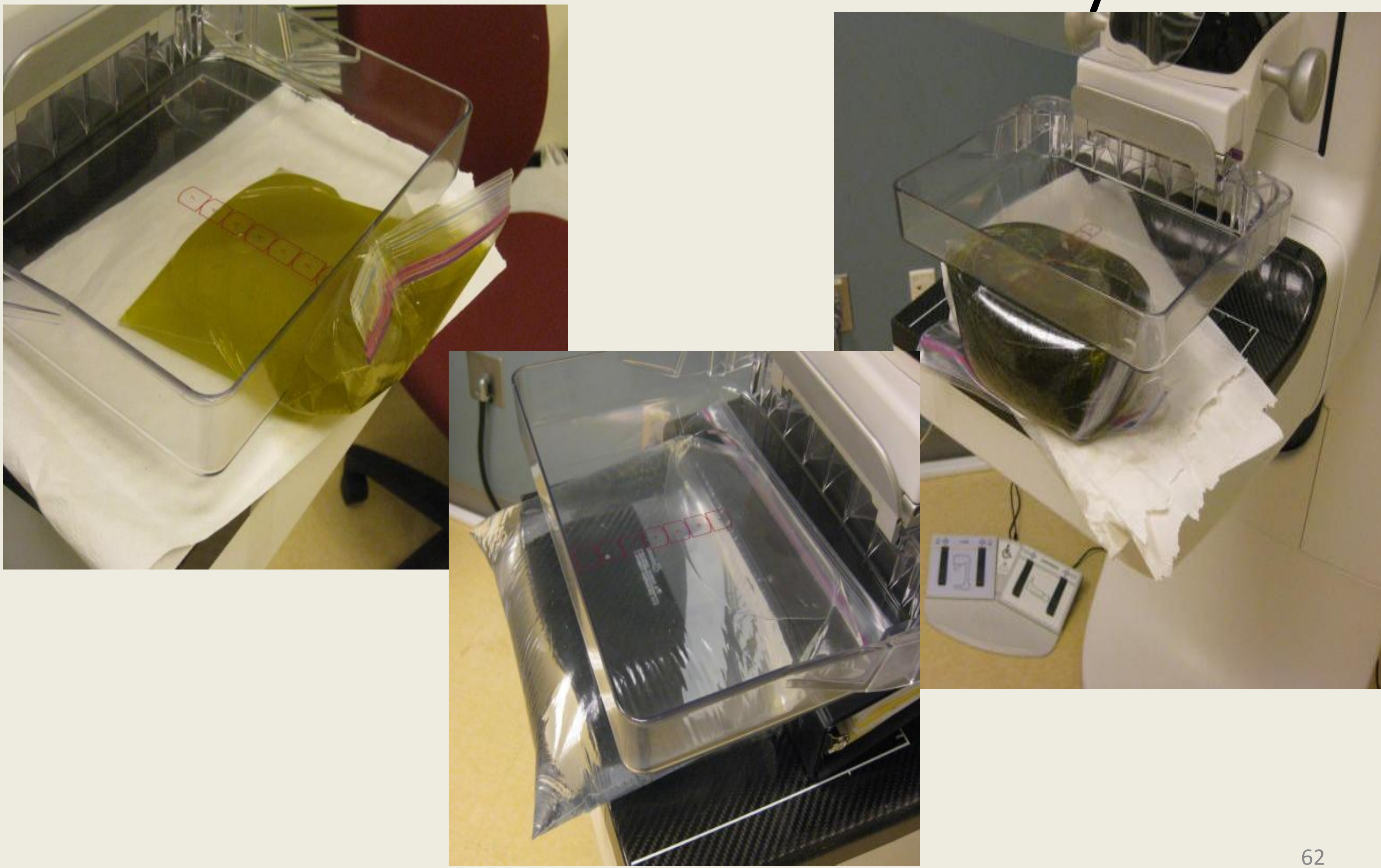

Feng and Sechopoulos, Radiology, 2012; 263(3): 35-42

	Tomosynthesis			Mammography		
Breast Thickness (cm)	**Filter**	**Tube Voltage (kVp)**	**1st HVL (mm Al)**	**Filter**	**Tube Voltage (kVp)**	**1st HVL (mm Al)**
2	Al	26	0.441	Rh	25	0.453
3	Al	28	0.476	Rh	26	0.494
4	Al	29	0.490	Rh	28	0.517
5	Al	31	0.541	Rh	29	0.551
6	Al	33	0.572	Rh	31	0.567
7	Al	35	0.600	Ag	30	0.586
8	Al	38	0.660	Ag	32	0.611

Feng and Sechopoulos, Radiology, 2012; 263(3): 35-42

TOMOSYNTHESIS RECONSTRUCTION

System	Fuji AMULET Innovality	GE Essential	Hologic Selenia Dimensions	IMS Giotto TOMO	Philips MicroDose	Planmed Nuance Excel DBT	Siemens MAMMOMAT Inspiration
Detector Type	Full field - Direct (a-Se) (Hexagonal pixels)	Full field - Indirect	Full field - Direct (a-Se)	Full field - Direct (a-Se)	Linear Slit Scan – Spectral Photon Counting (Si)	Full field - Direct (a-Se)	Full field - Direct (a-Se)
Detector Motion	Static	Static	Rotating	Static	Continuous Slit Scan	Rotating during exposure	Static
X-Ray Tube Motion	Continuous	Step-and-Shoot	Continuous	Step-and-Shoot	Continuous	Continuous	Continuous
Detector to Center of Rotation Distance (cm)	4	4	0	2	-40	4.37	4.7
Angular Range	15	25	15	40	11	30	50
Number of Projections	15	9	15	13	21	15	25
Scan Time (sec)	4	7	3.7	12	3 – 10	20	25
Reconstruction Method	Modified FBP	Iterative	FBP	Iterative with Total Variation Regularization	Iterative	Iterative	FBP
Development Stage	Commercial System**	Commercial System	Commercial System	Commercial System**	Prototype	Prototype	Commercial System

***Currently not approved for clinical use in the U.S. by the Food and Drug Administration (FDA)*

(really) Filtered Back Projection

$$H_{filter}\,(\omega_y, \omega_z) = H_{spectrum}(\omega_y) \cdot H_{profile}(\omega_z) \cdot H_{inverse}(\omega_y, \omega_z)$$

$H_{spectrum}(\omega_y)$: Hanning filter to control noise

$H_{inverse}(\omega_y, \omega_z)$: Ramp-type filter

$H_{profile}(\omega_z)$: Slice profile filter for constant depth resolution

Mertelmeier et al, SPIE 6142, 61420F (2006)

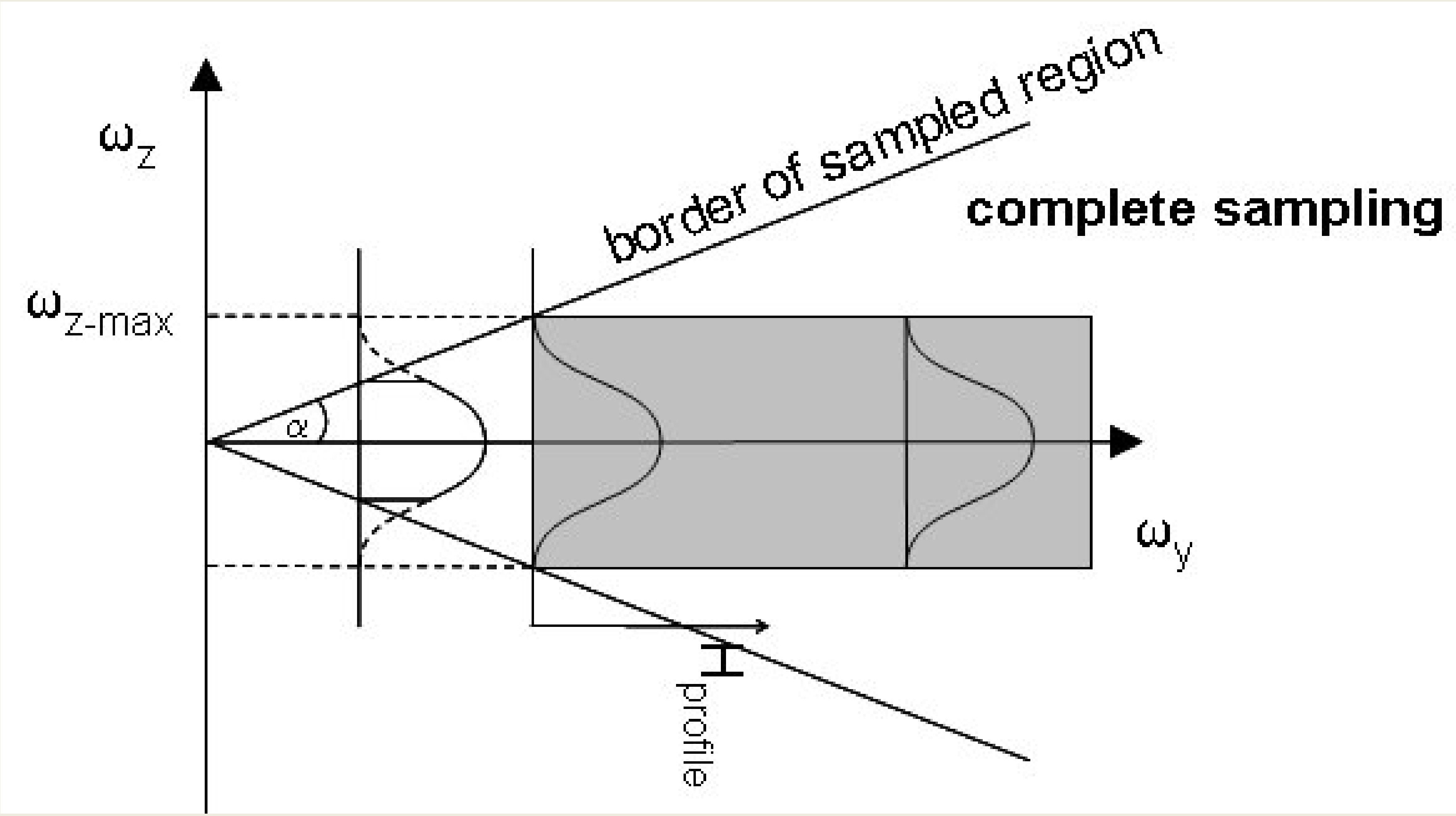

Mertelmeier et al, SPIE 6142, 61420F (2006)

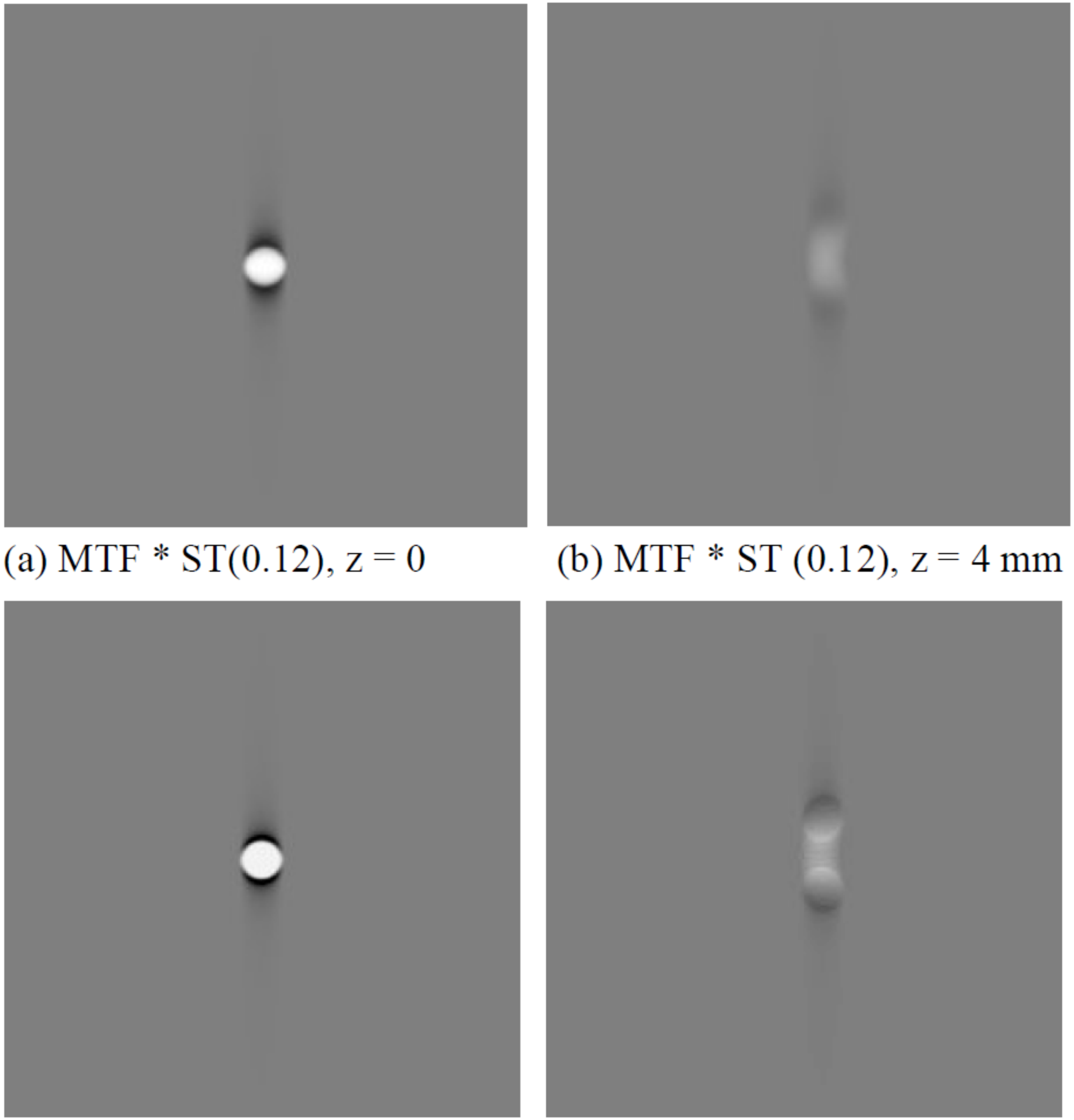

(a) MTF * ST(0.12), z = 0 (b) MTF * ST (0.12), z = 4 mm

(e) MTF, z = 0 (f) MTF, z = 4 mm

Mertelmeier et al, SPIE 6142, 61420F (2006)

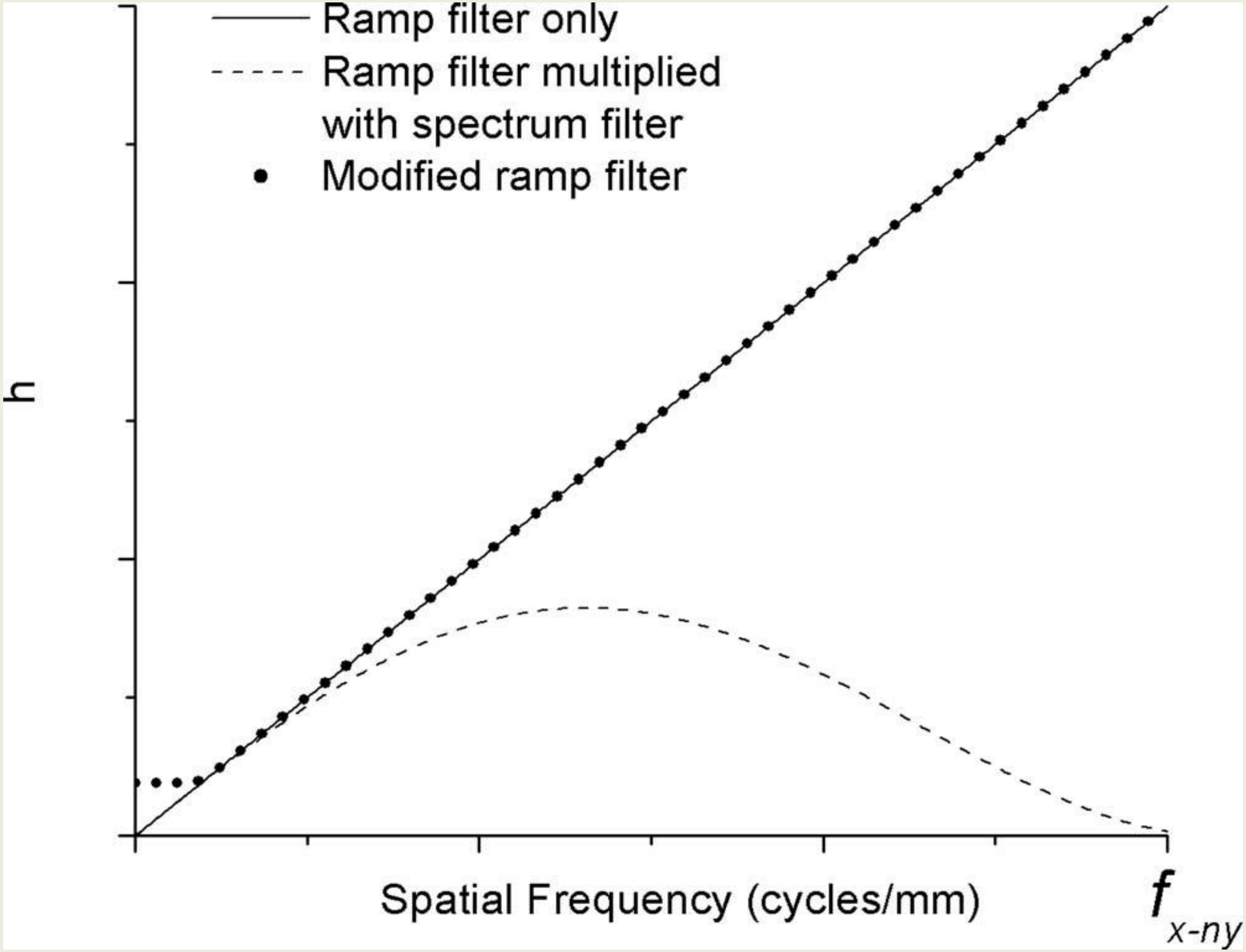

Zhou et al, Medical Physics, Vol. 34, No. 3, March 2007

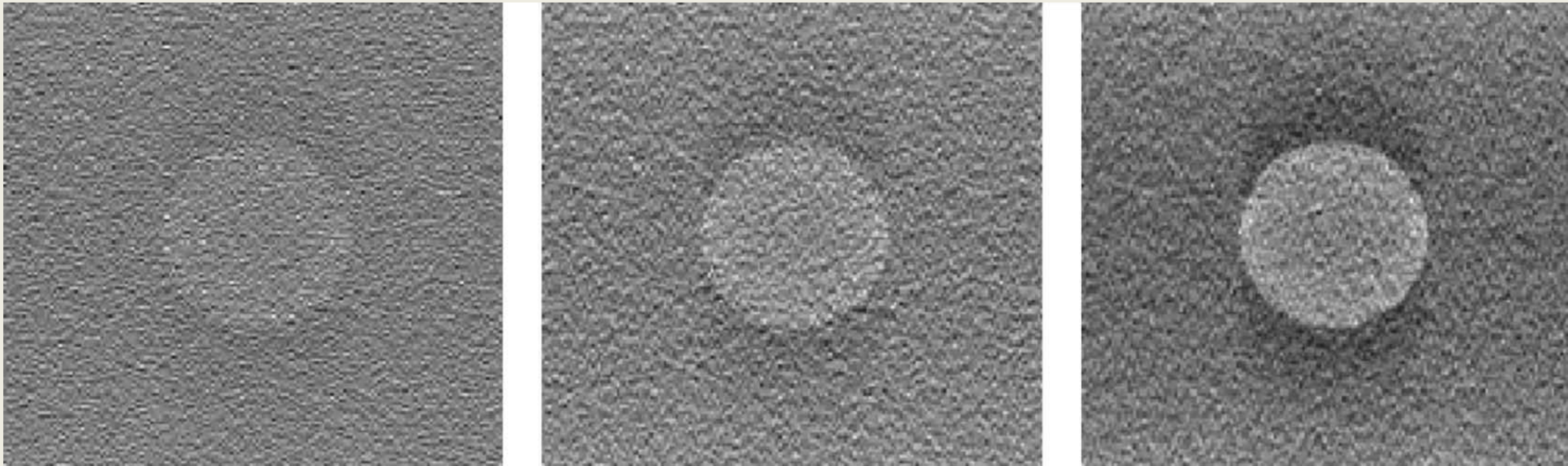

FBP w/ramp only | + Hanning & thickness filter | + Hanning & thickness filter 2

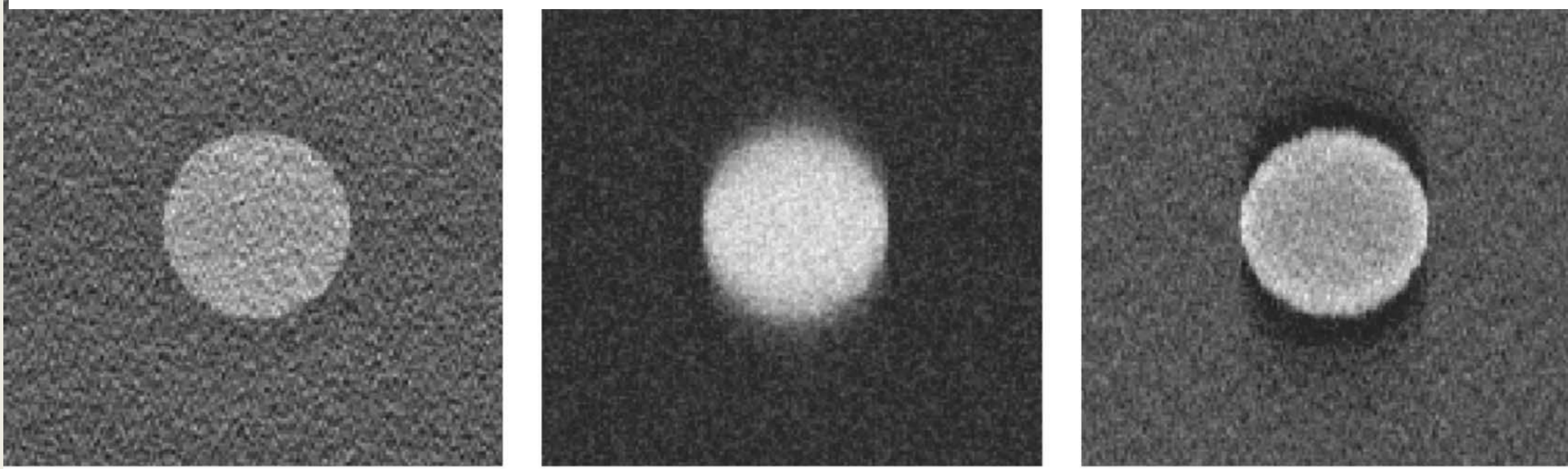

+ modified ramp | SBP | Iterative

Zhou et al, Medical Physics, Vol. 34, No. 3, March 2007

Iterative Reconstruction Methods

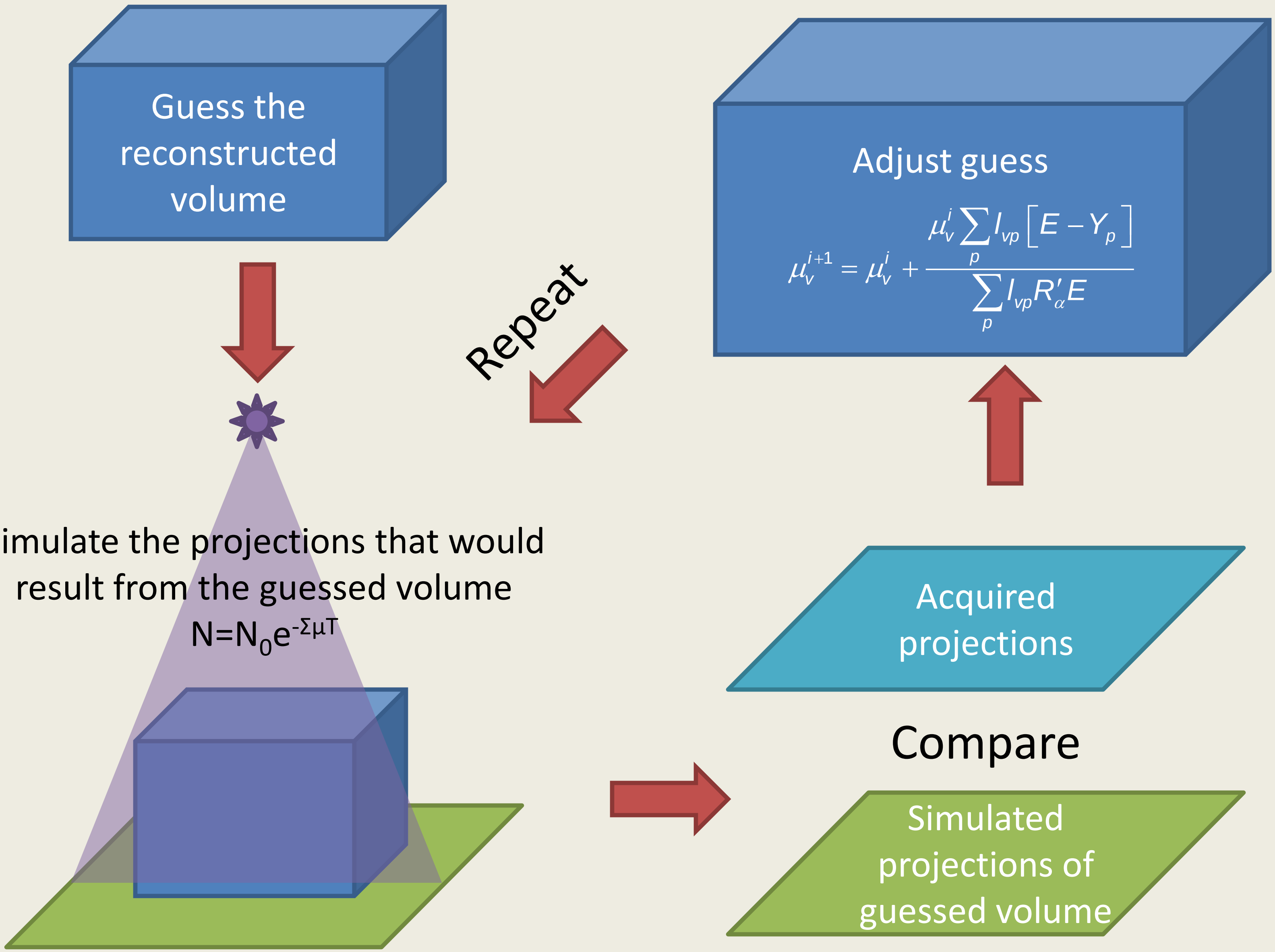

Other Reconstruction Methods

SIRT

SART

ART

MLEM

TVR

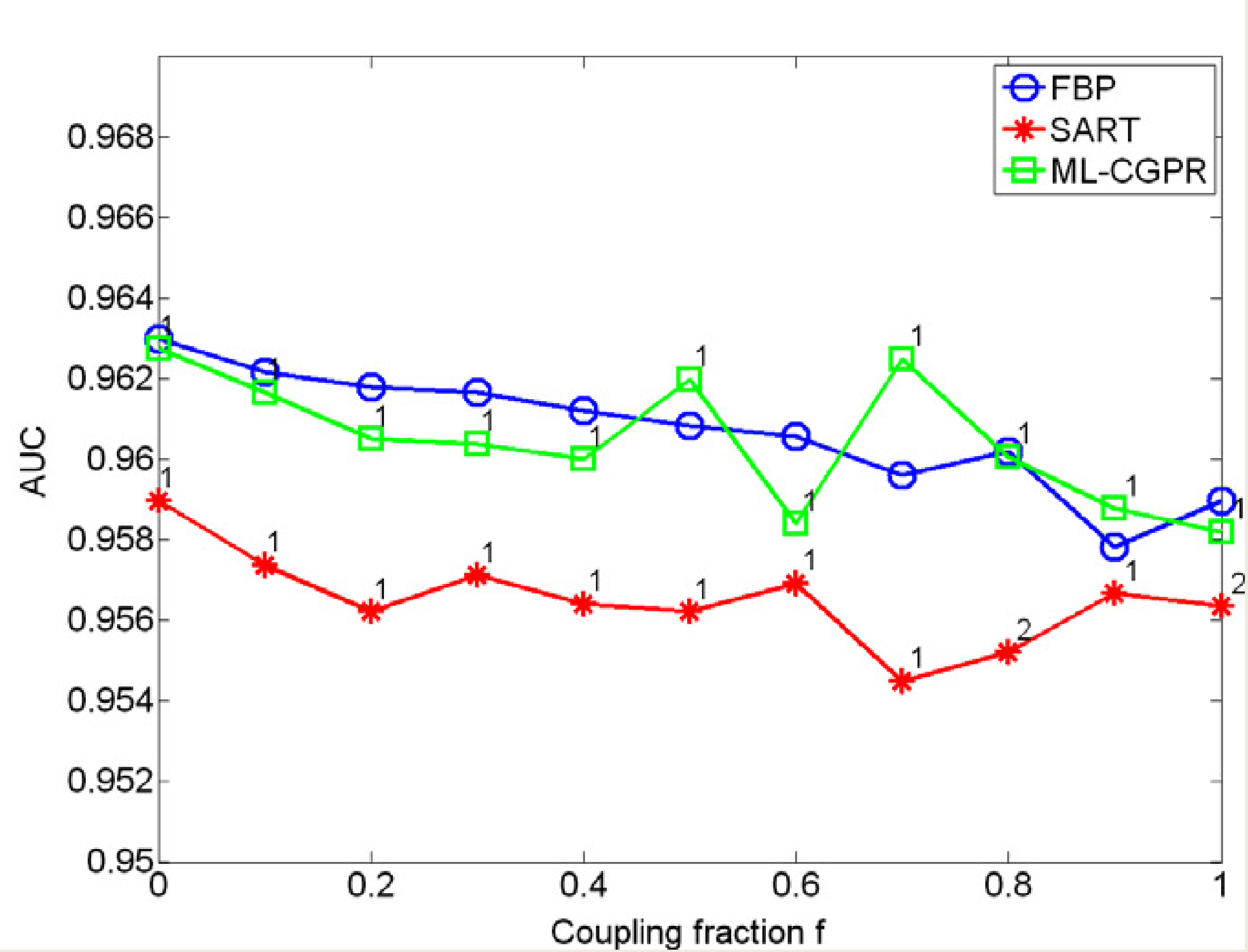

Van de Sompel et al, Medical Image Analysis 2011, 15, 53–70

Comparison of Reconstructions

Optimal acquisition might differ for different recons

Challenging for a single group to implement and optimize all recons

Most appropriate metric(s)?

Tomosynthesis Reconstruction

Mono-energetic Assumption

- Or constant spectral beam
- No explicit definition
- Same case with CT reconstruction algorithms

Standard Tomosynthesis Spectrum

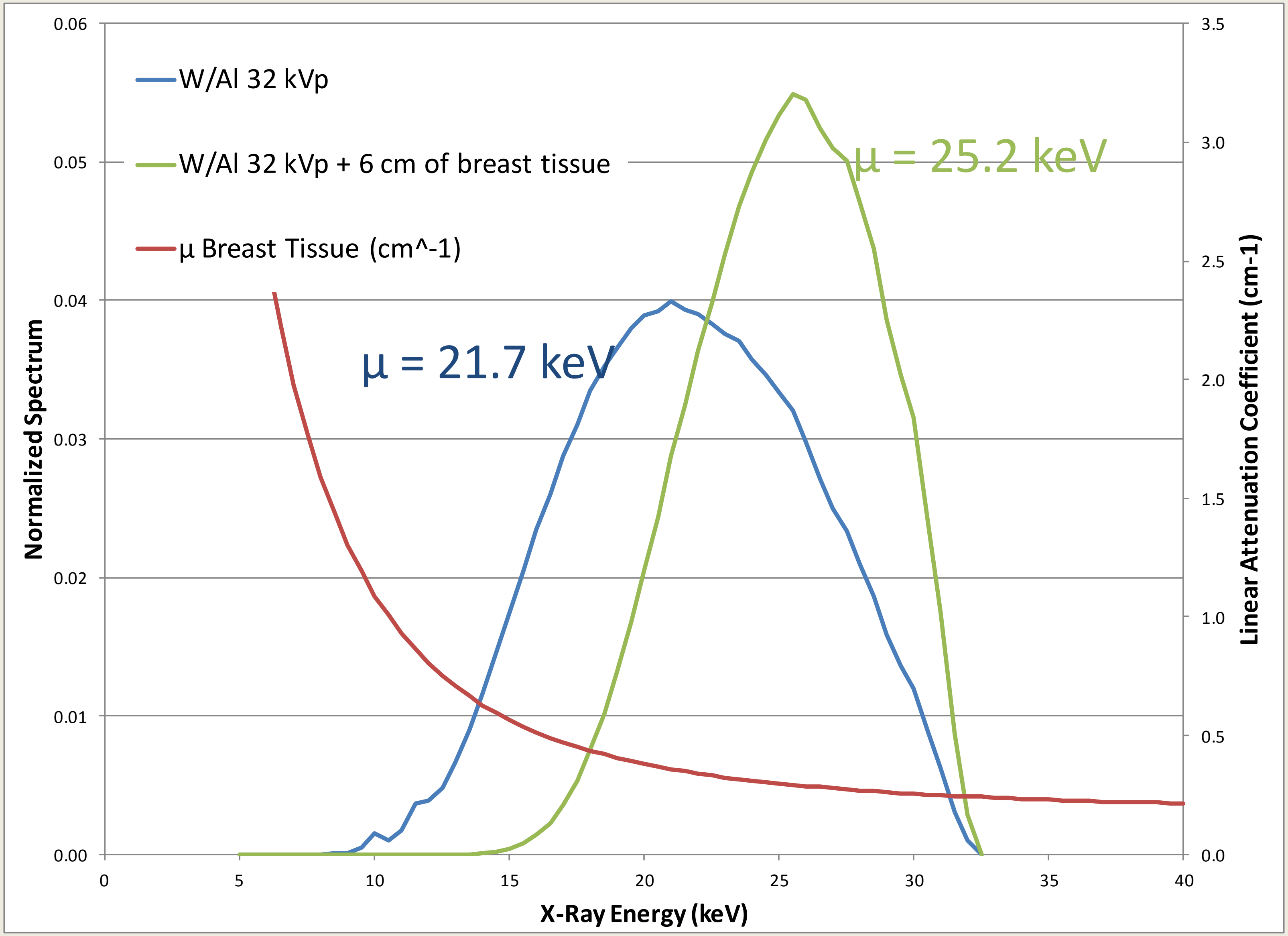

Breast Tomosynthesis Acquisition Model

$$b_i^\theta = \int_\varepsilon \psi(\varepsilon) e^{-\int_{L_{\theta,i}} \mu(\vec{x},\varepsilon) dl} d\varepsilon + \eta$$

b_i^θ → acquired signal at pixel i for projection θ

$\psi(\varepsilon)$ → incident energy fluence at energy ε

$\mu(\vec{x},\varepsilon)$ → linear attenuation coefficient of voxel $\vec{x}$ at energy ε

$L_{\theta,i}$ → line from source to pixel i for projection θ

Breast Tomosynthesis Acquisition Model

Minimize Poisson likelihood :

$$\boldsymbol{X}_{MLE} = \arg\min\left\{\sum -L_{\theta}\left(\boldsymbol{X}\right)\right\}$$

$$-L_{\theta}\left(\boldsymbol{X}\right) = \sum\left(\overline{b_{\theta}^{i}} + \overline{\boldsymbol{\eta}}\right) - b_{\theta}^{i}\log\left(\overline{b_{\theta}^{i}} + \overline{\boldsymbol{\eta}}\right)$$

Using iterative gradient descent optimization method

Sechopoulos et al, European Congress of Radiology, 2013

Homogeneous Phantom + Masses

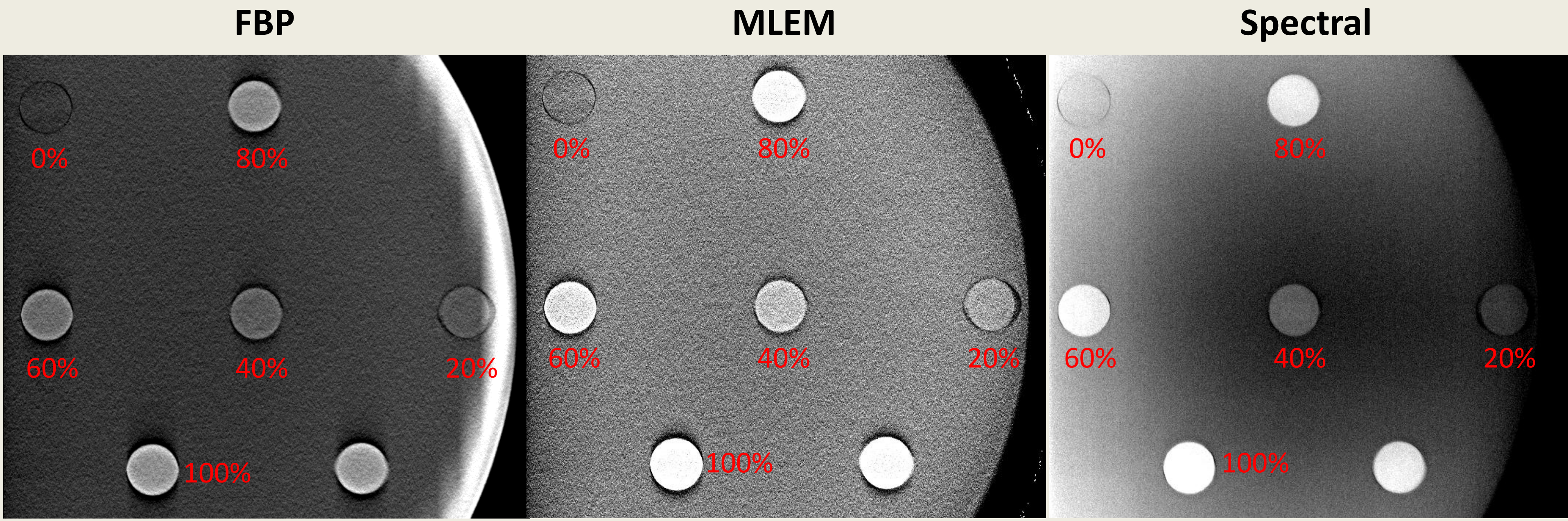

Homogeneous Phantom + Masses

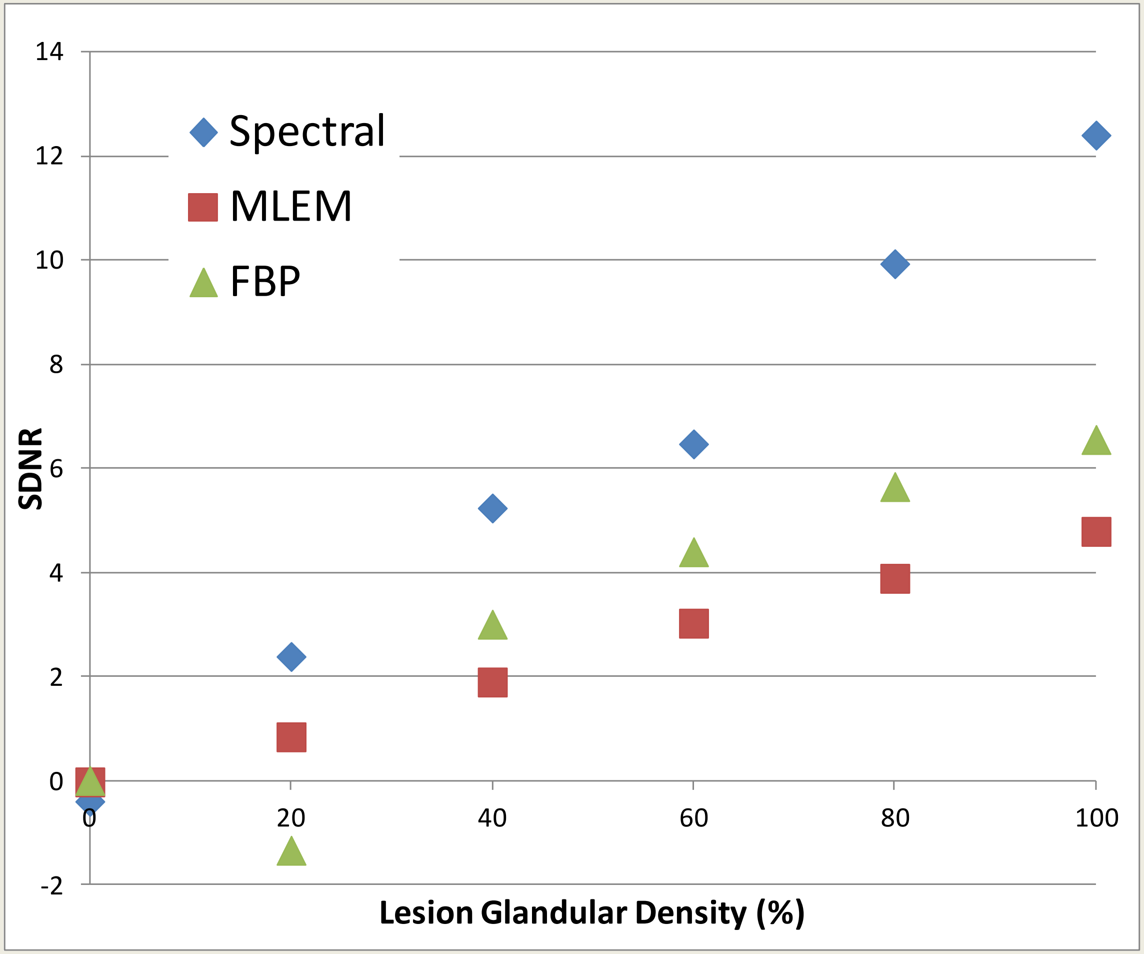

Homogeneous Phantom + Microcalcifications

FBP **Spectral**

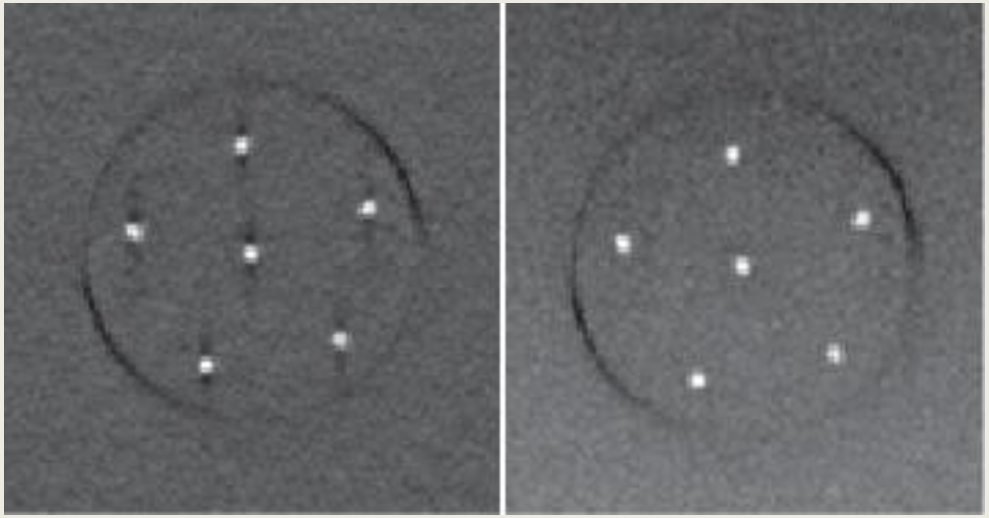

Homogeneous Phantom + Microcalcifications

FBP **Spectral**

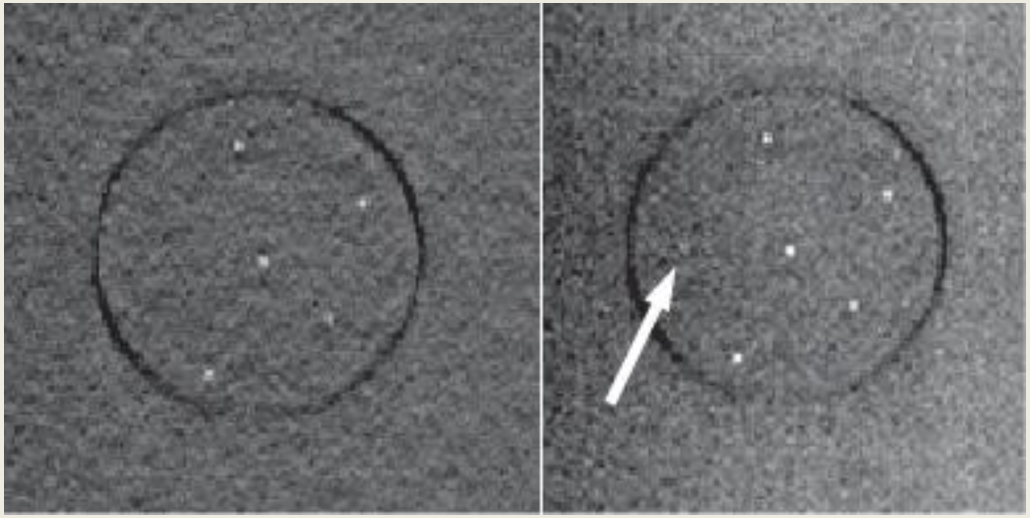

RADIATION DOSE

Breast Tomosynthesis Dosimetry Model

- Mammography:

$$AGD_{MAMMO} = D_g N_{MAMMO} AK$$

- Tomosynthesis:

$$AGD_{TOMO} = D_g N_{MAMMO} AK \underbrace{\left(\frac{\sum_{\alpha=\alpha_{MIN}}^{\alpha_{MAX}} RGD(\alpha)}{N_\alpha} \right)}$$

AAPM Task Group Report 234

Relative Glandular Dose

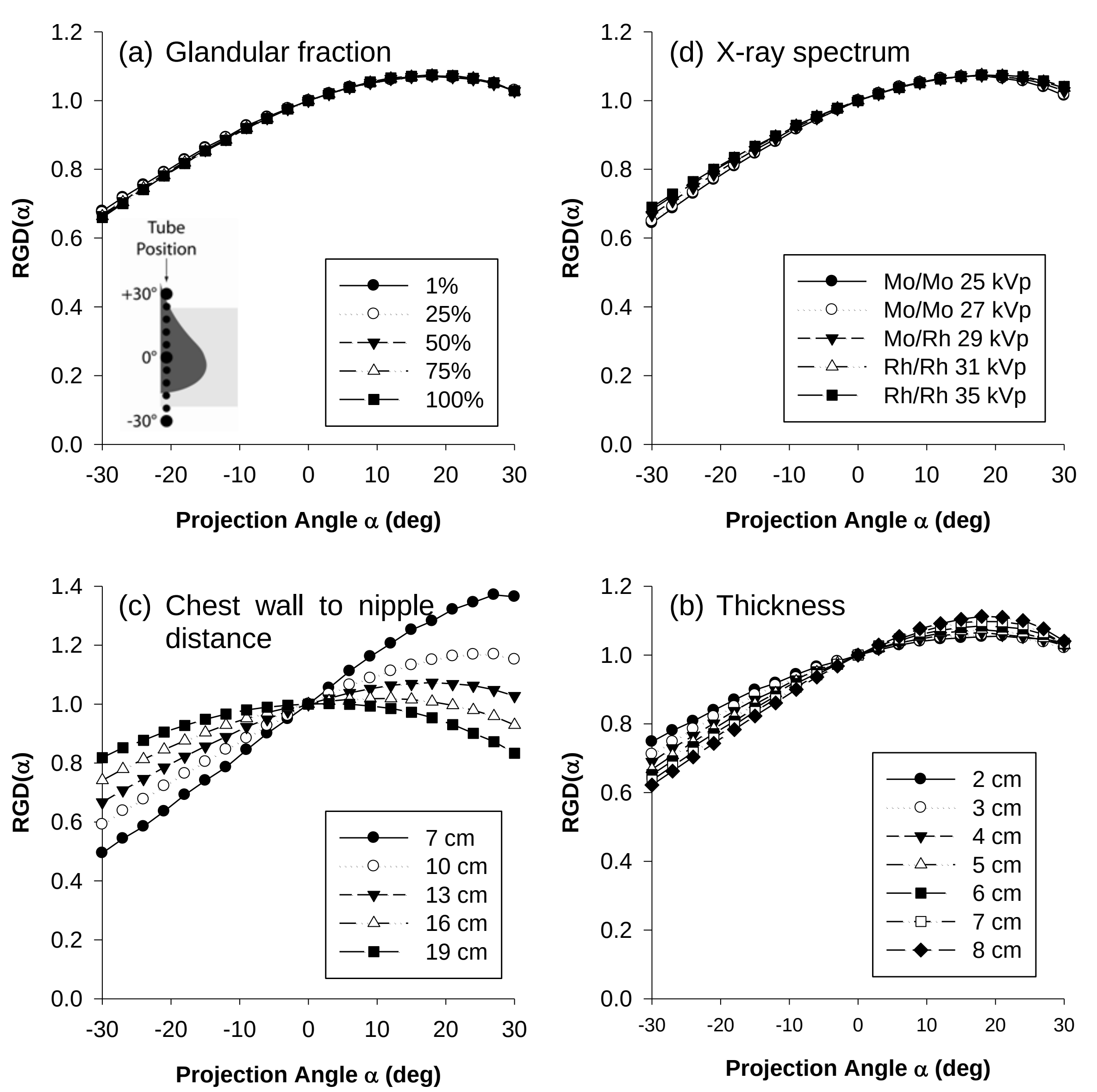

Sechopoulos et al, Med Phys, 2007; 3(1): 221-232

Mammography and Tomosynthesis Dose

Calculated Results for MGD for FFDM

Breast Thickness (cm)	1% Glandular Fraction	14.3% Glandular Fraction	25% Glandular Fraction	50% Glandular Fraction	75% Glandular Fraction	100% Glandular Fraction
2						
3						
4						
5						
6						
7						
8						

Note.—

Calculated Results for MGD for DBT

Breast Thickness (cm)	1% Glandular Fraction	14.3% Glandular Fraction	25% Glandular Fraction	50% Glandular Fraction	75% Glandular Fraction	100% Glandular Fraction
2	0.764	0.735	0.727	0.670	0.657	0.857
3	0.813	0.774	0.744	0.703	0.721	0.624
4	1.21	1.14	1.10	0.994	0.989	1.22
5	1.56	1.48	1.41	1.30	1.51	1.52
6	2.07	2.12	2.18	2.10	2.43	2.85
7	2.76	2.60	2.48	2.23	2.45	2.71
8	3.26	3.07	2.93	2.64	3.08	3.52

Note.—Data are MGDs (in milligrays).

Feng and Sechopoulos, Radiology, 2012, 263(1): 35-42

AGD Ratio of Tomo / Mammo

Breast Thickness (cm)	Glandular Density (%)			
	1	**14.3**	**25**	**50**
2	2.47	2.34	1.87	1.78
3	2.40	1.94	1.49	1.39
4	2.66	2.11	1.84	1.28
5	2.37	1.90	1.53	1.08
6	1.91	**1.83**	1.94	1.25
7	2.26	1.75	1.38	1.12
8	2.13	1.85	1.46	1.16

Feng and Sechopoulos, Radiology, 2012, 263(1): 35-42

Mean AGD [mGy]
GE SenoClaire Essential

Breast Thickness	N	Mammo	Tomo
All	236	1.62	1.49
<40 mm	28	1.13	1.14
41-50 mm	46	1.34	1.33
51-60 mm	74	1.48	1.41
61-70 mm	55	1.82	1.62
>70 mm	33	2.39	1.98

Paulis et al, Investigative Radiology, online ahead of print

Chest Imaging Effective Dose [mSv]

2-View CXR	Chest Tomo	Chest CT
0.056	0.124	7

Sabol, Medical Physics, Vol. 36, No. 12, 2009

Does the exposure distribution have to be uniform?

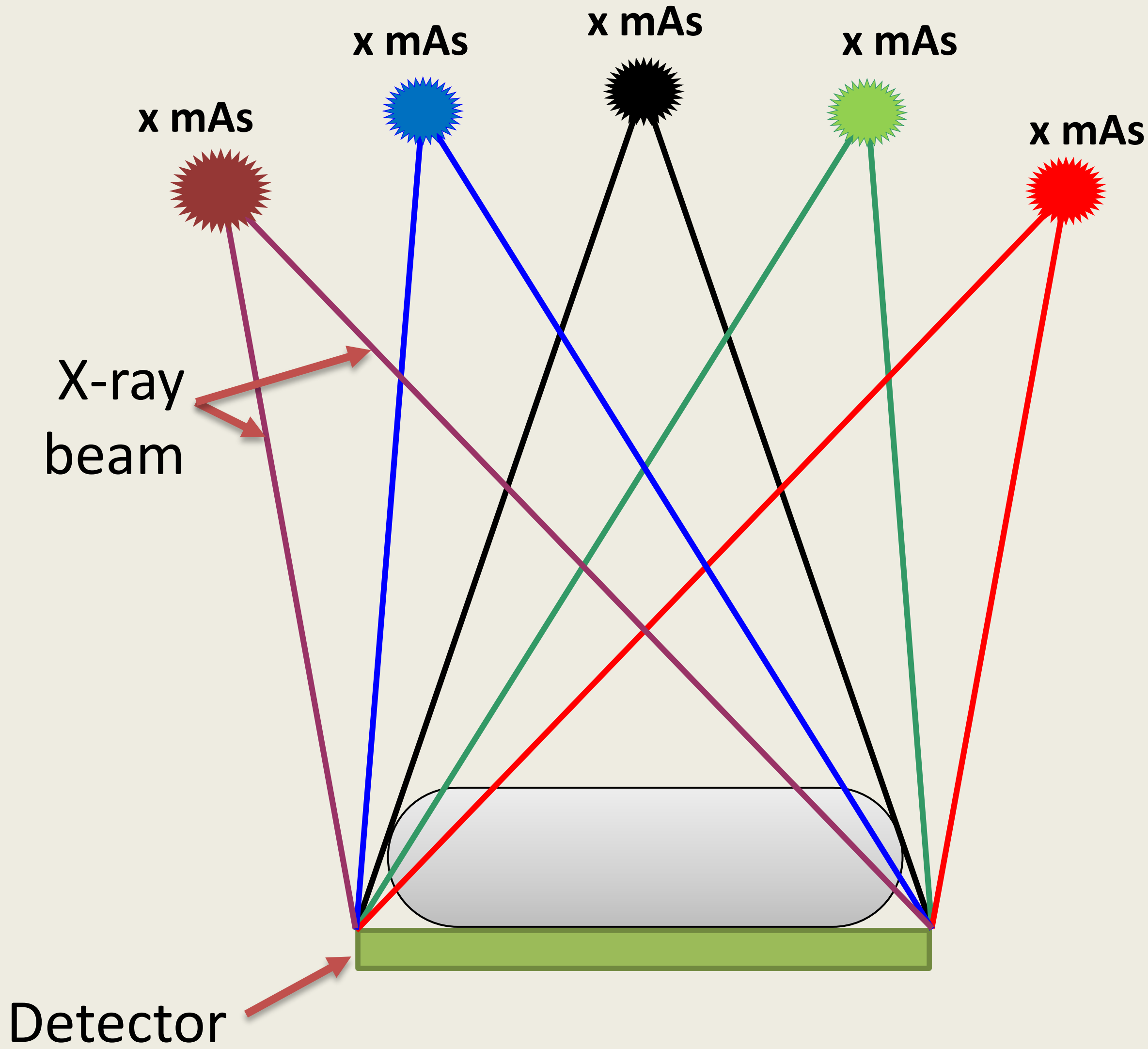

How about:

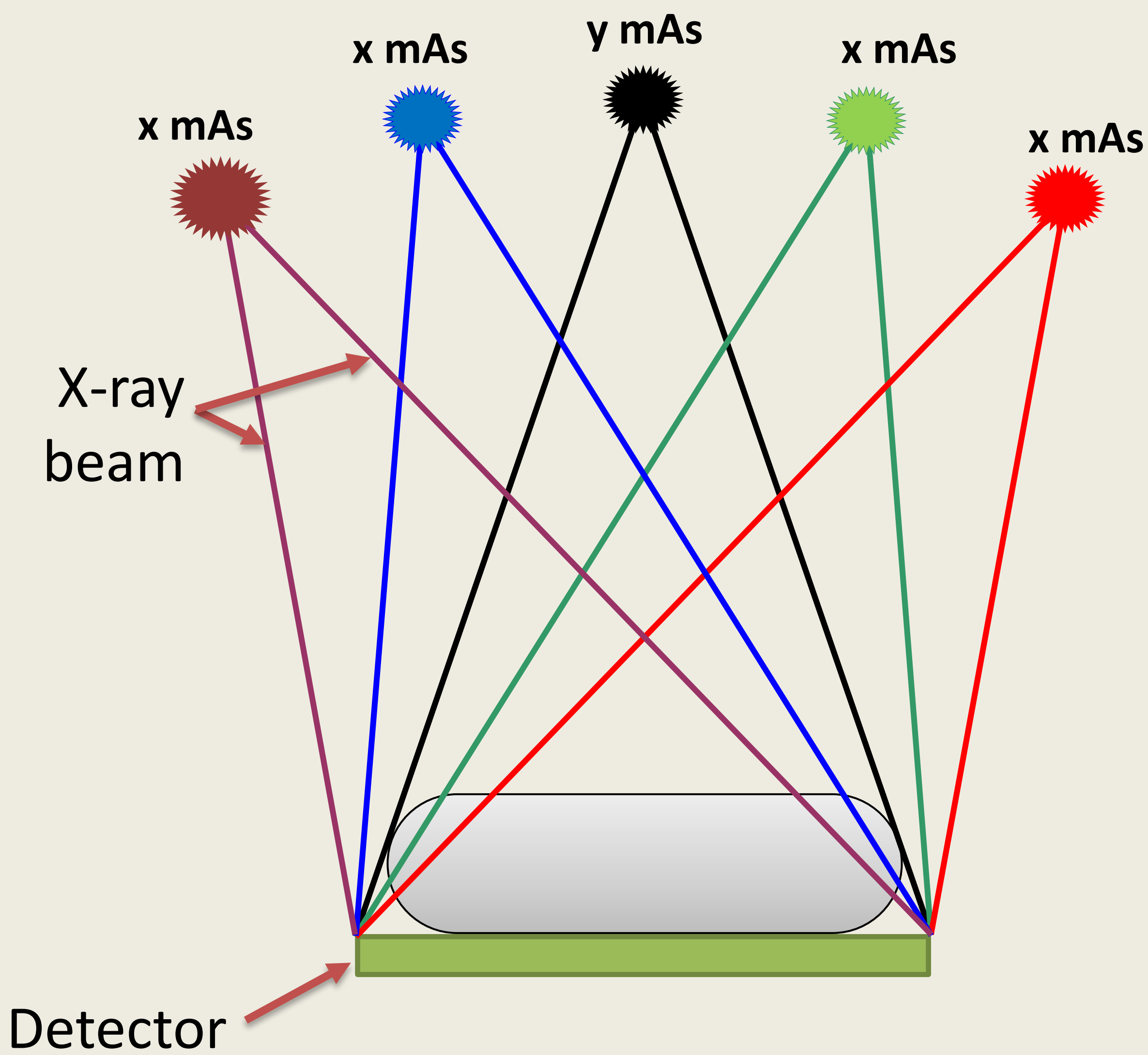

$y < x$?

$y > x$?

Or even:

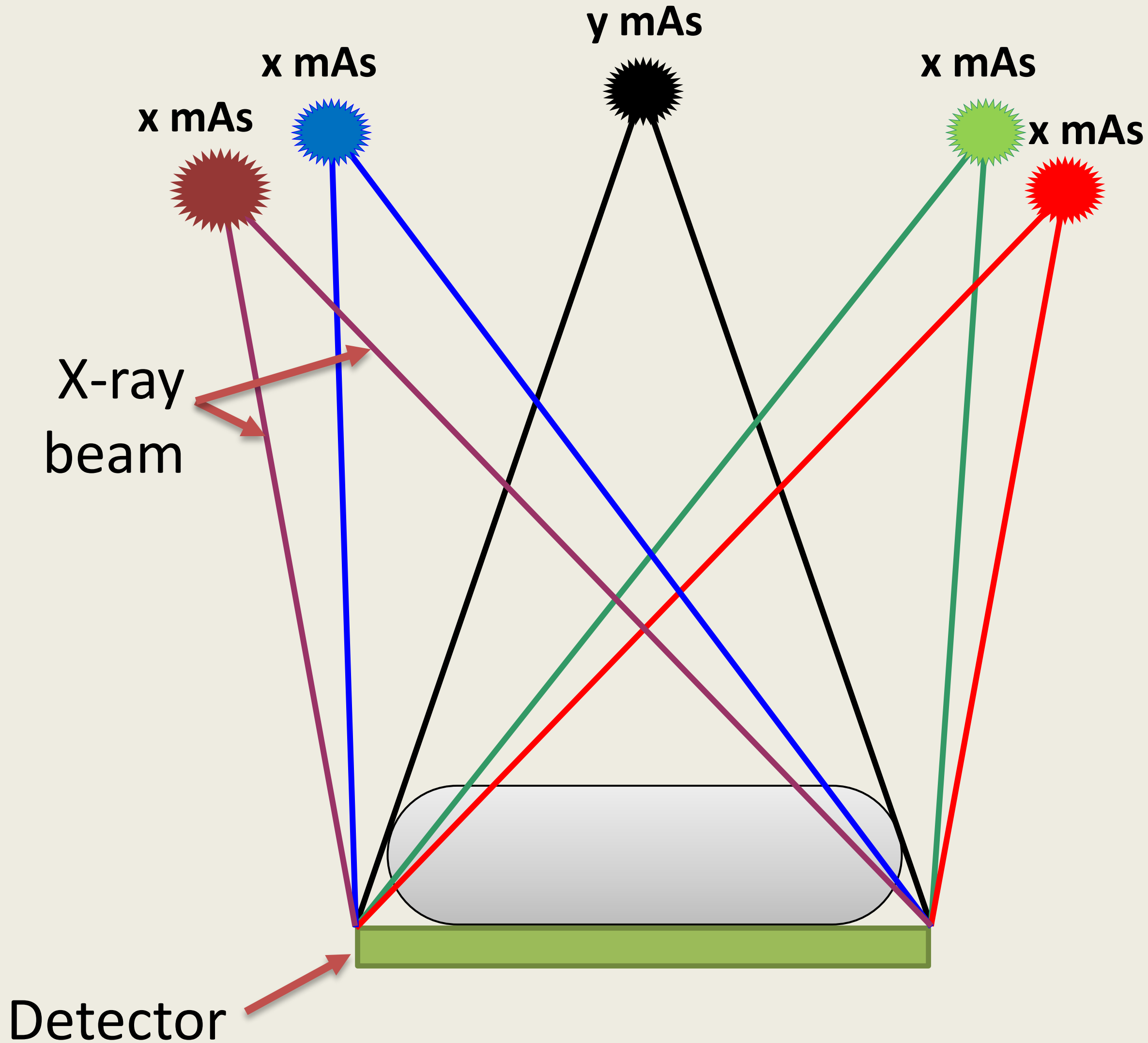

$y < x$?

$y > x$?

Mammo Tomo Proposal

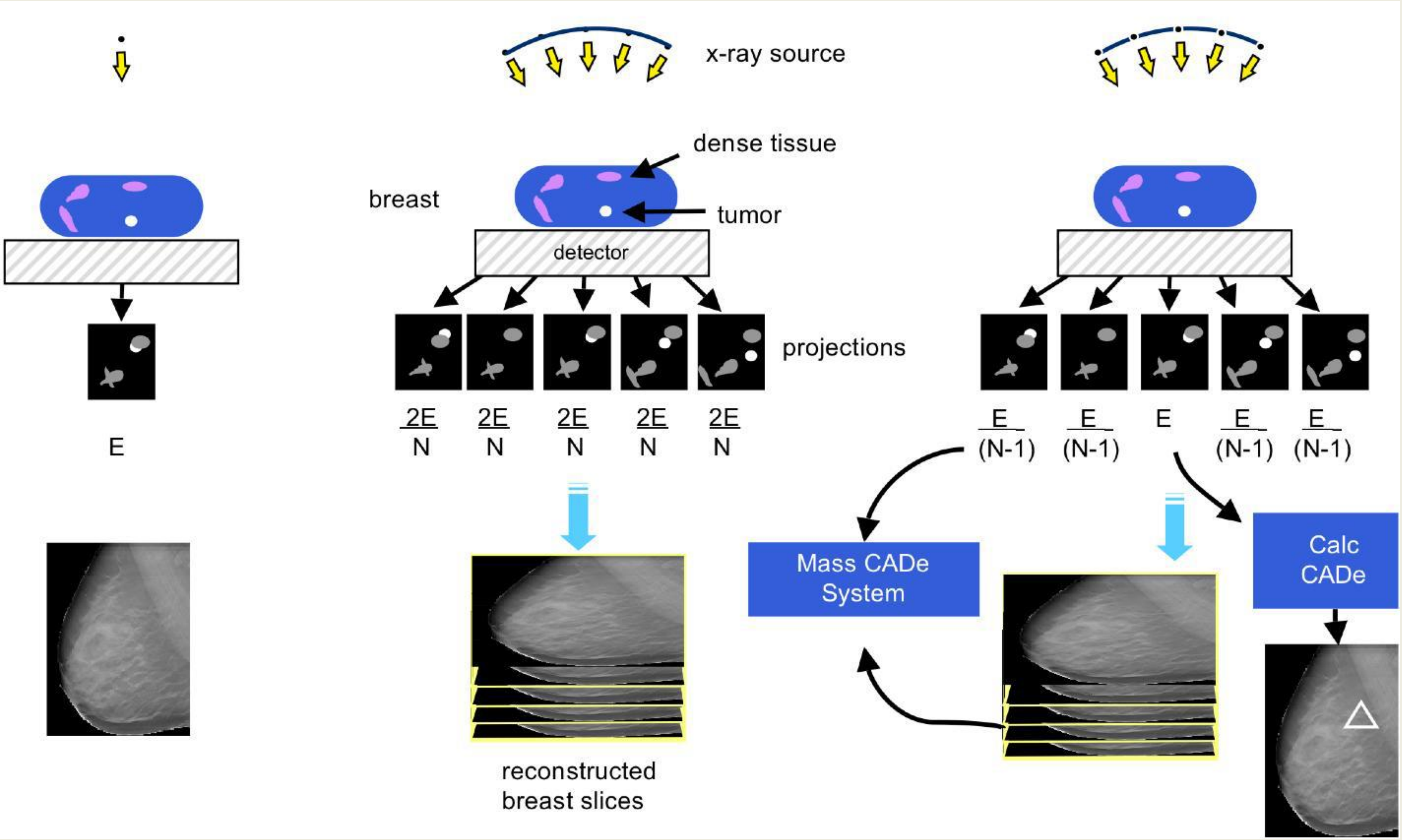

Nishikawa, Reiser et al, Proceedings of SPIE 6510, 65103C–65108C (2007).

µCa detectability: center projection < single center slice of reconstruction

Mass detectability: no statistically significant difference

Das et al, Medical Physics 2009, 36(6), 2009

Standard Tomo

Variable
7 central / 18 total proj

Variable
5 central / 20 total proj

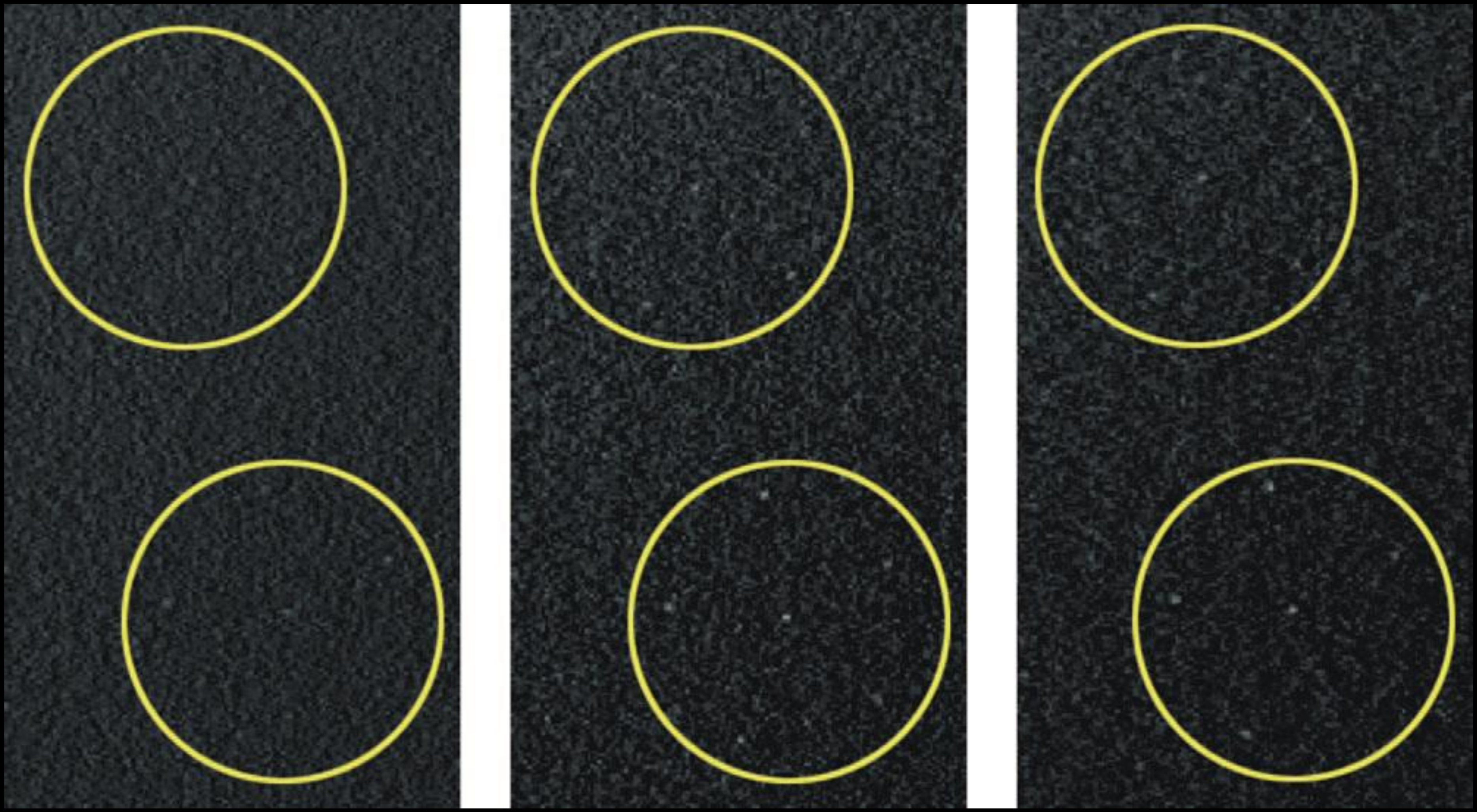

Hu and Zhao, Med. Phys. 38(5), 2455–2466 (2011).

Uneven distribution of exposure and non-uniform angular sampling used by one commercial manufacturer in systems outside the US.

What if??

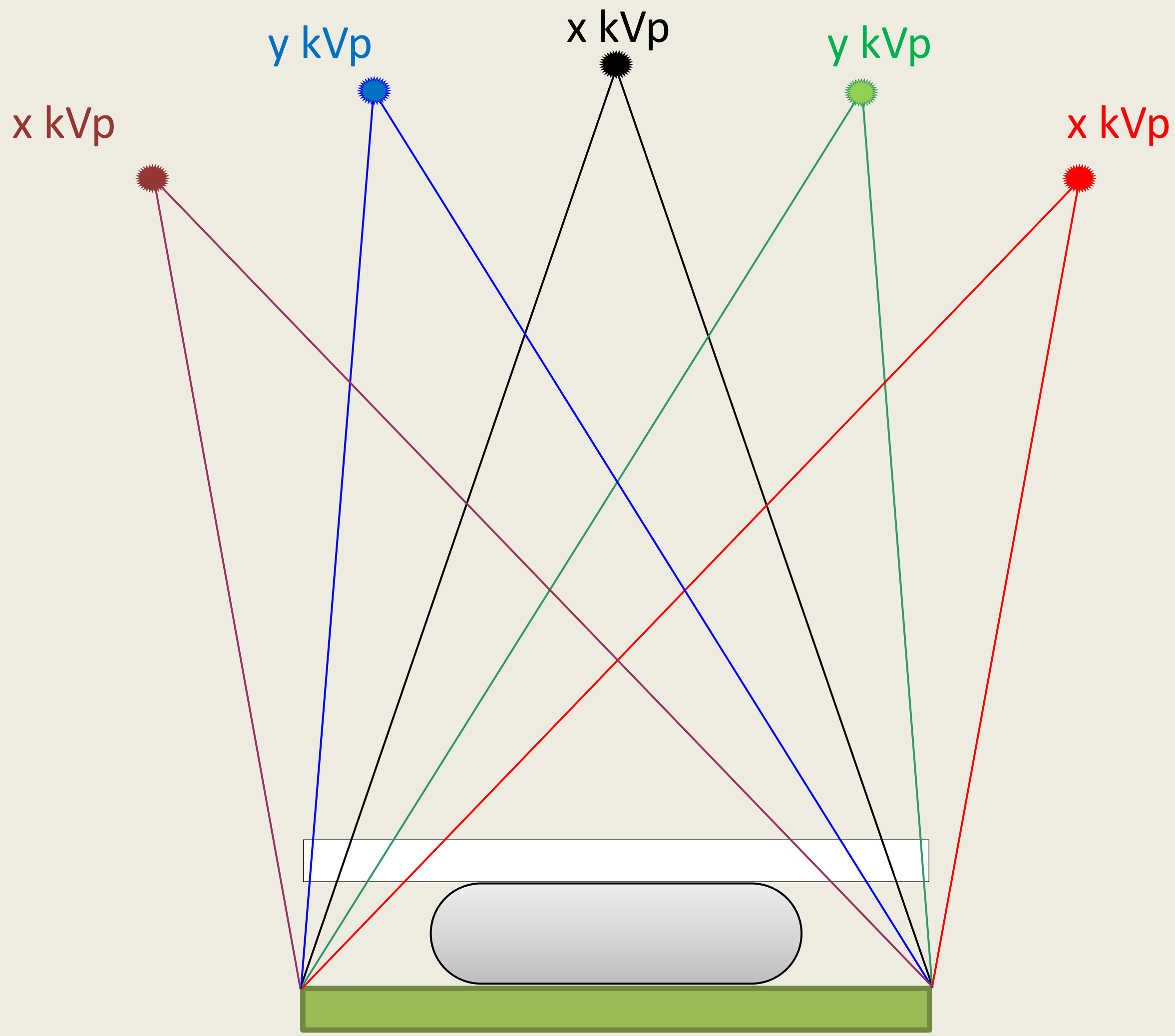

Improved image quality?

Dose reduction?

Single-pass contrast enhanced imaging?

Dual Spectrum Single Pass Tomo

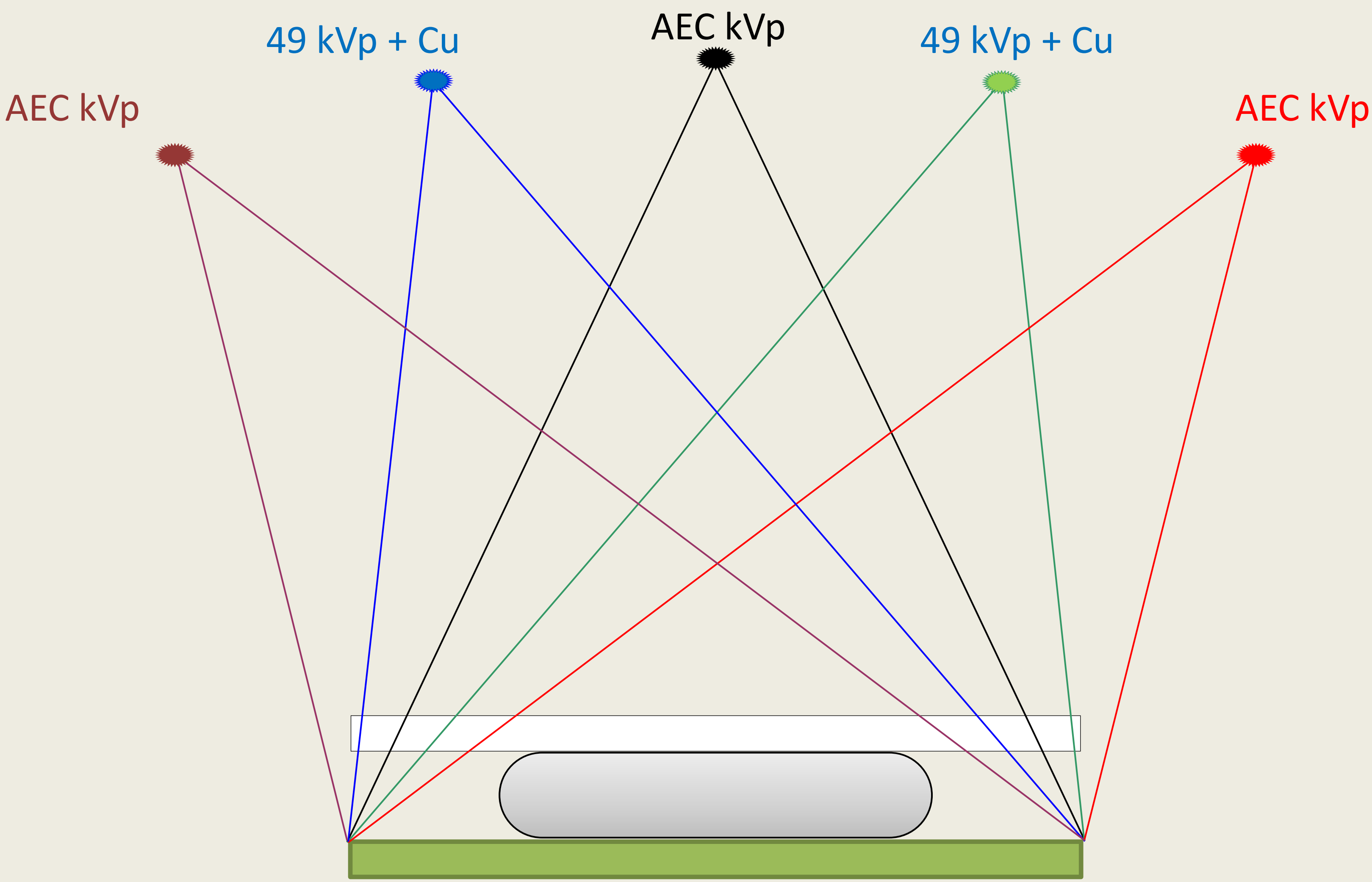

Sechopoulos et al, European Congress of Radiology, 2015

8 cm Homogeneous Phantom + Masses

AEC (38 kVp, 84 mAs)

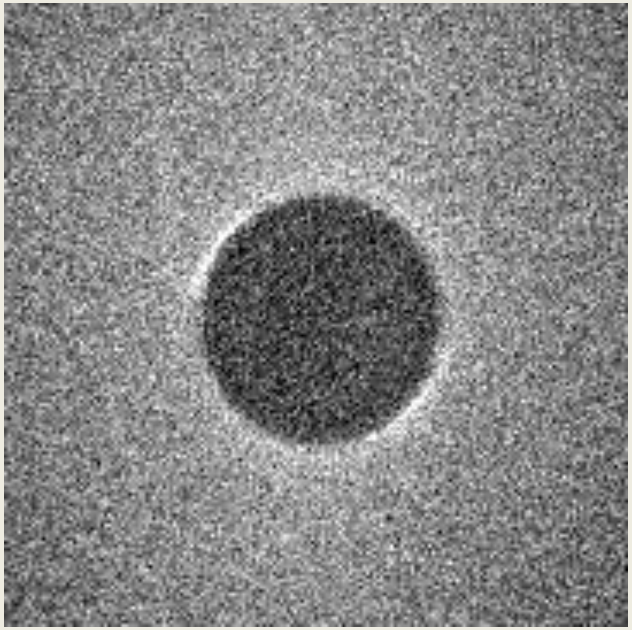

AEC + 49 kVp/0.254 mm Cu

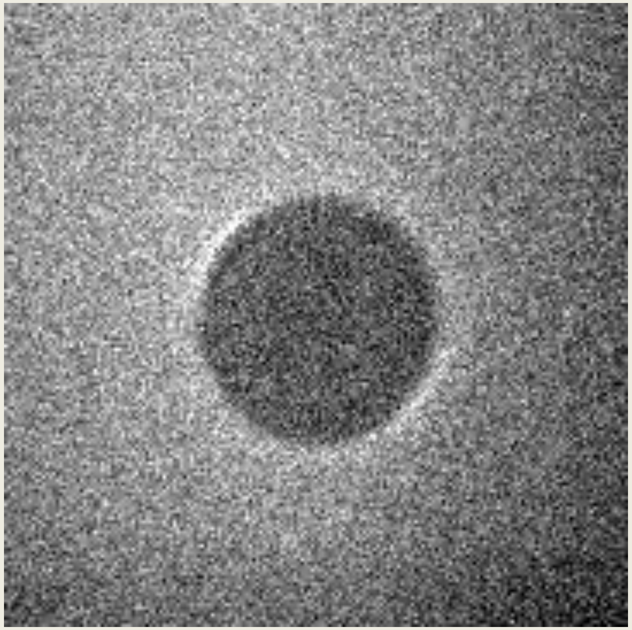

Sechopoulos et al, European Congress of Radiology, 2015

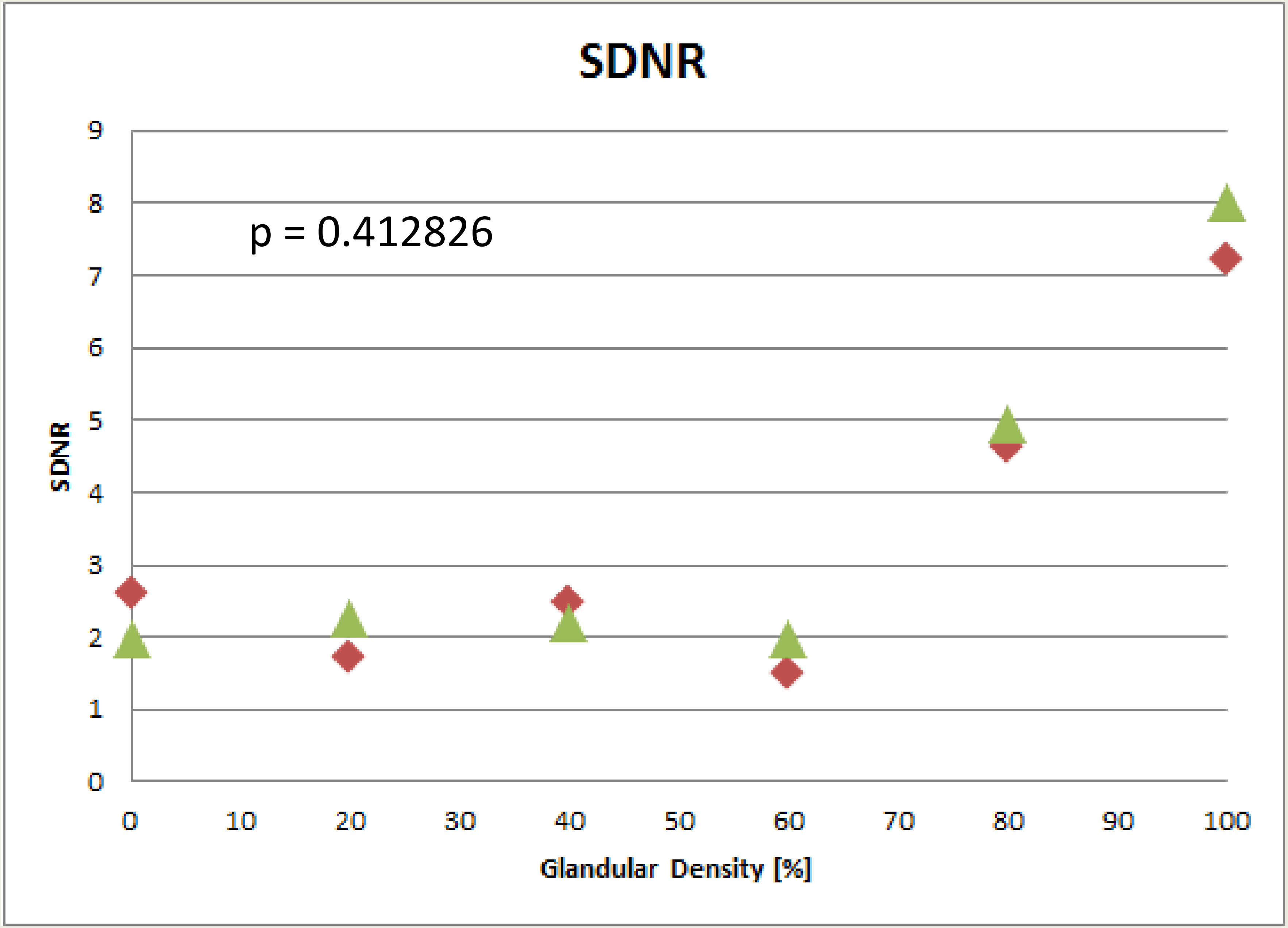

Sechopoulos et al, European Congress of Radiology, 2015

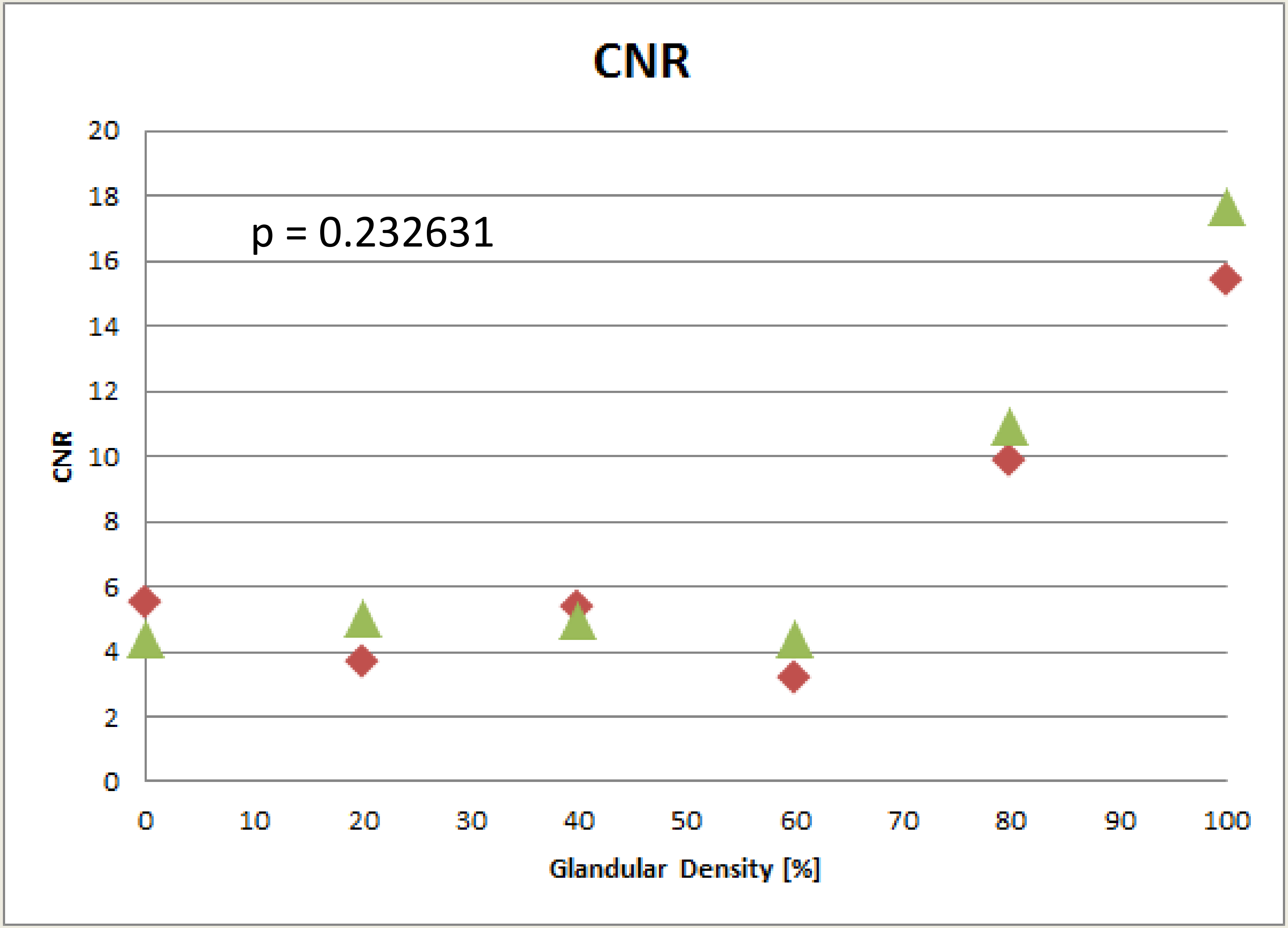

Sechopoulos et al, European Congress of Radiology, 2015

Results

Thickness	SDNR Difference	Dose
5 cm	-16.0 ± 9.25% (p>0.08)	-48%
8 cm	-3.2 ± 19.9% (p>0.41)	-28%

Sechopoulos et al, European Congress of Radiology, 2015

X-RAY SCATTER

Effect of Scatter in Tomosynthesis

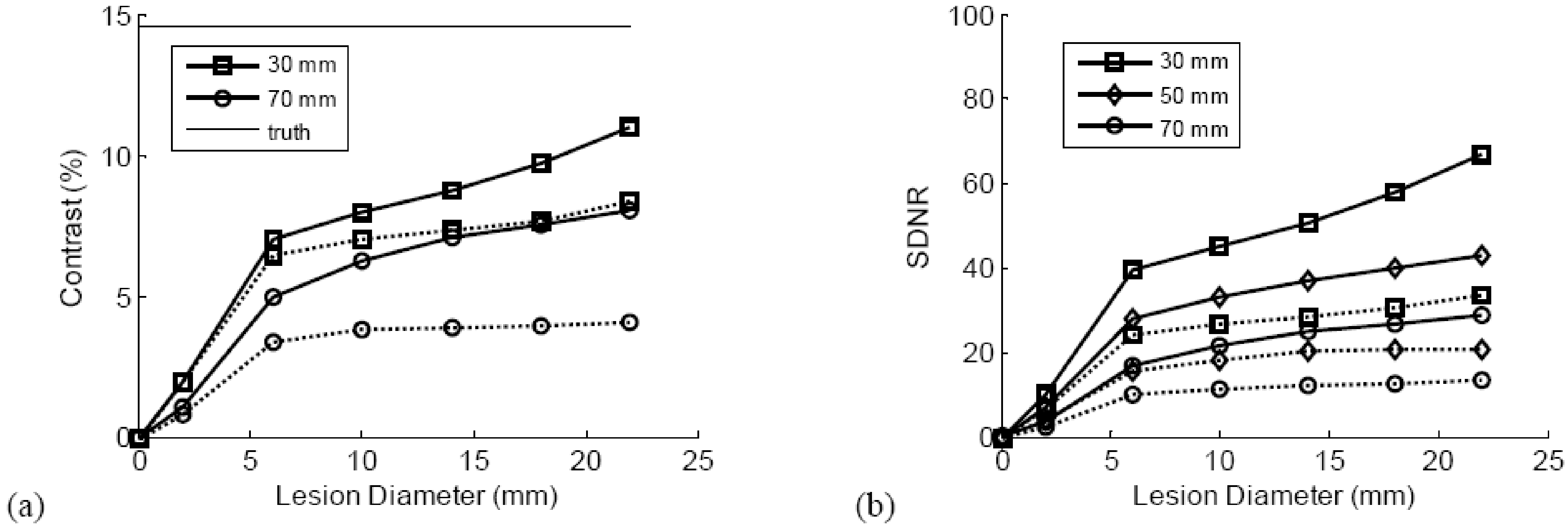

Figure 5. (a) The degrading effect of scatter radiation on contrast is illustrated for different breast thickness. (b) Scatter radiation markedly reduces the SDNR.

Wu et al, Proc SPIE, 2007

How is Scatter Normally Dealt With?

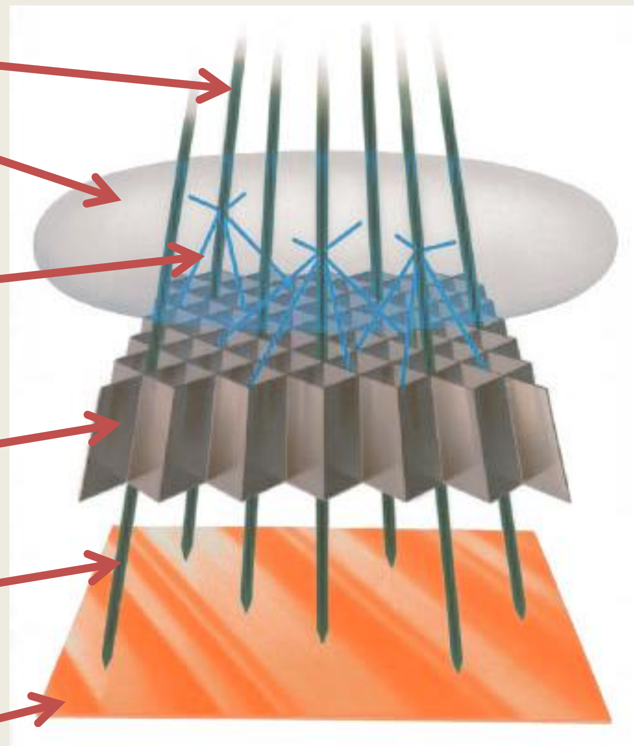

Cellular Grid

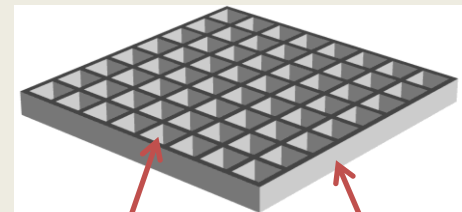

Linear Grid

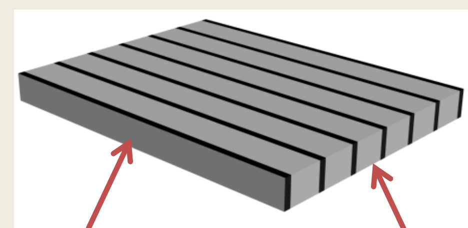

A clinical grid transmits ~80% of primary and ~20% of scatter x-rays

Grids in Tomosynthesis

Cut-off at higher projection angles

Primary photon absorption

Prone to image artifacts

GE SenoClaire Essential

Uses anti-scatter grid for DBT acquisition

Septa perpendicular to standard position

High number of lines per unit length

Alternatives

Post-acquisition processing

Correction during reconstruction

TOMOSYNTHESIS ARTIFACTS

High contrast off-plane objects introduce artifacts

“Voting” strategy to identify projections in which appropriate information is included, others ignored

Especially important for acquisitions with low number of projections

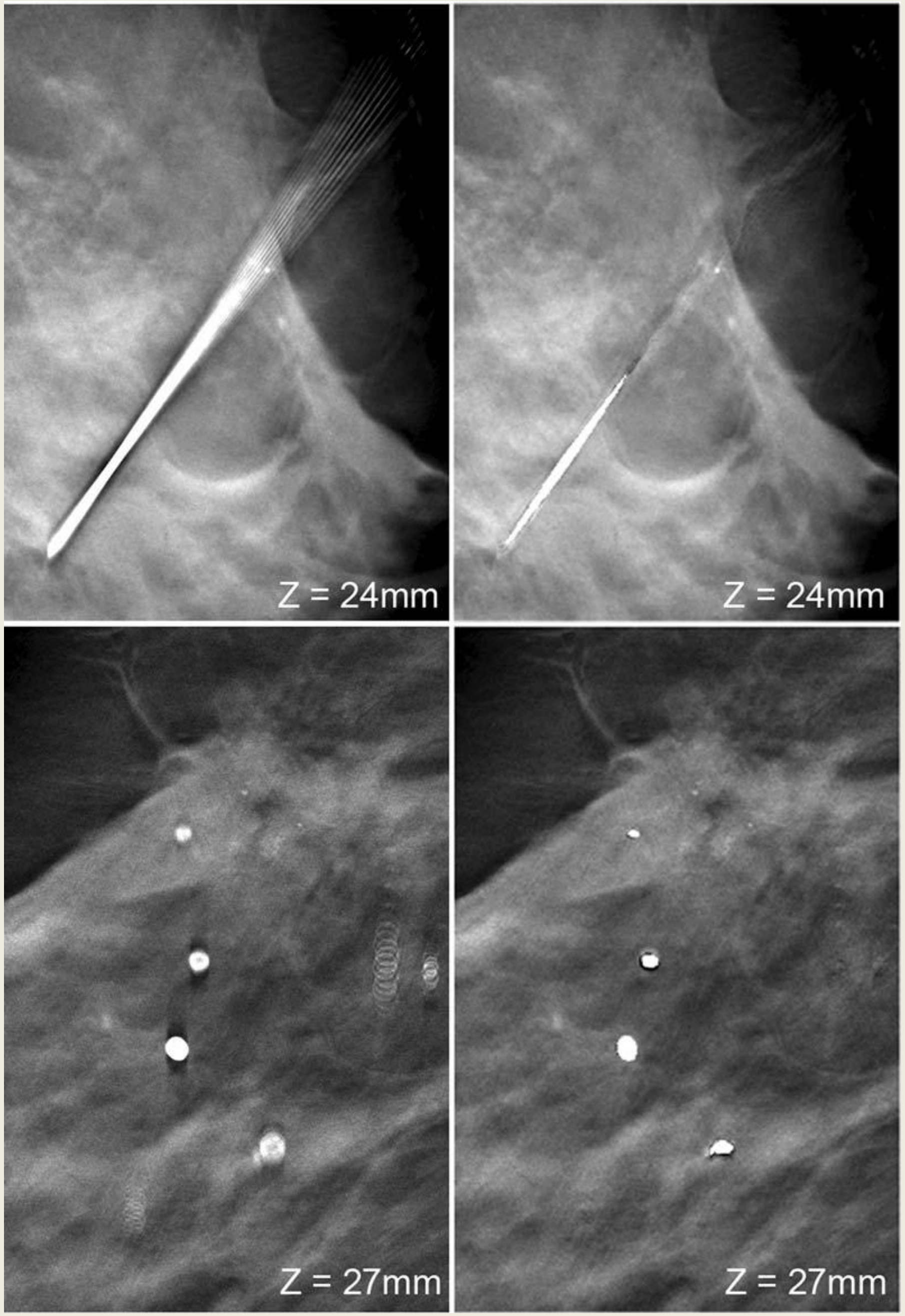

Wu et al, Medical Physics. 33(7), 2461–2471 (2006).

“Mask” to reconstruct only inside the breast

Faster reconstruction

Avoids artifacts outside breast

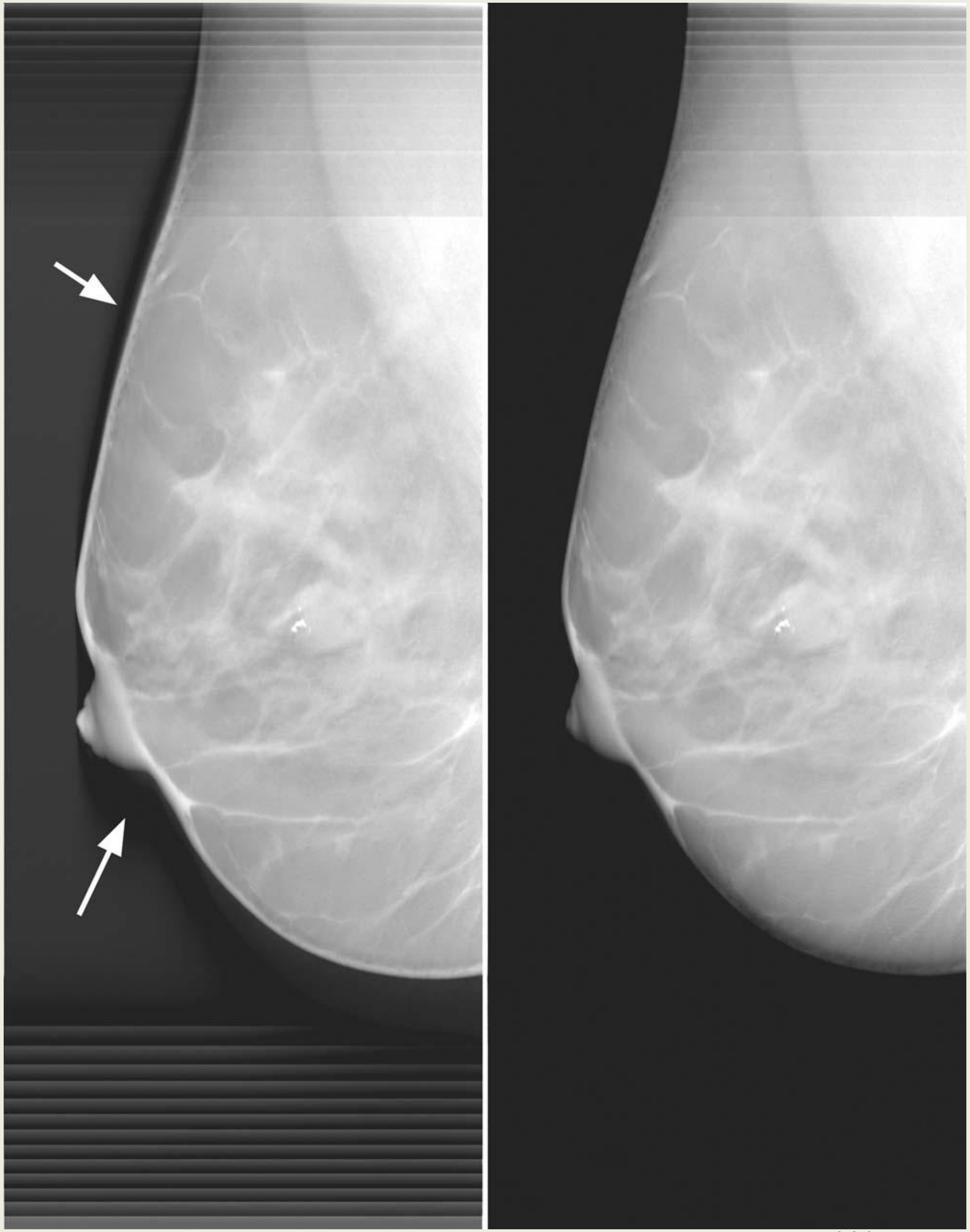

Zhang et al, Med. Phys. 34(9), 3603–3613 (2007)

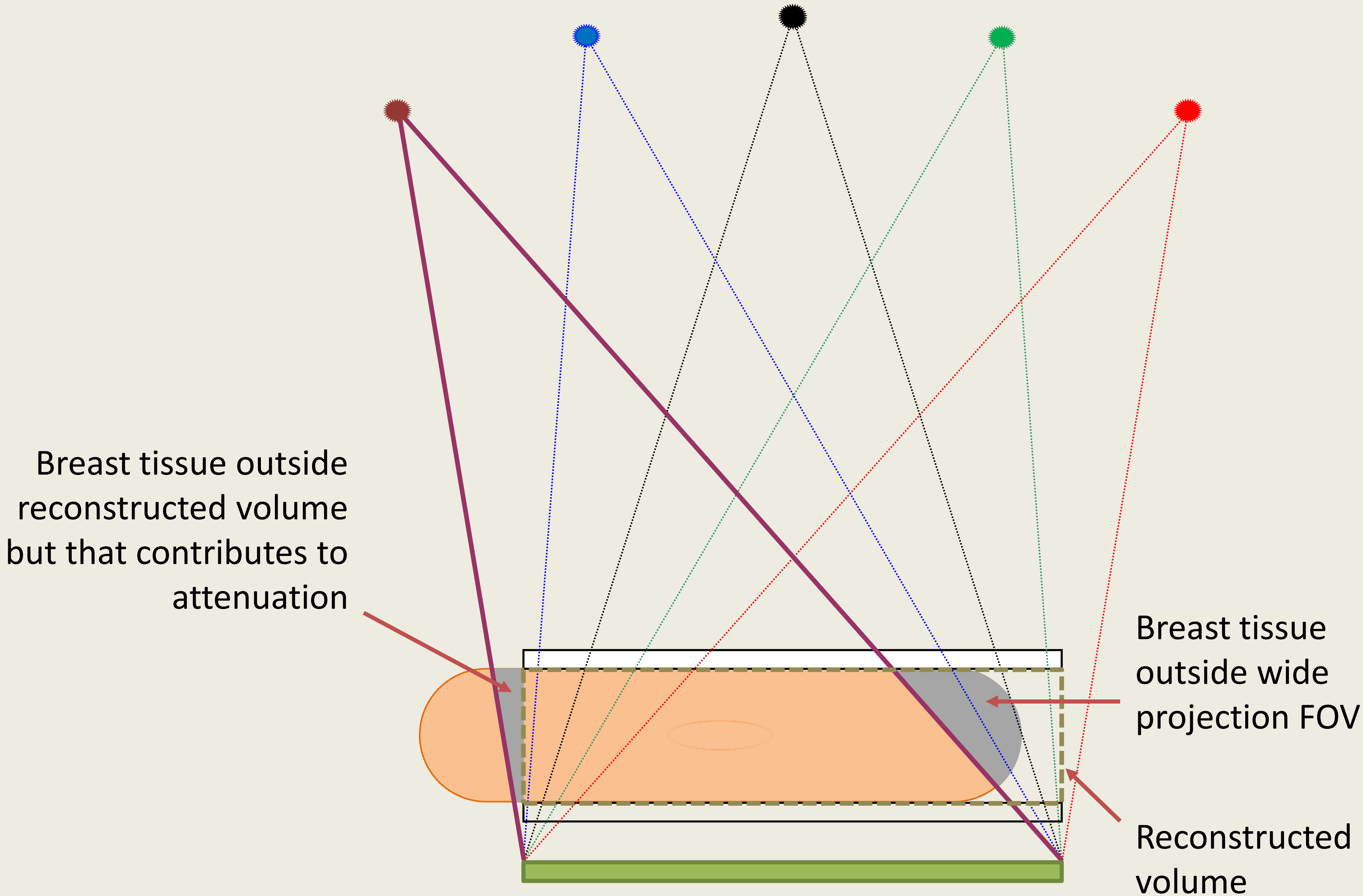
Breast tissue outside reconstructed volume but that contributes to attenuation
Breast tissue outside wide projection FOV
Reconstructed volume

Varying number of projections contributes to the volume update, introducing discontinuities: introduced equalization using neighbor values updated by previous projection

Bright artifact due to tissue attenuation outside volume: assume extension of “average” breast tissue outside of field of view to avoid bright artifact

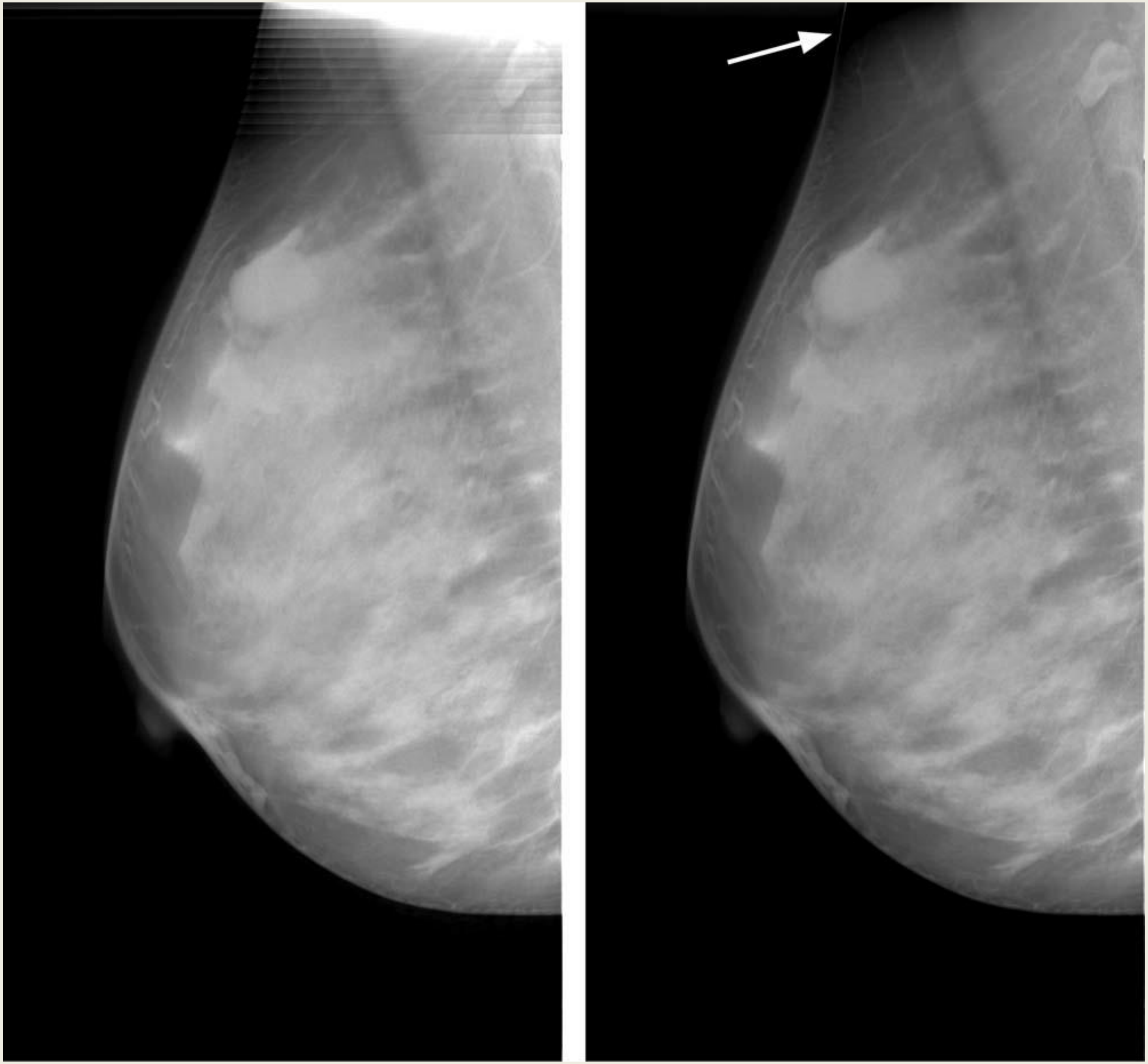

Zhang et al, J. Comput. Assist. Tomogr. 33(3), 426–435 (2009).

Uncorrected Previous Improved

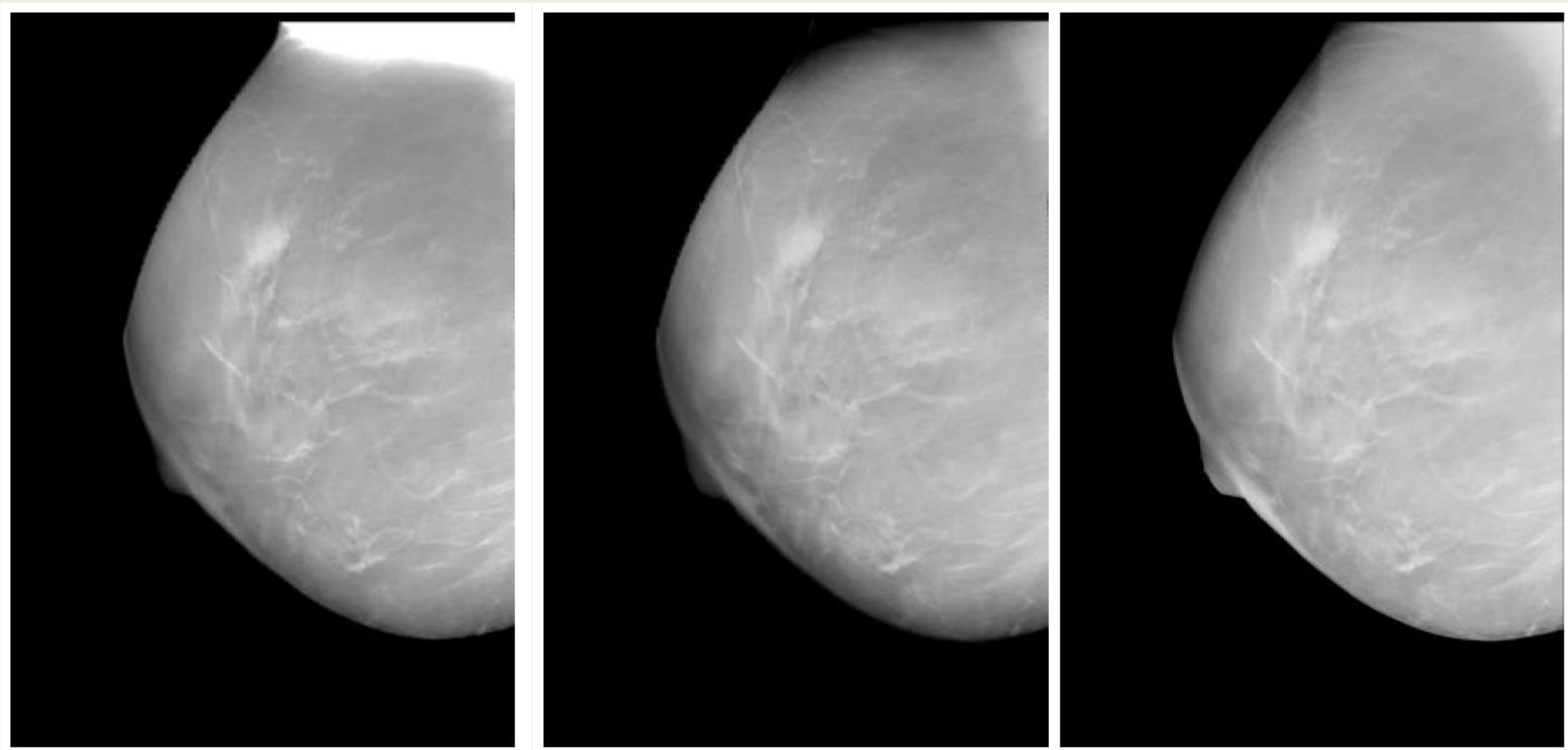

Improved estimation of x-ray path length in tissue outside field of view

Lu et al, Proceedings of the 11th IWDM 2012, pp. 745–752.

SYNTHETIC MAMMOGRAMS

Mammogram Orig. Synthetic Tomo Slice

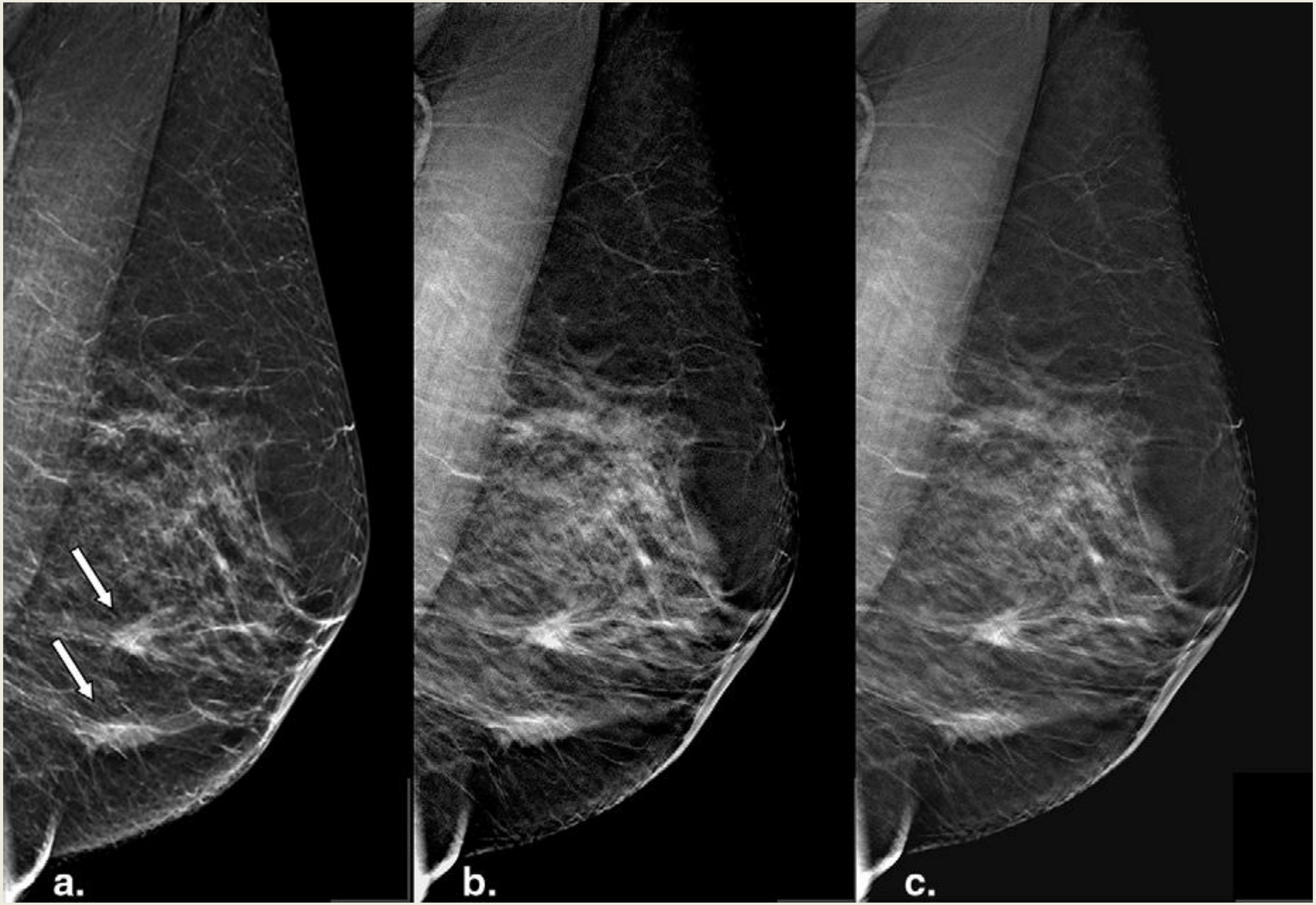

Gur et al, Academic Radiology, Vol 19, No 2, 2012

Recall Rates

	DBT + FFDM		DBT + Synthetic	
	False Positive Rate	% Detected Cancers	False Positive Rate	% Detected Cancers
1st Generation	53.1	83.5	46.1	77.7
2nd Generation	45.6	87.3	45.2	85.5

Skaane et al, Radiology, Vol 271(3), 2014

Synthetic Mammograms

Included in various commercial systems

Current Research

CADe and CADx for tomosynthesis

Need to lower reading time

Contrast enhanced tomosynthesis

Phase contrast tomosynthesis

Tomosynthesis elastography

Multimodality Imaging

Tomosynthesis

+ US

+ SPECT

+ Electrical Impedance

+ Optical

Summary

Fast digital detectors → Advanced imaging

Need to lower anatomic noise

Tomosynthesis similar to planar radiography

- System footprint
- Workflow
- Image interpretation

Summary

Acquisition geometry large impact on image quality

Dosimetry > but similar to planar radiography

Ongoing research in:

- Reconstruction algorithms
- Other techniques (enhanced, phase, etc.)
- Multimodality

QUESTIONS

In terms of image acquisition, what is the main difference between linear tomography and digital tomosynthesis?

1. Linear tomography acquisition takes substantially longer than digital tomosynthesis.
2. Linear tomography results in a single plane being in focus per acquisition while in digital tomosynthesis any number of planes can be reconstructed to be in focus.
3. Linear tomography results in circular images while digital tomosynthesis results in rectangular images.
4. In linear tomography the x-ray tube moves in a straight line while in digital tomosynthesis it moves in a circle.

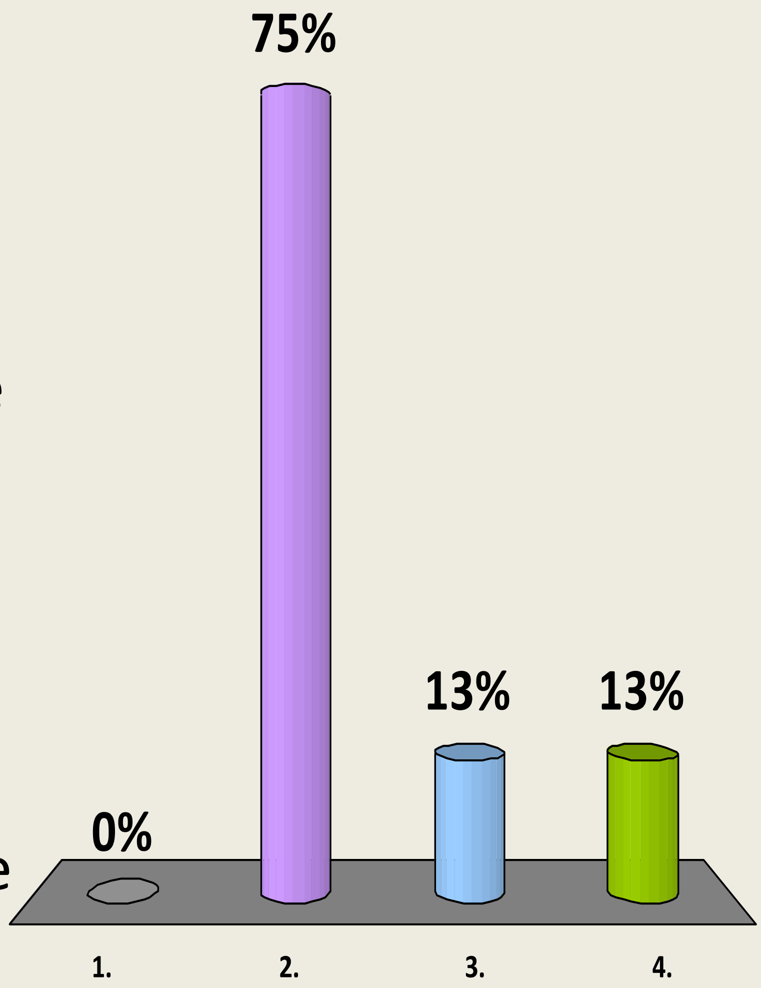

In terms of image acquisition, what is the main difference between linear tomography and digital tomosynthesis?

(2) In linear tomography, the in-focus plane has to be selected before acquisition, while in digital tomosynthesis, the reconstruction of the acquired projections results in many planes being in focus.

Bushberg et al, “The Essential Physics of Medical Imaging”, 3rd Edition

How does increasing the angular range of the tomosynthesis scan affect the vertical resolution of the reconstructed image?

1. Consistently decreases
2. Decreases up to a point, then remains constant
3. Vertical resolution does not increase with increasing angular range
4. Increases up to a point, then remains constant
5. Consistently increases

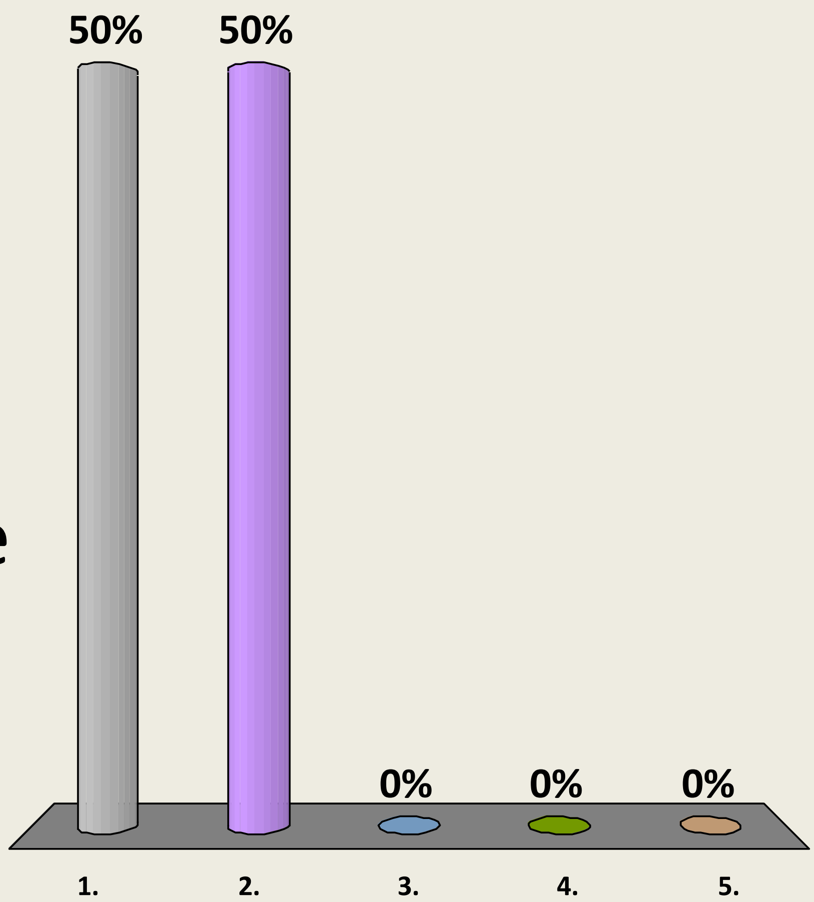

How does increasing the angular range of the tomosynthesis scan affect the vertical resolution of the reconstructed image?

(5) Increasing the angular range covered by the swing of the x-ray source consistently increases the vertical resolution of the reconstructed tomosynthesis image.

Sechopoulos and Ghetti, Medical Physics 2009, 36, 1199-1207.

How does increasing the number of projections of the tomosynthesis scan affect the vertical resolution of the reconstructed image?

1. Consistently decreases
2. Decreases up to a point, then remains constant
3. Vertical resolution does not increase with increasing number of projections
4. Increases up to a point, then remains constant
5. Consistently increases

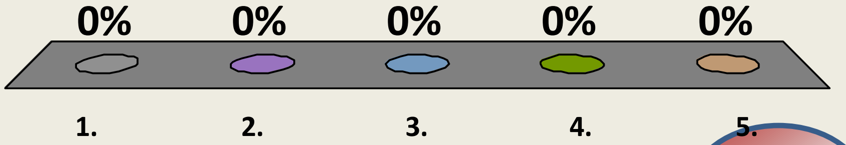

10

How does increasing the number of projections of the tomosynthesis scan affect the vertical resolution of the reconstructed image?

(4) Increasing the number of projections during a tomosynthesis acquisition increases the vertical resolution up to a certain threshold, beyond which the resolution remains constant unless the angular range is increased.

Sechopoulos and Ghetti, Medical Physics 2009, 36, 1199-1207.

Why is there a high interest in chest tomosynthesis?

0% 1. Much lower dose than chest radiography with out-of-plane blurring

0% 2. Much lower dose than chest CT with out-of-plane blurring

0% 3. Same vertical resolution as chest CT but lower dose

0% 4. Improved vertical resolution as chest CT at same dose

0% 5. Same vertical resolution and dose as chest CT, but considerably cheaper

10

Why is there a high interest in chest tomosynthesis?

(2) Chest tomosynthesis involves, in general, higher dose than chest radiography, but considerably lower than chest CT. Although it doesn’t result in true tomographic images as chest CT, it provides enough vertical resolution to be superior to chest radiography and sufficient for some clinical applications.

Sabol, Medical Physics, Vol. 36, No. 12, 2009
Dobbins and McAdams, European Journal of Radiology 72 (2009) 244–251

EMORY UNIVERSITY SCHOOL OF MEDICINE

EMORY WINSHIP CANCER INSTITUTE

NCI–Designated

Introduction to Tomosynthesis

Ioannis Sechopoulos, Ph.D., DABR
Diagnostic Medical Physics Laboratory
Department of Radiology and Imaging Sciences
& Winship Cancer Institute
Emory University
Atlanta, Georgia